

# Optimization of Laminated Dies Manufacturing

by

Hossein Ahari

A thesis

presented to the University of Waterloo

in fulfillment of the

thesis requirement for the degree of

Doctor of Philosophy

in

Mechanical Engineering

Waterloo, Ontario, Canada, 2011

©Hossein Ahari 2011

I hereby declare that I am the sole author of this thesis. This is a true copy of the thesis, including any required final revisions, as accepted by my examiners.

I understand that my thesis may be made electronically available to the public.

## Abstract

Due to the increasing competition from developing countries, companies are struggling to reduce their manufacturing costs. In the field of tool manufacturing, manufacturers are under pressure to produce new products as quickly as possible at minimum cost with high accuracy. Laminated tooling, where parts are manufactured layer by layer, is a promising technology to reduce production costs. Laminated tooling is based on taking sheets of metal and stacking them to produce the final product after cutting each layer profile using laser cutting or other techniques. It is also a powerful tool to make complex tools with conformal cooling channels. In conventional injection moulds and casting dies the cooling channels are drilled in straight paths whereas the cavity has a complex profile. In these cases the cooling system may not be sufficiently effective resulting in a longer cooling time and loss of productivity. Furthermore, conventional cooling channels are limited to circular cross sections, while conformal cooling channels could follow any curved path with variable and non circular cross sections.

One of the issues in laminated tooling is the surface jaggedness. The surface jaggedness depends on the layers' thicknesses and surface geometry. If the sheets are thin, the surface quality is improved, but the cost of layer profile cutting is increased. On the other hand, increasing the layers' thicknesses reduces the lamination process cost, but it increases the post processing cost. One solution is having variable thicknesses for the layers and optimally finding the set of layer thicknesses to achieve the minimum surface jaggedness and the number of layers at the same time. In practice, the choice of layers thicknesses depends on the availability of commercial sheet metals. One solution to reduce the number of layers without compromising the surface jaggedness is to use a non-uniform lamination technique in which the layers' thicknesses are changed according to the surface geometry. Another factor in the final surface quality is the lamination direction which can be used to reduce the number of laminations. Optimization by considering lamination direction can be done assuming one or multiple directions.

In this thesis, an optimization method to minimize the surface jaggedness and the number of layers in laminated tooling is presented. In this optimization, the layers' thicknesses are selected from a set of available sheet metals. Also, the lamination direction as one of the optimization parameters is studied. A modified version of genetic algorithm is created for the optimization purpose in this research. The proposed method is presented as an optimization package which

is applicable to any injection mould, hydroforming or sheet metal forming tool to create an optimized laminated prototype based on the actual model.

## Acknowledgements

I should be grateful to my supervisors professor A. Khajepour and professor S. Bedi for all their helpful guidance and supports during this research.

I would like to express my gratitude to Professor Jean-Christophe Cuilliere of Université du Québec à Trois-Rivières for serving as my external examiner.

I also would like to express my appreciation to professor W. Melek of University of Waterloo for his technical guides regarding the Genetic Algorithms.

I also thank my PhD committee: Professor Jahed, Professor Eihab and Professor Melek for their suggestions and advises.

I would like to thank my fellow PhD candidates in our research group: J. Seo and M.K.Ghovanlou for all the good experiences we shared during this research.

Also, special thanks to Jason Benninger of CNC machine shop in University of Waterloo for helping in machining process.

Moreover, a very special thanks to Mr. Dean Dajko, Vice president of Webplas company for all the helps during the experimental analysis.

Finally to my father and mother, who always believed in me.

To my wife, Mozhgan  
and  
my daughter, Raha.

# Contents

List of Tables . . . . .	<b>viii</b>
List of Figures . . . . .	<b>ix</b>
<b>1 Introduction</b>	<b>1</b>
1.1 Overview . . . . .	1
1.2 Motivations . . . . .	1
1.3 Objectives . . . . .	2
1.4 Thesis Organization . . . . .	3
<b>2 Literature Review and Background</b>	<b>5</b>
2.1 Introduction . . . . .	5
2.2 Definitions . . . . .	5
2.3 Introduction to Laminated Tooling . . . . .	6
2.4 Laminated Tooling in Literature . . . . .	10
2.5 Overview of Genetic Algorithms . . . . .	16
2.5.1 What are Genetic Algorithms? . . . . .	17
2.5.2 Fundamentals of Genetic Algorithms . . . . .	18
2.5.3 Example . . . . .	27
<b>3 Optimization of Laminated Dies</b>	<b>31</b>
3.1 Introduction . . . . .	31
3.1.1 Slicing Based on STL Data . . . . .	31
3.1.2 Direct Slicing Technique . . . . .	33
3.2 Slicing Process . . . . .	33
3.3 Optimization Methodology . . . . .	36
3.3.1 Why Genetic Algorithms? . . . . .	39

3.4	Optimization and Simulation Modules . . . . .	47
<b>4</b>	<b>Optimization Results</b>	<b>49</b>
4.1	Introduction . . . . .	49
4.2	Case Studies . . . . .	49
4.2.1	Case 1 - A trivial example . . . . .	49
4.2.2	Case 2 - Hydroforming tool . . . . .	53
4.3	Actual Experimental Test . . . . .	56
4.3.1	Case 1 . . . . .	57
4.3.2	Case 2 . . . . .	60
4.4	Improving the Search Technique . . . . .	63
4.5	Premature convergence and its treatment . . . . .	64
4.5.1	Parallel genetic algorithm and niching methods . . . . .	64
4.6	Weak elimination crowding method . . . . .	66
4.6.1	Termination criterion . . . . .	67
4.7	Results . . . . .	69
4.8	Conclusion . . . . .	78
<b>5</b>	<b>Slicing Direction Optimization in Laminated Dies</b>	<b>79</b>
5.1	Introduction . . . . .	79
5.2	The Effect of Surface Topology on Slicing Direction . . . . .	80
5.2.1	Error Triangle . . . . .	81
5.3	Surface Analysis Method . . . . .	83
5.4	Direction Analysis Results . . . . .	87
5.4.1	Single direction . . . . .	87
5.4.2	Multiple Directions . . . . .	87
5.5	Global Search for The Best Direction . . . . .	95
5.6	Conclusion . . . . .	97
<b>6</b>	<b>Experimental Analysis</b>	<b>100</b>
6.1	Introduction . . . . .	100



6.2	Experimental Results . . . . .	101
6.3	Conclusion . . . . .	107
7	<b>Concluding Remarks and Future Works</b>	109
7.1	Thesis Contributions . . . . .	109
7.1.1	Volume deviation and number of slices were minimized at the same time .	110
7.1.2	Considering a set of available sheets in the optimization process . . . . .	110
7.1.3	A customized version of genetic algorithm was proposed for this specific application . . . . .	110
7.1.4	Geometry of CAD model was considered for slice thickness calculations .	110
7.1.5	Slicing direction as an important parameter in laminated tools optimization was studied. An analytical method to find the best slice direction was developed . . . . .	111
7.1.6	A user friendly software for laminated dies manufacturing . . . . .	111
7.1.7	Experimental analysis to show the performance of the suggested method was performed . . . . .	111
7.2	Future Work . . . . .	111
Appendix		
A	<b>Optimization Program</b>	113
	Bibliography	118

# List of Tables

2.1	Results for the first randomly selected population . . . . .	22
2.2	Example1 - Results for the first randomly selected population . . . . .	28
2.3	Example1 - Selection results for the first generation . . . . .	28
2.4	Example1 - final next generation . . . . .	29
3.1	Different cases in crossover operation . . . . .	45
4.1	Different case studies in optimization of injection mould laminated manufacturing	71
5.1	Co-operator normal vectors and the areas of well-located tiles for model in Figure 5.9 . . . . .	87
5.2	Co-operator normal vectors and the areas of Well-located tiles for model in Figure 5.10 . . . . .	90
5.3	Areas of well-located tiles in different portions for the model in Figures 5.10 and 5.12 . . . . .	91
6.1	Operation results for conventional and conformal cooling channels for the sample injection mould tool . . . . .	107

# List of Figures

2-1	A tool with conventional cooling channel . . . . .	7
2-2	An illustration of a conformal cooling system . . . . .	8
2-3	Schematic of laminated tooling process steps . . . . .	8
2-4	2-D profile created by intersecting a 3-D CAD model by a sample slice plane . . . . .	9
2-5	Volume deviation between (a) actual CAD model, and (b) laminated tool . . . . .	10
2-6	Volume patches [17] . . . . .	12
2-7	conventional (a) and conformal (b) cooling channels employed on performance evaluation in [20] . . . . .	13
2-8	The importance of an optimized slicing direction . . . . .	14
2-9	a) a sample tool, b) the same tool created in PEL method . . . . .	16
2-10	2D profile created by intersecting a 3-D CAD model by a cutting slice plane . . . . .	17
2-11	Schematic representation of reproduction process in genetic algorithm . . . . .	21
2-12	Single point crossover: (a) randomly chosen crossover point on the parents' chromosomes, and (b) two new chromosomes . . . . .	24
2-13	Double point crossover: (a) randomly chosen crossover points on the parents' chromosomes, and (b) two new chromosomes . . . . .	25
2-14	Cut and splice crossover: (a) randomly chosen two different crossover points on parents' chromosomes, and (b) two new chromosomes with different size of data . . . . .	25
2-15	Original distribution of 10 randomly selected initial data . . . . .	30
2-16	Final result after 20 iterations . . . . .	30
3-1	A tessellated sample CAD model . . . . .	32
3-2	A sample slice with one slice plane in each side . . . . .	34

3-3	An isometric view of back and front profiles . . . . .	34
3-4	Back and front profiles for a sample slice . . . . .	35
3-5	Compare back and front profiles to find the union profile . . . . .	35
3-6	Union profile . . . . .	36
3-7	Schematic of slicing process in simulation module . . . . .	37
3-8	(a) A sample model; (b) Uniform slicing with minimum thickness; (c) Uniform slicing with maximum thickness; (d) Adaptive slicing with optimization outcome thicknesses. . . . .	38
3-9	A sample CAD model with conformal cooling channels . . . . .	40
3-10	Schematic of how genetic algorithm works . . . . .	42
3-11	A sample CAD model with two critical sections . . . . .	44
3-12	Location of the slice planes in either side of critical section . . . . .	45
3-13	The effect of internal mutation on a thickness vector. (a) before mutation; (b) after mutation . . . . .	46
3-14	Schematic of genetic algorithm procedure in the current research . . . . .	48
4-1	First case, a simple model . . . . .	50
4-2	Fitness values at the beginning of the optimization process and after 11 iterations. . . . .	51
4-3	The best relative fitness for each iteration. . . . .	51
4-4	Slice planes arrangement; (a) the best set at the first randomly selected population, (b) final result . . . . .	52
4-5	Fitness values at the beginning of optimization process and after 20 iterations . . . . .	53
4-6	The best relative fitness for each iteration. . . . .	54
4-7	Optimization results for 200 population size; (a) Isometric preview of original CAD model, (b) Top view of original CAD model; and The best slice planes locations: (c) For the first randomly selected generation, (d) After 5 iterations, (e) After 7 iterations, (f) After 10 iterations, and (g) After 20 iterations . . . . .	55
4-8	The original injection mould tool and the section selected for the case study . . . . .	56
4-9	The portion of CAD model used in the optimization process . . . . .	57
4-10	A conformal cooling system can follow the cavity shape . . . . .	58
4-11	The best relative fitness trough iterations for a population size of 50 . . . . .	59

4-12	The fitness values of the best thickness vectors in each iteration . . . . .	59
4-13	The best relative fitness trough iterations . . . . .	60
4-14	The fitness values of the best thickness vectors in each iteration . . . . .	61
4-15	Fitness values of all thickness vectors at the first and last iterations . . . . .	61
4-16	Volume deviations of all thickness vectors at the first and last iterations . . . . .	62
4-17	The top view of the slice planes arrangement for the second case study, a) The best set in the first generation b) The optimization result . . . . .	63
4-18	Schematic of the modified genetic algorithm procedure in the current research . .	68
4-19	Comparison of volume deviations with the ideal value for the first generation in the left and the last generation in the right ( — ideal volume deviation, —●— calculated volume deviation) . . . . .	72
4-20	Comparison of fitness values with the average value at the first generation in the left and the last generation in the right(— average fitness value, —●— calculated fitness value) . . . . .	74
4-21	The best fitness value in each generation. T: the unique termination criterion is satisfied; T1: the first termination criterion is satisfied; T2: the second termination criterion is satisfied. . . . .	75
4-22	The top views of the results for the first and last runs . . . . .	76
4-23	Side views of results for the first and last runs . . . . .	77
5-1	A change in slice direction from (a) to (b) eliminates the volume deviation value	80
5-2	The effect of different slice directions on the slicing process performance . . . . .	81
5-3	CAD model tile behavior in different slice directions . . . . .	82
5-4	Error triangle . . . . .	82
5-5	Tiles and normal vectors on a sample model . . . . .	84
5-6	Suggested algorithm for optimal direction finding . . . . .	85
5-7	A non-planar tile in a CAD model . . . . .	86
5-8	Planar representation of a non-planar tile . . . . .	86
5-9	A sample model without non-planar tiles (Dimensions are in millimeter) . . . . .	88
5-10	A sample model with non-planar tiles (Dimensions are in millimeters) . . . . .	89
5-11	STL representation of tile A <sub>6</sub> or A <sub>7</sub> . . . . .	89

5-12	Model is divided into different portions to investigate different slicing directions	91
5-13	Performance of each favorite direction on CAD model	92
5-14	The hydroforming tool	93
5-15	The suggested slicing directions from program output	93
5-16	Model is divided to different territories to investigate different slicing directions	94
5-17	Performance of each favorite direction based on CAD model length	94
5-18	All potential slicing directions in the space	95
5-19	Suggested algorithm for globally optimal direction search	96
5-20	Histogram of well-located tile areas produced by favorite directions, $D_1$ to $D_6$	97
5-21	Rank of favorite slicing directions	98
5-22	The outcomes of the global best direction investigation	98
6-1	Slice planes location at the end of optimization procedure	101
6-2	One sample after laser cutting process	102
6-3	The laminated tool after brazing process	102
6-4	The CNC machining process	103
6-5	Inside of the cavity and joined layers	104
6-6	The laminated injection mould tool during the operation, with the sensors installed to investigate the cooling channels performance	105
6-7	The final product	106
A-1	The first dialog box in the program	114
A-2	Dialog box to input the multiple direction slicing information	115
A-3	CAD model length and gain value are needed if the slicing direction(s) is found by the program	116
A-4	Optimization parameters input dialog box	116
A-5	The intersection of a slice plane with the actual model	117
A-6	An individual slice built by the program	117

# Chapter 1

## Introduction

### 1.1 Overview

Laminated tooling is a promising technology to create tools with complex shapes. It reduces the manufacturing costs by increasing the production speed. In production of injection mould tools, it enables conformal cooling channels which follow the cavity shape and provide more control on the cooling process. Conformal cooling channels also can be created in different cross-section profiles. This will allow the designer to control the cooling speed at different portions of the tool providing a more uniform cooling process in the part.

Despite the benefits inherent in the laminated tooling technique, it suffers from some disadvantages. One of the most important issues in laminated tooling is surface jaggedness. Since the surface of the tool is divided into various layers, there is always a discrepancy between the actual model and the assembled layers. Therefore, a post-processing step, which is usually a CNC machining, is needed to achieve the desired tolerances. To reduce the amount of CNC post-processing, a reduction in the volume deviation between the assembled slices and the actual model is desirable.

### 1.2 Motivations

Although the volume deviation is reduced if the thicknesses of layers are small, the cost of laser cutting increases. Therefore, in this research an optimization problem is defined to minimize

the surface jaggedness and the number of slices at the same time. Volume deviation, which represents surface jaggedness and the number of slices are the two parameters of the objective function in the optimization procedure.

Thus far, most of the laminated tooling optimization techniques are derived from rapid prototyping (RP), where parts are produced by deposition of material layer by layer. It should be mentioned that in the most rapid prototyping machines, optimized output, which is a set of thicknesses, can be used in the manufacturing process. In laminated tooling however, this is not always true, as only certain thicknesses are commercially available. This is a significant issue that makes the rapid prototyping based algorithms less effective in laminated tooling.

### 1.3 Objectives

The objectives of this thesis are:

**1. Find the optimum arrangement of standard thicknesses which minimizes the surface jaggedness and the number of slices at the same time.**

The slicing process is simulated and the volume deviation between the assembled layers and the actual model is calculated. The result is used in an optimization process to find the best arrangement of the commercially available thicknesses which minimizes the post - processing and the laser cutting costs.

**2. Consider a set of available thicknesses for selecting the sheets used in the laminated tooling process.**

Unlike the rapid prototyping based techniques, here a set of available thicknesses is selected and these are the only thicknesses that can be used in laminated tooling process. Therefore, the optimization procedure is based on these thicknesses.

**3. Slicing direction is considered as one of the important parameters to minimize the surface jaggedness.**

It is desirable to investigate the best slicing direction beforehand, in order to find the direction along which the surface jaggedness is minimized. In the industry, slicing direction usually is selected manually by a well trained technician, while here an analytical method is presented which finds the best slicing direction considering the CAD model surface geometry.



On the other hand, in some occasions, it might be helpful to have more than one slicing direction in the tool to have a better surface quality in final product. The proposed method can also suggest different slicing directions for different portions of the entire CAD model, based on the changes on the surface geometry.

**4. All process steps are followed to make a laminated injection mould and test the conformal cooling channels performance in order to compare with the conventional one.**

The final step in this research is the experimental analysis of the proposed optimization method. An injection mould tool with conventional cooling channels is selected as the test model. A new injection mould with conformal cooling channels is designed. The proposed optimization method is applied to this tool, the optimum arrangement of the thicknesses is found. The tool then is fabricated and tested to compare the performance of conformal and conventional cooling channels.

## **1.4 Thesis Organization**

This thesis is divided into seven chapters and one appendix. The current chapter started with an overview and motivations of this research.

Chapter 2 contains the definitions used in this research. Also, it includes an explanation about the laminated tooling .The literature review is presented in this chapter and finally genetic algorithm is introduced in this chapter..

The proposed optimization method is explained in Chapter 3. Moreover, the slicing process as one of the most important part of the optimization procedure is explained in this chapter.

Chapter 4 starts with the results for the optimization in a single slicing direction. The premature convergence as one of the common problems in the optimization of multi-objective functions is introduced in Chapter 4. Then a new crowding method implemented to prevent the premature convergence is explained. Finally, the optimization process results with and without crowding method application is presented to show the improvement.

Slicing direction as one of the important parameters in volume deviation reduction is studied in Chapter 5. The analytical method presented in this chapter finds the best slicing direction

based on the CAD model surface geometry. Some examples are presented in this chapter to show the performance of the proposed analytical method. The method is also expanded such that it can find different slicing directions based on the geometry of different portions of CAD model surface.

Chapter 6 contains the experimental results of the research. The proposed optimization method is applied to an injection mould tool. A new tool with conformal cooling system based on an injection mould tool with conventional cooling system has been designed and fabricated. The results show the effect of using laminated tools in cooling rate improvement. As it is explained in this chapter, the results also can represent the performance of the proposed optimization method in CNC machining cost reduction, very well.

Finally, Chapter 7 includes the conclusion statement and a list of the publications. For thesis completion, the optimization program is explained in Appendix A. Also a CD-ROM which contains the program is attached to this report.

## Chapter 2

# Literature Review and Background

### 2.1 Introduction

In this chapter, first some definitions that are frequently used in this report are introduced. Then, the laminated tooling method is discussed. The literature review is presented in the next section. Since the optimization procedure in this research is based on genetic algorithms, a brief discussion about these algorithms is provided in the last section of the chapter.

### 2.2 Definitions

#### **Laminated Tool**

Laminated tool is a tool that is created by joining metal sheets. The metal sheets can have the same or different thicknesses.

#### **Slice Plane**

Slice planes are used to create laminations or slices. Each slice is formed by intersecting the slice plane with the tool 3D CAD model.

#### **Thickness Vector**

A thickness vector is a combination of the standard thicknesses that can cover the entire CAD model surface. The ability to cover the entire CAD model surface means the summation of all thicknesses in a thickness vector must be greater or equal to the CAD model length along the slicing direction.

### **Standard Set**

A set of commercially available metal sheet thicknesses that is used in the optimization procedure.

### **Volume Deviation**

Each slice is formed by considering all the features of the two slice planes surrounding it. This is to ensure that the tool can be fully fabricated and there is enough material for CNC machining. This causes an extra volume of material in each slice comparing to the section of the actual model represented by that slice. In general, the volume of the laminated tool created by assembling all individual slices is greater than the actual model's. This difference is called volume deviation. To reduce the post processing cost, this volume deviation must be minimized.

### **Number of Slices**

It represents the number of metal sheets that is used to cover the entire CAD model surface. Since each individual layer is cut by a cutting machine, less number of slices means less profile cutting costs. Therefore the number of slices is used as another optimization parameter.

### **Conventional Cooling Channel**

As depicted in Figure 2-1, a conventional cooling channel is created traditionally by straight drilling in the tool. Due to manufacturing limitations, this kind of cooling channels can not follow the cavity.

### **Conformal Cooling Channel**

Figure 2-2 introduces a conformal cooling channel. A conformal cooling channel follows the shape of the tool's cavity. Moreover, it can have different cross section profiles. These characteristics provide more control on the cooling rate.

## **2.3 Introduction to Laminated Tooling**

Laminated tooling, as a manufacturing method, uses Computer Aided Design (CAD) to produce tools. This technology involves designing a tool using 3D CAD software, slicing the model into cross sections, cutting off the 2D profiles for each slice, bonding the sheets together and finally machining the near net surface into a finished product.

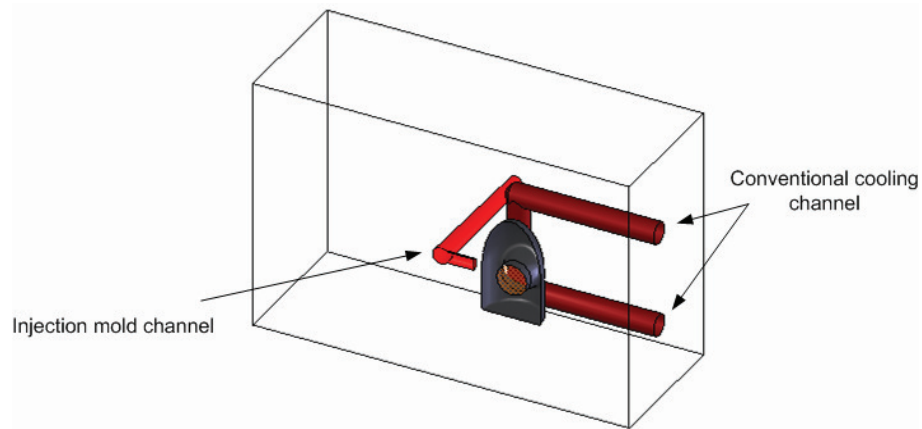


Figure 2-1: A tool with conventional cooling channel

Laminated dies can be used in hydroforming or injection moulds. In hydroforming tools, the die surface should be smooth to allow the tube to form into a desired shape. In injection molding the material must be cooled during processing. The uniformity of the cooling directly affects the quality of the final product.

The conventional cooling channels shown in Figure 2-1 are created by drilling through the entire tool. As depicted, some portions of the cooling system which are farther away from the cavity result in non-uniform cooling rate with undesirable effects on the part's physical properties.

Figure 2-2 represents a conformal cooling channel that follows the cavity. The use of conformal cooling channels allows fast and uniform heat removal from the die, and thus contributes to reducing the cycle time, accumulation of internal stresses and part distortion.

The process steps of laminated tooling, depicted in Figure 2-3, are as follows:

### **Solid Modeling**

The first step in laminated tooling is making a CAD model of the tool. Here all the CAD models are created in SolidWorks<sup>®</sup>. It is not only a powerful CAD software, but also compatible with VisualBasic that is used for optimization programming. SolidWorks<sup>®</sup> also has Application Programming Interface (API) functions that are powerful tools for slicing process simulation.

### **Slicing Data Gathering**

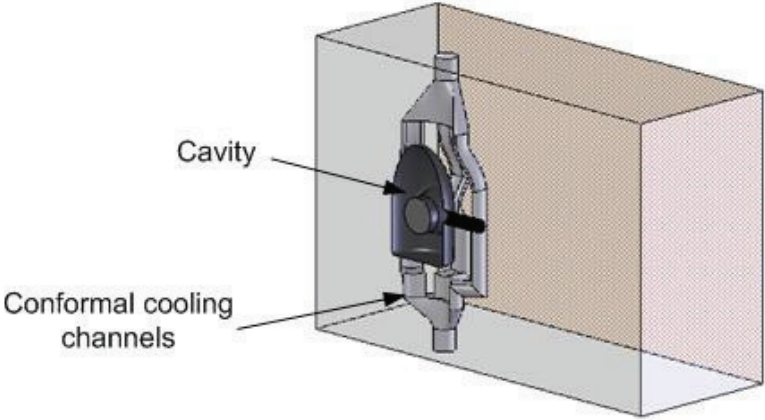


Figure 2-2: An illustration of a conformal cooling system

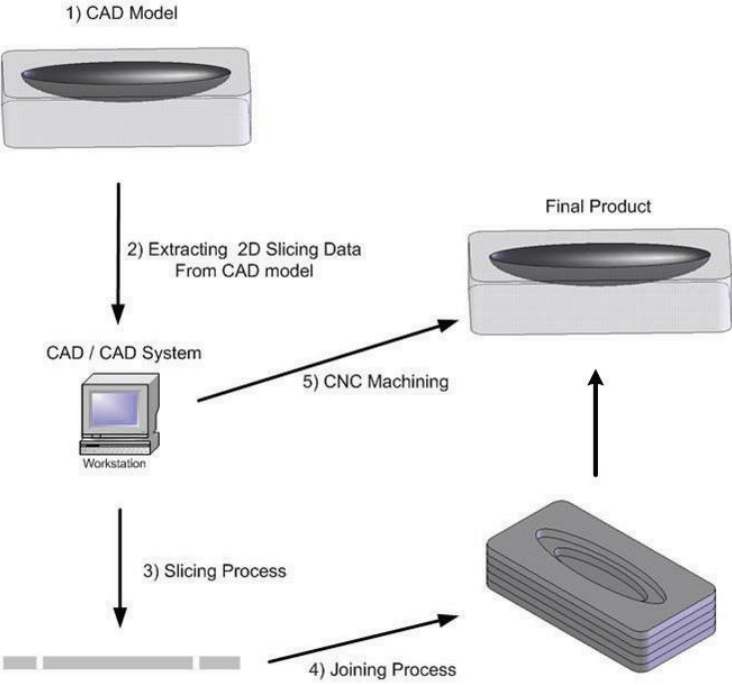


Figure 2-3: Schematic of laminated tooling process steps

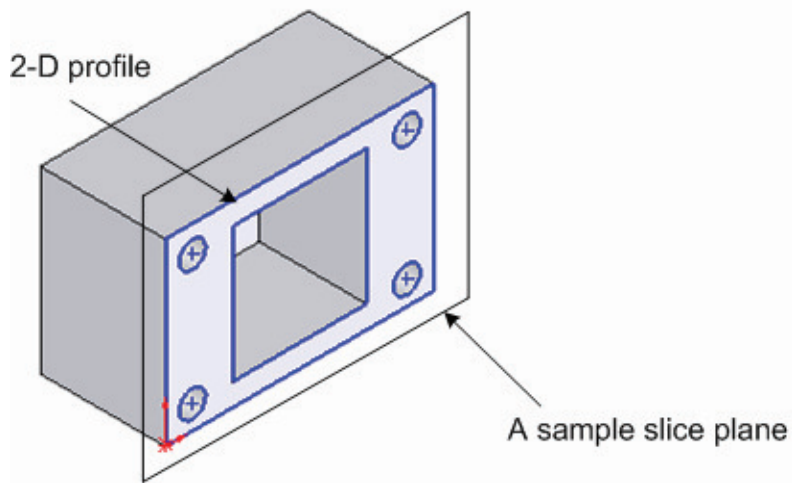


Figure 2-4: 2-D profile created by intersecting a 3-D CAD model by a sample slice plane

Both CAD model and slice planes information is used to create the data for the slicing process. These are the information of 2D profiles coming from the intersection between the 3D CAD model and slice planes. Figure 2-4 illustrates one of these 2D profiles in a sample model.

### **Laser Cutting**

The slices are then cut using techniques such as laser cut, Abrasive Water Jet (AWJ) [1], plasma cutting or wire electro discharge machining [2]. However, a 2D laser cutting machine is employed for cutting process in this research.

### **Joining**

After cutting the 2D profile corresponds to each sheet, the sheets need to be assembled. There are several joining methods and some of them are explained in the literature review section. In this work, brazing is used for joining.

### **CNC Machining**

The assembled slices will undergo a CNC machining process to bring the near net shape to the desired tolerances.

One of the challenging issues in laminated tool manufacturing is reducing the CNC machining costs. This means minimizing the surface jaggedness in the laminated tool before CNC post processing, as illustrated in Figure 2-5. The extra material needs to be minimized in assembled slices in order to have less CNC machining costs.

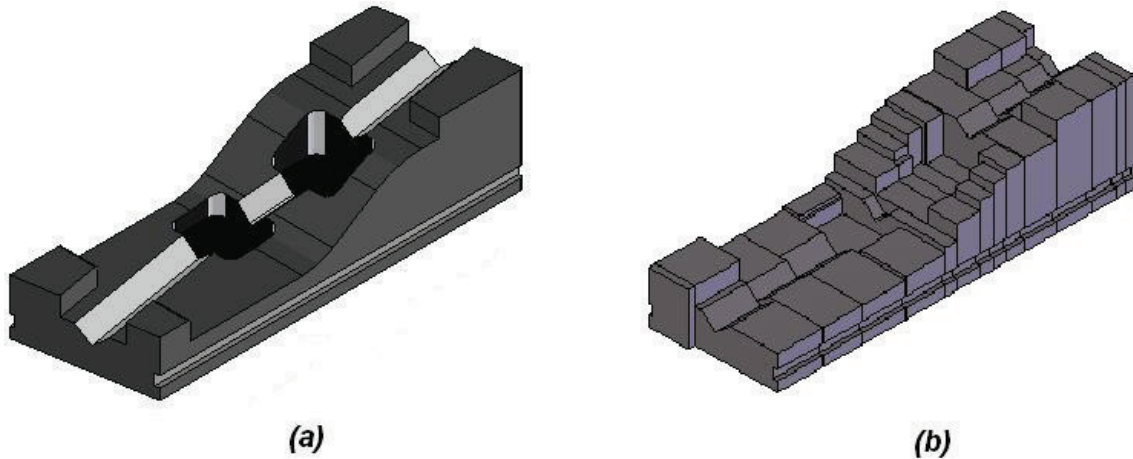


Figure 2-5: Volume deviation between (a) actual CAD model, and (b) laminated tool

## 2.4 Laminated Tooling in Literature

One of the first works on laminated tooling, was reported by Nakagawa et al. [3], [4]. He introduced laminated tooling process steps and showed how the sheets can be cut by laser, and stacked in an adhesive bonding process. Then at the beginning of the 1990s, Dickens [5] introduced the potential problems that can occur while clamping the sheets. He was also the first to introduce the idea of changing the slice thicknesses and slicing direction in order to achieve a better surface quality. However he considered the same thickness for all slices and limited the slicing directions to only vertical and horizontal.

Kulkarni and Dutta [6] investigated the sources of surface inaccuracy in layered manufacturing. This inaccuracy comes from the approximation of the actual CAD model surface in each slice with a first degree profile. Dolenk et al.[7] and Hope et al. [8] introduced the cusp height and stair case effect concepts to predict the amount of surface roughness of the final product in rapid prototyping. Smith and Farouki [9], [10] performed a CAD model surface study based on the surface normal vectors, which can be used to find the optimum slicing direction in laminated tooling process. Lee and Choi [11] introduced a new adaptive slicing method based on the 2D contours in the intersection of slice plane and CAD model. Majhi et al. [12] considered the slicing optimization to improve the surface quality and minimize the volume of support structure. Cormier et al. [13] considered variable cusp height based on the geometry of CAD



model to have a smoother surface at the end of an adaptive slicing. Haipeng and Tianrui [14] and Dai et al. [15] proposed a stereolithography based optimization method to improve the surface accuracy rapid prototyping and computer graphics, respectively.

Renner [16] was one of the first researchers who considered genetic algorithm to solve some optimization problems in CAD/CAM.

In Kumar and Choudhury's [17], each 2D contour is approximated based on the cutter linear motion. As it is shown in Figure 2-6, a cusp volume quantity is defined for each patch as the volume enclosed between the actual CAD model surface and a four-sided patch. By keeping this cusp volume within a specified user-defined tolerance, the thickness of the layer is found. Since this technique is based on the CAD model, the result is a thickness for each layer that can vary from one layer to the next. This method of slicing is called adaptive slicing in contrast with the uniform slicing, which assumes the same thickness for all slices. Adaptive slicing improves the surface quality by considering variable slice thicknesses. While Zhao and Laperriere's [18] research is similar to Kumar and Choudhury's [17], they considered an area deviation between two consecutive slices. The area deviation should be less than or equal to a user-defined value. The geometry of a CAD model surface between two consecutive slices is missing in their study, as they only consider the shape of a CAD model surface where slices are located.

Beside the CNC machining, Himmer et.al [19] considered multiple laser processing such as laser cutting, laser welding, and direct laser metal deposition to increase the surface quality. They considered a uniform thickness for all the slices. There is no investigation on finding an optimum thickness in their research. As they mentioned, "the layer thickness must be determined before", and is selected based on two parameters: sheet metal tolerances that are available and also shrinkage of adhesive material during the joining process. Both of these parameters have a direct impact on the slicing process as well as the final product shape. The authors in [19] suggested some laser processing to increase the surface quality. It is however more desirable if the same accuracy can be achieved with lesser need to high tech manufacturing processes.

One of the main advantages of laminated tooling is the ability of creating conformal cooling systems. Gibbons et al. [20] studied the manufacturing process in laminated tooling and the effect of conformal cooling system on increasing the cooling performance of the tool. They

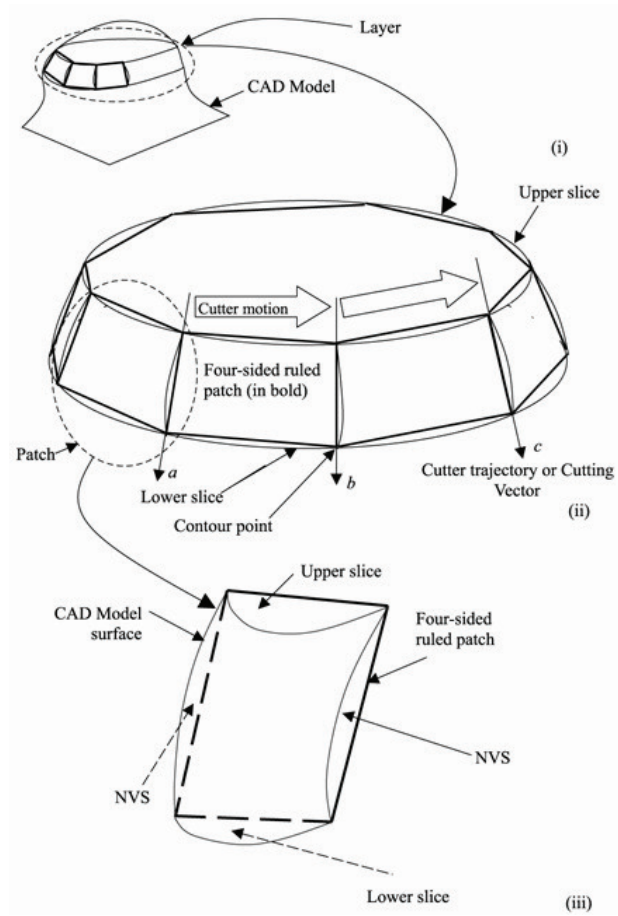


Figure 2-6: Volume patches [17]

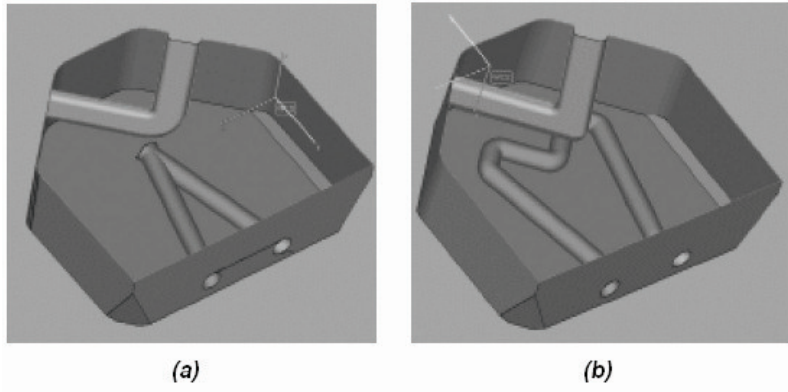


Figure 2-7: conventional (a) and conformal (b) cooling channels employed on performance evaluation in [20]

considered angled laser cutting to reduce the cost of CNC machining.

Their research is focused on die casting tools and they considered only two vertical and horizontal slicing directions. Also there is no surface analysis to find out either vertical or horizontal slicing in more suitable for a portion of CAD model. However they did a reliable investigation on the performance of conformal cooling system in a die cast tool created by laminated tooling. They compared the results with the same tool manufactured by traditional method. Outcomes showed higher performance of the cooling system of the tool fabricated by laminated tooling technique. Figure 2-7 shows the conformal and conventional models they considered for cooling channels performance evaluation. They considered oblique laser cutting by a 3D laser machine to reach a better surface quality at the end. Since 2D laser cutting machine is more available than a 3D machine, some researchers studied the manufacturing optimization of laminated dies based on using 2D laser cutting machine. However, the methodology to optimize the volume deviation and the number of slices is independent from the type of cutting machine which is used.

In addition to adaptive slicing, direction of slicing is another parameter that can be considered for surface quality improvement. Figure 2-8 illustrates the effect of slicing direction on the volume deviation in a simple case. As depicted in this figure, choosing the right slicing direction could even eliminate the surface jaggedness. Moreover, it should be mentioned that in some cases, having different slicing directions for an individual part can reduce the manufacturing

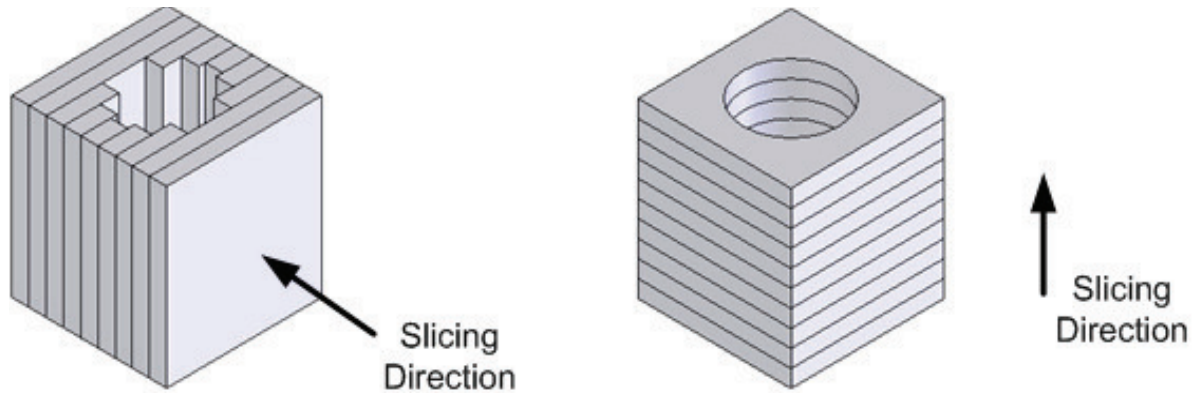


Figure 2-8: The importance of an optimized slicing direction

complexity as well as volume deviation.

Hur and Lee [21] investigated the effect of build-up orientation on product surface accuracy in rapid tooling, focusing on the stereolithography method. In their research, the proposed method is based on trial and error and no systematic method is suggested to find an optimum orientation. Therefore, there is a possibility that a better direction will be overlooked or missed while the program tries to find the best direction among the preferred candidates.

Paul et al. [22] investigated the sources of surface roughness in the laminated object manufacturing (LOM). They considered the orientation angle and the slice thickness as the control parameters on surface quality. Although results showed their model was not sufficiently accurate at surface roughness prediction for thick slices in large orientation angles, it can nevertheless provide reliable results on smaller thicknesses and orientation angles.

Himmer et al. [19] considered different directions based on surface topology, developing software that can choose slice direction. Their results show that they are limited to vertical and horizontal directions.

Gibbons et al. [20] investigated the effect of direction in die performance. Their research is focused on die casting tools, and they considered only two vertical and horizontal slicing directions. Also, there is no surface analysis to discover more suitable slicing orientation for a portion of the CAD model.

Another research was coordinated by Massod and co-workers [23], [24]. They suggested the

best deposition orientation in layered manufacturing can be ascertained by finding the direction in which the difference in volume between the CAD model and the LM part is minimal. The best direction is then selected as the direction which produces minimal volume difference. Their approach is based on assuming some pre-defined candidate directions. The number of directions that can be tested is limited. Consequently there is always a chance of missing a potentially good slicing direction just because it is not selected as one of the candidate directions by the user. On the other hand, since volume deviation has to be found for each candidate direction, the number of candidate directions is limited due to the time needed for the volume deviation calculation.

On the other hand, joining the layers of sheets is another important procedure in laminated tooling. In some cases such as the one explained in [3], there might be liquid seepage into the cavity or vice versa during operation. Bryden et al. [25] showed that brazing is more reliable as a joining process than other bonding techniques, since it is effective in any range of operation temperatures. Brazing, as a type of welding process, is widely used in industry to produce an assembled product from two or more individual components. In the brazing process, a filler metal in the form of foil, plating, wire, paste or powder, with a melting point of above 450° C and below the molten temperature of base metal, is melted and distributed between the facing surfaces of the individual components to join them following solidification.

Brazing produces less thermal distortion than fusion welding as the individual parts are uniformly heated to the brazing temperature. Some additional advantages of the use of brazing, rather than conventional welding processes, include: the economical fabrication of complicated assemblies, capability of joining large parts in a stress free condition, superior heat transfer properties, the possibility of joining metals of a wide range of thicknesses, the preservation of special metallurgical properties of the base metals, and the feasibility of producing joints with high precision in tolerances [26].

The leakage problems and also the stacked-layers bonding problem, pushed researchers to try other techniques such as *profile edge lamination* (PEL) for stacking the layers.

In the profile edge lamination (PEL) technique, first proposed by Walczyk and Hardt in 1994 [27], the laminations, are then oriented in a vertical plane and clamped together in a frame. Figure 2-9 represents a sample PEL tool. In fact in reality the edge of the laminas

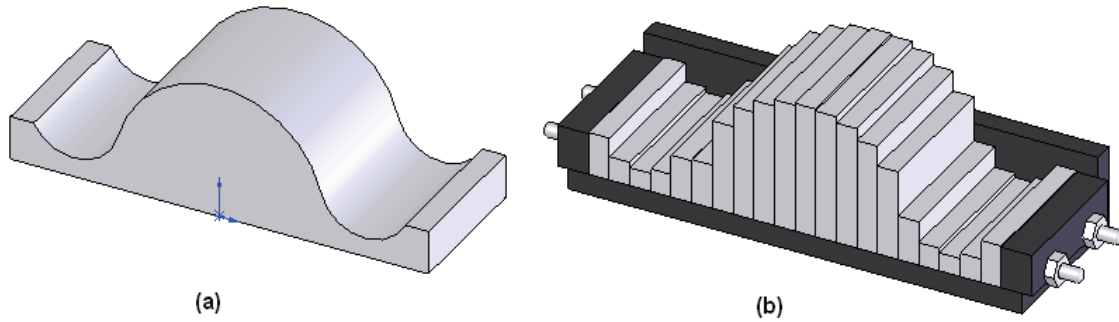


Figure 2-9: a) a sample tool, b) the same tool created in PEL method

in Figure 2-9(b) should be profiled to follow the actual tool geometry in Figure 2-9(a), more closely; whereas here to have a better preview of a PEL tool the difference between assembled slices and the actual model is exaggerated. In general, this kind of tool is ideally suited for sheet metal tools that require re-configuration. This is due to the fact that there is no bonding process, and all the sheets are clamped together by bolts along the entire length of the tool.

In 2005 and 2007, Yoo and Walczyk [1], [28] developed a CAD-based PEL tooling system, along with a cutting trajectory algorithm for fabricating PEL tools with a five-axis CNC AWJ cutting machine. It was based on extracting a 2D profile for each lamina from the SolidWorks® CAD model of the PEL tool. In this method, the model is sliced at predefined cutting planes. The information about the resulting intersection curves is obtained by using a SolidWorks® Application Programming Interface (API) function. These intersection curves are then used in both the adaptive slicing and cutting trajectory algorithms, specifically developed for cutting PELs. Figure 2-10 displays a 2D profile which is created by intersecting a sample CAD model with a slice plane.

## 2.5 Overview of Genetic Algorithms

Since the optimization process in this research is based on genetic algorithms (GAs), the fundamentals of GAs are established in the following sections.

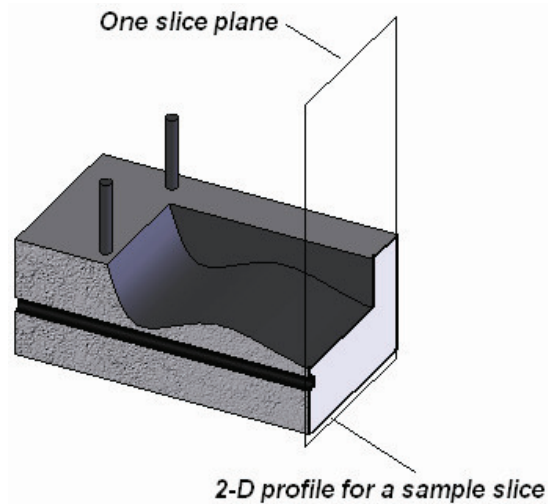


Figure 2-10: 2D profile created by intersecting a 3-D CAD model by a cutting slice plane

### 2.5.1 What are Genetic Algorithms?

Traditional optimization algorithms are prone to inherent difficulties; some of them such as gradient-based methods not only need the derivative or partial derivatives of the objective function, but also do not guarantee a global optimum. Since traditional algorithms become stuck at a local optimum most of the times, some specific cooperative methods are required to jump from a local optimum to seek a global optimum. Another weakness is that traditional methods can be applied only in well defined systems with simple objective functions.

*Evolutionary computing* can offer new approaches to optimization as alternatives to traditional single point methods [29]. Evolutionary computing is effective on problems with complex or not completely defined objective functions; Such computing is based on biological evolution, where different methods have been developed by different scientists over the last 40 years. *Evolutionary strategies* have been developed in Germany by I. Rechenberg and H.P. Schwefel. *Evolutionary programming*, has been developed by L.J.Fogel ,A.J. Owens, and M.J. Walsh in America; and finally, genetic algorithm has been reported by J. H. Holland in America in the 1970s.

Genetic algorithms (G.A.) type of evolutionary computing, are used to find the exact or at least, the approximate *global* solution for an optimization problem. A G.A. is based on the

Darwinian theory of natural selection, where in a population, some individuals with specific characteristics have a greater chance of surviving than others; therefore, if the best characteristics of the parents can be transferred to the next generation, the possibility of survival for that specific population is increased. However, chance is always a factor and even the fittest can die in an "unlucky circumstances" [29].

### 2.5.2 Fundamentals of Genetic Algorithms

GAs are introduced as computer iterative algorithms, based on a random set of solution candidates. This random set prepares a solution for the optimization problem, and the task of a GA is to arrive at the best solution by reproducing the best or *fittest* members, and ignoring the weak members of the set.

There are two different kinds of Genetic Algorithms, *binary coded* and *real coded*, however the methodology is almost the same for both. In the binary coded GAs, each member of the solution set is converted to a binary number. For example, to find the maximum value of a function such as:

$$f = \frac{1}{x^2 + 2}. \quad (2.1)$$

In a specific interval of real numbers between 0 and 120, the possible solutions are all the real numbers between 0 and 120. In this simple example, the maximum digit of these binary numbers is 7 which means all the integer numbers in this interval can be represented by a seven digit binary number. It should be mentioned that there is a formula in the literature to find the maximum number of binary digits to represent all the possible solutions as binary numbers [29].

In real coded GAs there is no need to convert the possible solutions to binary numbers. In this approach, all the possible solutions are directly represented as vectors of real parameters. Consequently, the set of possible solutions in this case is

$$\{x|x \in \mathfrak{R} \ \& \ x \in [0, 120]\}. \quad (2.2)$$

Typically, a real coded GA is more suitable and convenient for most practical engineering



applications.

### **Chromosomes, Genes, Alleles, and Fitness**

In biology, a *chromosome* is defined as an organized structure in the DNA which transfers the characteristics of the parents to the next generation. In GAs, a chromosome represents a possible solution to optimization problem. For instance, in the optimization problem, presented by 2.1, an encoded possible solution such as [0001010] which represents integer number "8" is defined as a chromosome.

Each chromosome includes some elements which determine the characteristics of that chromosome. As in biology, these elements are called *genes*, and any of the alternative forms of a gene that can occur at a given locus are called *allele*. As a result, in a chromosome such as [0001010], each binary element is a gene. The values that each gene can take, which is 0 or 1 in the binary coded GA, are alleles.

The chance for a specific chromosome to be reproduced in the next generation depends on the *fitness value*. It is a quantity which shows how the optimization result based on this specific solution, is close to the ideal solution. Consequently, the higher the fitness value for a specific chromosome, the greater the chance for the solution to be reproduced in the next generation. All the solutions which have produced better results for the optimization problem converge to establish the final solution. This convergence depends on the existence of a possible solution, and the application of two GA operators. In other words, in many applications, despite the existence of an optimization solution, the algorithm can not converge to the global solution, since these two operators are not used appropriately. They will be introduced in the following after the GAs are further investigated.

### **Population**

GAs work on a population of solutions. In an optimization problem, where finding the optimum of an objective function in a specific interval is desirable, the first step is produce a set of possible solutions, called the *initial population*. The size of the initial population and how it is created directly affects the accuracy of final solution. Typically, the initial population consists of a random choice of possible solutions.

## Relative Fitness

In biology, the *relative fitness* represents the capability of an individual, in comparison with other individuals, to be reproduced in offspring. In GAs, it is a particular number for each member of the population which shows how close a specific possible solution is to the final solution in comparison with other members of the population. Therefore, to find this quantity for each chromosome, the value of the objective function  $f$  for that specific chromosome needs to be determined ( $f_i$ ). To find how this specific member is close to the solution among other members of the population, the relative fitness is represented as

$$(\text{RelativeFitness})_i = \frac{f_i}{\sum f_i}. \quad (2.3)$$

where  $\sum f_i$  represents the summation of the fitness values of all the individuals in the population. In the next section, how the relative fitness affects the possibility of reproducing a specific individual is assessed.

## Generation and Reproduction

As mentioned in Section A.3, a GA is an iterative procedure that by repeatedly applying genetic operators should reach the solution of the optimization problem. During this process, which starts with a randomly selected population, a new population is created after each iteration. Each population is called a *generation*. Hence, the number of iterations is the same as the number of generations.

The series of actions carried out to produce a new generation is called *reproduction*. This process starts with finding the fitness values for all the individuals in an initial randomly selected population. After the relative fitness values are found, as described in previous section, the fitter individuals can be chosen and the weaker ones ignored in order to generate the new generation. It is evident that this new set of solution must have the same number of members as the previous generation. Consequently, in this new set, for each weak element of the population which has been ignored, one of its members that has a higher value of relative fitness is replaced. As it is shown in Figure 2-11 at the end of the reproduction process, the new generation has the same number of possible solutions as the old one. A *selection* process must be conducted to

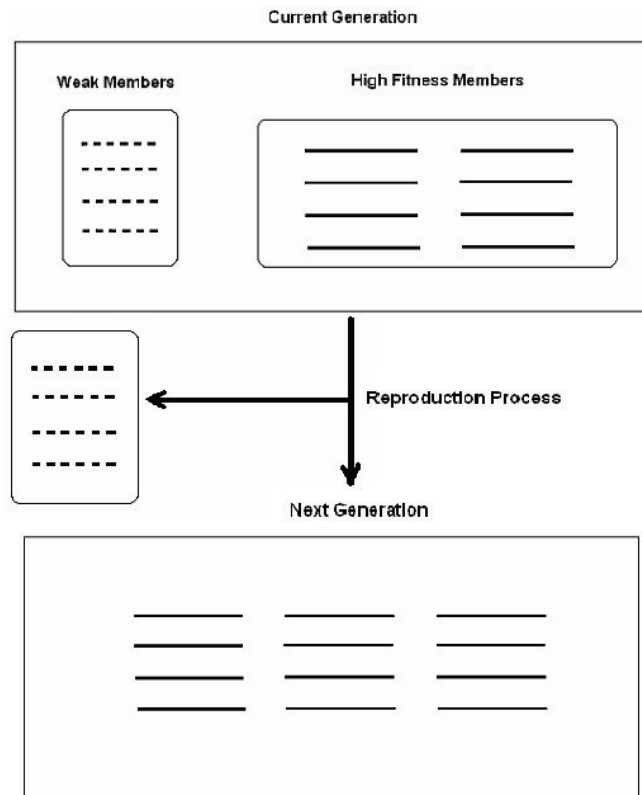


Figure 2-11: Schematic representation of reproduction process in genetic algorithm

determine which members can not exist in the next generation and which members not only exist in the new generation but also may be selected for one or more times of repetition.

## Selection

*Selection* is a genetic operator that chooses chromosomes from the current generation to create the next generation. Here are some of the most commonly used selection methods that exist in the GA tool box.

**Roulette Wheel Selection** This method is based on the positive values for relative fitness values, therefore scaling would be necessary sometimes. In the roulette wheel selection method,

Table 2.1: Results for the first randomly selected population

<u>Chromosomes</u>	<u>Decimal Value</u>	<u>Binary encoded</u>	<u>Fitness</u>	<u>Relative Fitness</u>
1	5	0000101	0.0385	0.82
2	12	0001100	0.0069	0.147
3	28	0011100	0.0013	0.027
4	75	1001011	0.00018	0.004
5	115	1110011	0.00008	0.0017

first a random number  $a \in [0, 1]$  is selected. Then by comparing all the relative fitness values with this number, based on the order of the chromosome in the population, if  $a < F_1$ , where  $F_1$  is the relative fitness of the first chromosome, this chromosome is selected; otherwise,  $i^{th}$  chromosome is selected such that

$$\sum_{j=1}^{i-1} F_j < a \leq \sum_{j=1}^i F_j. \quad (2.4)$$

This is the first chromosome in the next generation. Since  $M$  chromosomes are needed, where  $M$  is the size of population, the roulette wheel process is repeated  $M$  times, and each time, with a new randomly selected  $a$ . At the end, a new population, based on the fitter chromosomes is generated. In the simple example in section A.3, assume that the first generation is

$$\{5, 12, 28, 75, 115\}. \quad (2.5)$$

(in reality a longer population is preferred since more possible solutions are considered at the beginning, resulting in a better chance to find the global solution accurately)

Table 2.1 reflects that since in the first round of selection,  $a = 0.95$  is selected randomly, and  $0.82 < a < 0.82 + 0.147 = 0.967$ , the first member of the next generation is 12 which represented by [0001100]; in the next round,  $a = 0.23$  and since  $a < 0.82$ , the next selected chromosome is [0000101]. By following the same procedure, the next population is

$$\{[0001100], [0000101], [0000101], [0000101], [0001100]\} \quad (2.6)$$

Therefore, in the next population the previous population members that have the last three smallest relative fitness values do not exist.

It should be mentioned that the population set created by the selection process is not the final next generation. There are two pivotal genetic algorithm operators that should be applied on this set to generate the final next generation. These two operators are discussed in the following sections.

The other selection methods are as follows [30].

**Tournament Selection** In this method, first,  $N$  individuals are selected, and then the one that has the best relative fitness among them is selected for the next generation; this process is repeated  $M$  times, where  $M$  is the size of the population.

**Truncation Selection** With this method, all the individuals are ordered according to their relative fitness values. Then, a randomly chosen portion  $p$  (e.g,  $p = \frac{1}{2}$  or  $p = \frac{1}{3}$ ) of the fittest ones are selected, and by repeating  $p$  times, the next generation population is created.

**Linear Ranking Selection** In this method, the weakest individual is assigned by 1 and the fittest one by  $N$ . Then based on the rank of each individual and a selection equation, the selection probability is linearly assigned to each individual.

**Exponential Ranking Selection** The only difference between this method and the previous one is exponentially weighted probabilities for the individuals.

Once the new population is generated, the next two important operators of GAs will be applied to create the next generation.

## Crossover

*Crossover* is the principal operator in GAs. It gives this chance to the offspring to gather the characteristics of both parents. After the best individuals are selected for the next population, the crossover operator acts on two parents (e.g, chromosomes  $i$  and  $j$  of the new population) to produce two children based on the characteristics of both parents. The number of chromosomes that are involved in the crossover process are determines by a real number between 0 and 1 which is called the *crossover rate*. For example with a crossover rate of 0.6 and a population size of 100, 60 chromosomes are selected for the crossover. As a result, the crossover process

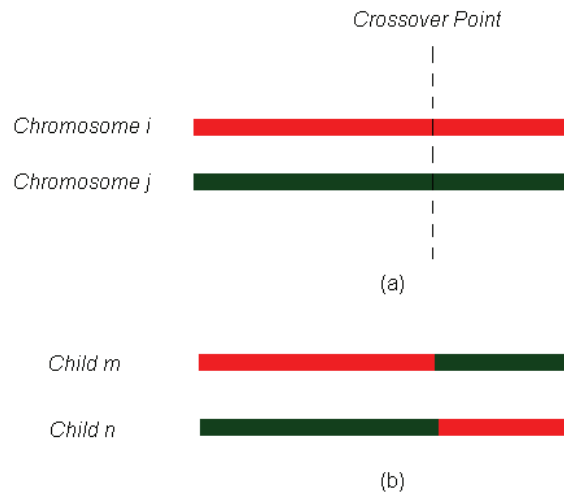


Figure 2-12: Single point crossover: (a) randomly chosen crossover point on the parents' chromosomes, and (b) two new chromosomes

is repeated 30 times, each time on two different parents to produce two different children. The crossover rate is usually chosen around 0.6, but can vary depending on the nature of the problem.

In the following, some of more practical crossover techniques are discussed.

**Single Point Crossover** In this method, one randomly selected location on both chromosomes is selected as the crossover point. All the data (genes) beyond this point are switched between the two parental chromosomes to create two children Figure 2-12.

**Double Point Crossover** Two points on parental chromosomes are selected as crossover points, and the data between these two points are exchanged between the parents; Figure 2-13 illustrates this kind of the crossover.

**Cut and Splice Method** In this method, each parent string chooses its own crossover point. As a matter of fact, as it is shown in Figure 2-14, the results are two children with different sizes of data.

In the following, the other GA operator that has a significant effect in this optimization

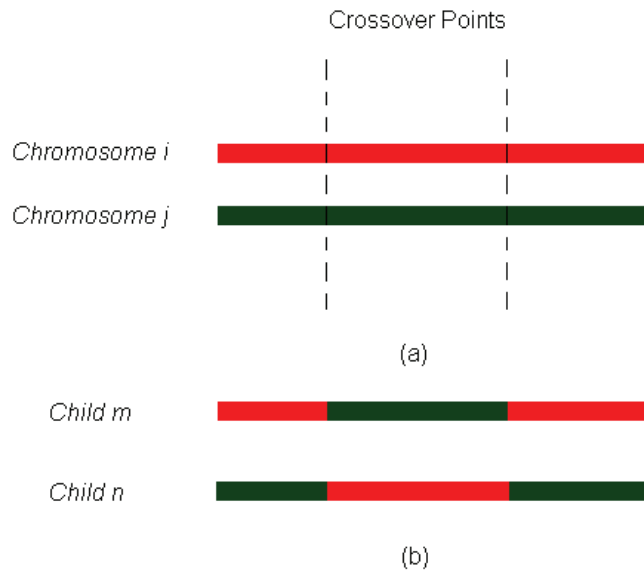


Figure 2-13: Double point crossover: (a) randomly chosen crossover points on the parents' chromosomes, and (b) two new chromosomes

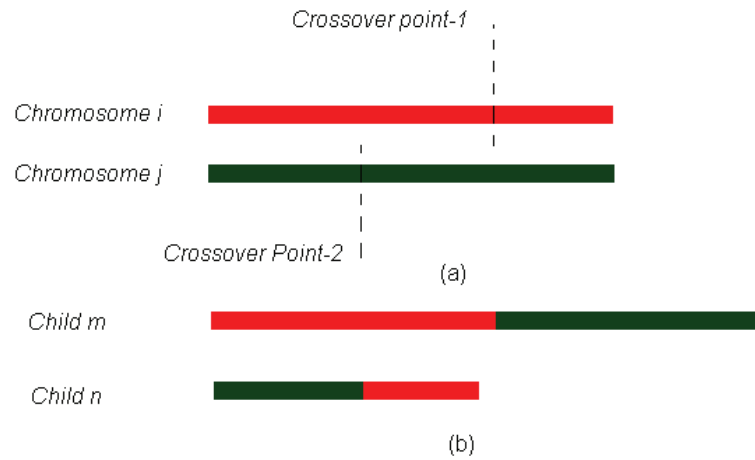


Figure 2-14: Cut and splice crossover: (a) randomly chosen two different crossover points on parents' chromosomes, and (b) two new chromosomes with different size of data

method is introduced.

## Mutation

*Mutation* has a perturbation effect on a randomly chosen chromosome. It produces a child chromosome with new characteristics that did not exist in the parent chromosomes. It helps the GAs to avoid a local optimum in order to approach a global optimum. The same as crossover, the mutation is not applied to all the members of the population. The mutation rate varies based on the optimization problem and it is usually around 4% of the entire population.

Mutation is carried out by different methods, including the two most commonly used ones which are presented in the following.

**Flip Bit Mutation** In this method, which is used for binary coded GAs, a chromosome is chosen randomly. Between genes inside that chromosome, the allele of one randomly selected gene flips from 0 to 1, or vice versa. For example, if the chromosome [1001101110110] with 13 genes is one of the members of the population, a randomly selected number between 1 to 13, say 7, introduces the genes selected for mutation. Since the allele for that gene is currently 1, becomes 0 during the mutation process. Hence, the new chromosome is [1001100110110].

**Internal Mutation** The previous method can not be used for real coded GAs; however, *internal mutation* allows the application of mutation in real coded GAs, and in this research, this type of mutation has the best results. Here, in a randomly chosen chromosome, two different genes are selected randomly and the alleles of these two genes are switched during the mutation process. Consider a sample chromosome such as {5, 24, 12, 32, 84, 105, 7}. Since the size of the chromosome is 7, by randomly selecting two integer numbers between 1 and 7, if the numbers 2 and 6 are selected, the new chromosome is {5, 105, 12, 32, 84, 24, 7}.

## Termination Criteria

The last concept that is introduced is the termination criterion. After the GAs begin, it is necessary to know when the algorithm should stop. Different criteria for termination GAs process are listed below.



**Generation Number** The algorithm stops when user-defined maximum number of iterations is reached.

**Evolution Time** The algorithm ceases when it exceeds a user-defined maximum computing time.

**Fitness Threshold** The algorithm terminates, when the maximum fitness is greater than the user-defined maximum fitness.

**Maximum Fitness Convergence** The algorithm stops when in the user-defined times of iterations, the changes in maximum fitness values are less than a user-defined value.

Although there are some other termination criteria in the literature, the most commonly used ones were introduced in this section.

### 2.5.3 Example

In the following section, an example is presented to explain how GAs is used in some real optimization problems. However, this example is still more mathematical than practical.

#### Example [29]

Solve the optimization problem for the function,

$$f(x) = 20 + 100 \cos(4\pi x) \exp(-2x) \quad , \quad (2.7)$$

inside the interval  $[0, 1.5]$  with the precision of three decimals.

#### Solution

The crossover and mutation rates for this problem are chosen as 0.8 and 0.1, respectively. The population is assumed to have 10 chromosomes.

There is a formula to find the maximum digits for binary coded values [29]. It states that if the required precision is given by  $\gamma$ , then the maximum number of digits in the binaries is the smallest amount of  $n$  which satisfies

$$(\beta - \alpha)10^\gamma \leq 2^n \quad , \quad (2.8)$$

Table 2.2: Example1 - Results for the first randomly selected population

<u>Order of Chromosomes</u>	<u>Decimal Value</u>	<u>Binary Encoding</u>	<u>Fitness</u>	<u>Relative Fitness</u>
1	0.933	10011111011	29.778	0.1348
2	1.496	11111111010	27.497	0.1245
3	0.776	10000100100	4.490	0.0203
4	1.486	11111101100	27.492	0.1245
5	0.340	00111010000	12.668	0.0573
6	0.597	01100101111	26.188	0.1186
7	1.045	10110010010	30.919	0.1400
8	0.097	00010000101	22.721	0.1029
9	1.122	10111111011	20.466	0.0927
10	0.631	01101011101	18.672	0.0845

Table 2.3: Example1 - Selection results for the first generation

<u>Order of Chromosomes</u>	<u>Decimal Value</u>	<u>Binary Encoding</u>	<u>Fitness</u>	<u>Relative Fitness</u>
1	0.097	00010000101	22.721	0.089
2	1.486	11111101100	27.492	0.108
3	1.486	11111101100	27.492	0.108
4	0.631	01101011101	18.672	0.074
5	1.045	10110010010	30.919	0.122
6	0.340	00111010000	12.668	0.050
7	0.933	10011111011	29.778	0.118
8	0.097	00010000101	22.721	0.089
9	1.045	10110010010	30.919	0.122
10	0.933	10011111011	29.778	0.118

where  $\alpha$  and  $\beta$  are the lower and upper bounds of the solution interval, respectively. Since, in this example,  $\alpha = 0$  and  $\beta = 1.5$ , from Equation 2.8,  $n = 11$ .

The first population is selected randomly from the real numbers inside the interval, and Table 2.2 lists the results for this first possible solution.

To select the next generation, the roulette wheel method is used. Since the first amount of  $a$  is 0.8113, the eighth chromosome is selected for the next generation; by the iterative process, the other members of the next generation are selected as presented in Table 2.3.

By comparing Table 2.3 with Table 2.2, it can be seen that the third chromosome in the first population, which has a low relative fitness, is ignored in the new population. Now it is time to apply the crossover operator to this population. Since the crossover rate is 0.8, four pairs of chromosomes are selected to apply the crossover operator on them. If the first pair is selected

Table 2.4: Example1 - final next generation

<u>Order of Chromosomes</u>	<u>Decimal Value</u>	<u>Binary Encoding</u>	<u>Fitness</u>	<u>Relative Fitness</u>
1	0.097	00010011011	22.721	0.089
2	1.486	11111100101	27.492	0.108
3	1.486	11111101101	27.492	0.108
4	0.631	01101011100	18.672	0.074
5	1.045	10110010000	30.919	0.122
6	0.340	00111010010	12.668	0.050
7	0.933	10011111011	29.778	0.118
8	0.097	00010001100	22.721	0.089
9	1.045	10110010010	30.919	0.122
10	0.933	10011100101	29.778	0.118

as the first and the last chromosomes and the crossover location (a single point crossover is used) is randomly chosen as 5, then the new pair of chromosomes, based on these two parents, are:

[00010011011] and [10011100101]

By comparing these two chromosomes with the first and the tenth chromosomes in Table 2.3, it can be seen that two different chromosomes are generated. By repeating the same process on three other randomly selected pairs of chromosomes, the crossover is completed. As the last step, the mutation operator is applied to the system. After all, the next generation population is the same as that in Table 2.4

Figure 2-15 portrays the distribution of the first randomly selected population. In Figure 2-16, after 20 iterations, the system converges to the global maximum, but two chromosomes that are representing other points in solution area still remain.

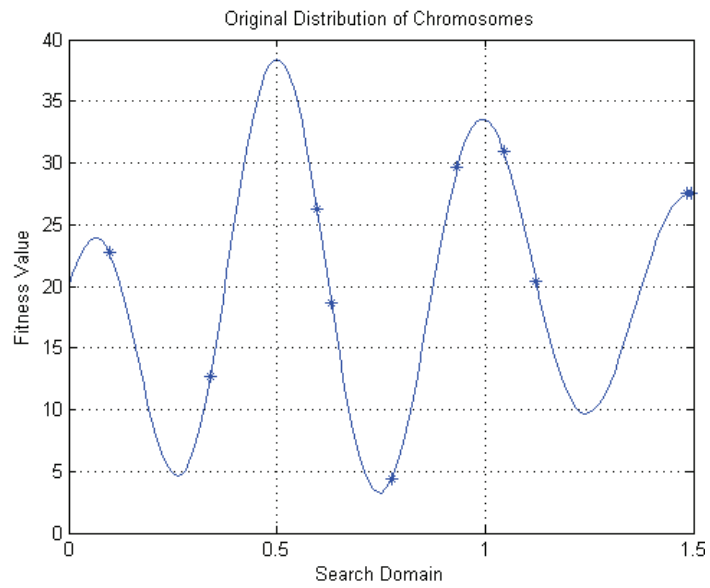


Figure 2-15: Original distribution of 10 randomly selected initial data

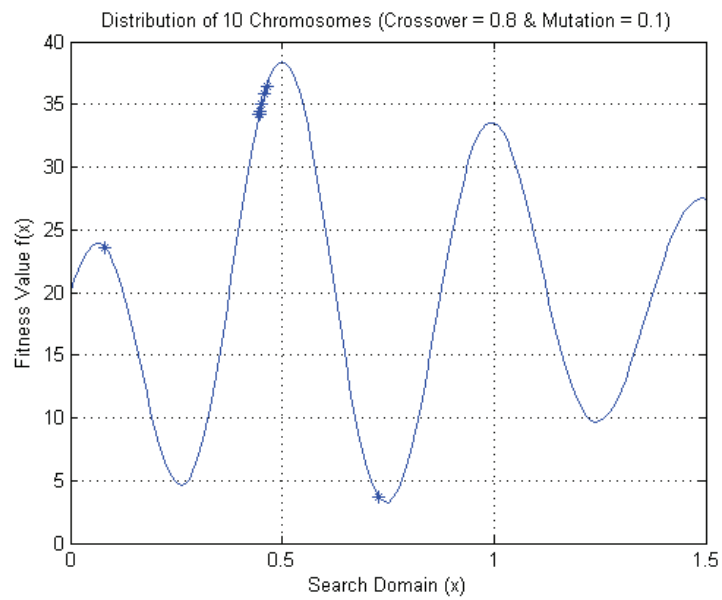


Figure 2-16: Final result after 20 iterations

## Chapter 3

# Optimization of Laminated Dies

### 3.1 Introduction

Since the slicing procedure is a crucial step in all laminated tooling and rapid prototyping methods, this chapter starts with the discussion about the slicing process and different methods developed for that in the literature. There are two slicing methods, first method is slicing based on STL representation of CAD model, and the second one is direct slicing.

In this research, to optimize the volume deviation and the number of slices, it is needed to simulate the slicing procedure and find these two quantities. This is necessary in objective function evaluation during optimization process. The slicing simulation module is developed in Visual Basic since it is compatible with SolidWorks<sup>®</sup>. In this module, the model is sliced at predefined cutting planes. The information about the resulting intersection curves is obtained by using a SolidWorks Application Programming Interface (API) function. The cutting algorithm used in the proposed research is based on a 3-axis cutting machine, mainly due to its availability.

In the next sections, the two slicing methods are described and then the slicing procedure in this study is presented.

#### 3.1.1 Slicing Based on STL Data

“The STL file is a tessellated representation where the solid model is represented by a number of three-sided planar facets (triangles)” [31]. Figure 3-1 displays a tessellated CAD model.

Each triangular facet is described by a set of x, y and z coordinates for every three vertices,

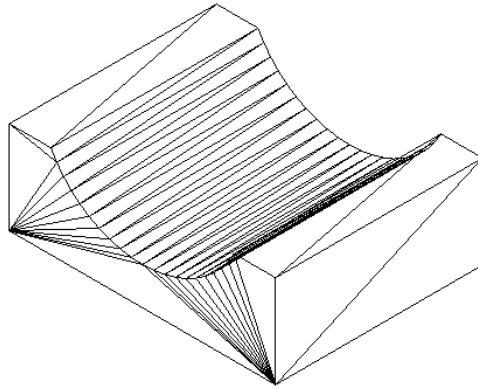


Figure 3-1: A tessellated sample CAD model

and a unit normal vector for each facet that shows the side of the facet. The patches of triangular facets define a section of the external surface of the object. In general, it takes many triangles to represent a 3D solid model. This causes problems which must be solved before adopting this kind of data for the slicing process.

The first limitation of the STL format representation is that some features in the original CAD model are lost because of the linear approximation of the CAD model surface. In STL representation, no more information about the original CAD model remains except a list of triangles and their unit normal vectors. This leads to some sources of errors. As Leong et al. [32] reported, these errors can be classified as follows

- 1) Gaps (cracks, holes or punctures) - that is, missing facets;
- 2) Degenerate facets, where all the edges are collinear;
- 3) Overlapping facets; and,
- 4) Non-manifold topology conditions.

Typically, the STL file is larger than the original CAD model. This causes difficulties when a STL file is transferred from the STL generator to the laser cut or the RP machine. Due to this, other slicing techniques such as direct slicing are used.

### 3.1.2 Direct Slicing Technique

The direct slicing technique is based on a geometrical process which determines the 2D contours by finding the intersections of horizontal planes with the geometrical representation of the actual CAD model surface. This avoids many disadvantages of the STL format, which was discussed in the previous section. A model of the slice is then built from the 2D contour. Building this model is a challenging problem that is addressed in this research.

The cutting algorithm in the proposed research is derived from Walczyk's studies [1], [27], [33]. However, since 2-axis laser cutting machines are readily available, a slicing process, based on 2-axis cutting machines, seems more practical. Therefore, the preference in this research is to use a 2-axis cutting machine, and then CNC surface machining to bring the part's dimensions to specific tolerances.

In the current research, a new method to find the volume deviation is proposed. This new method is more efficient than using STL format. The discussion of the slicing procedure is presented in the following section.

## 3.2 Slicing Process

As mentioned in Section 1, slicing the CAD model is a crucial step in all rapid manufacturing processes. In the current research, the slicing process is needed to find the volume of each slice in order to calculate the final volume deviation.

One of the benefits of the method presented here is the ability to change the slice thicknesses while slicing the CAD model. This capability reduces the time needed to implement the optimization process in the model while finding the best thicknesses for the laminated tooling process. To find the 2D profiles for each slice, the 3D CAD model needs to be cut by these slice planes to create an individual actual slice. Figure 3-2 shows an individual slice with one slice plane in each side.

The next step is to find the intersection profile between each slice plane and 3D CAD model. A SolidWorks<sup>®</sup> API function is used for this purpose. Figure 3-3 represents the intersection between the 3D CAD model, and each slice plane is the area surrounded by a 2D profile.

As soon as these profiles are found, the next step is to find a unique 2D profile which contains

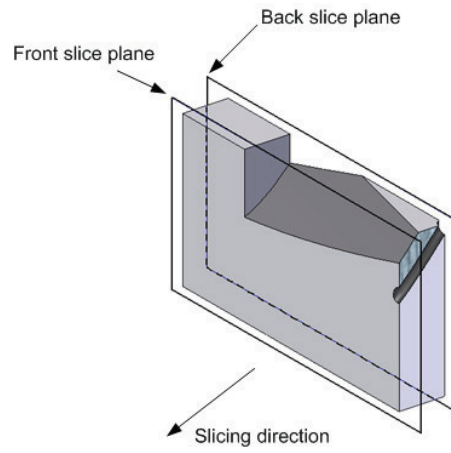


Figure 3-2: A sample slice with one slice plane in each side

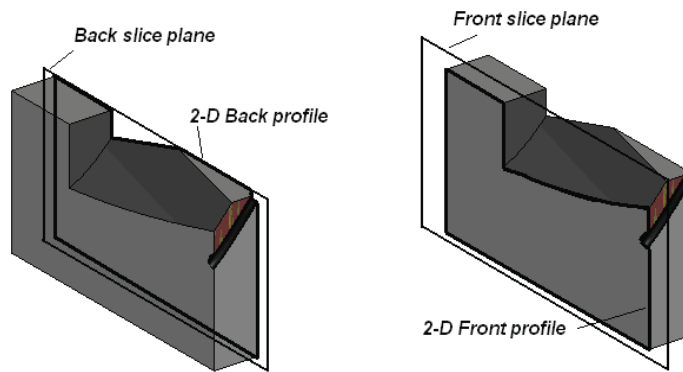


Figure 3-3: An isometric view of back and front profiles



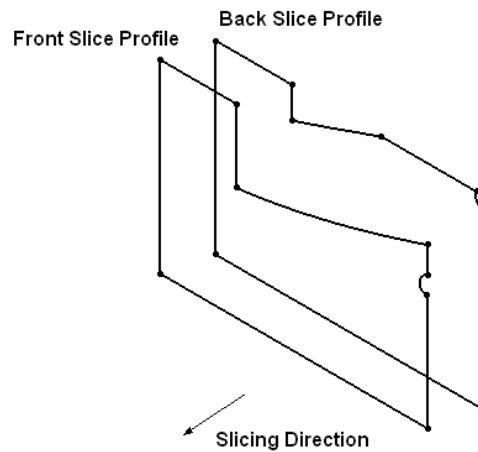


Figure 3-4: Back and front profiles for a sample slice

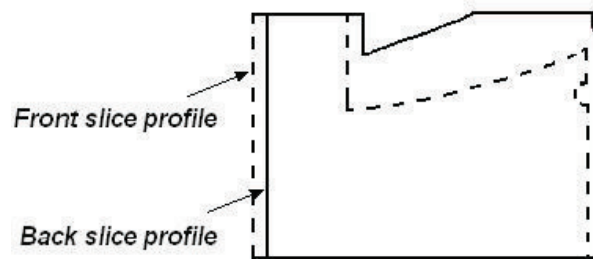


Figure 3-5: Compare back and front profiles to find the union profile

all the features located on the back and front profiles.

So far, for each slice, back and front profiles are found, Figure 3-4 represents the back and front profiles for the sample slice in Figure 3-2. The next step is to find a union profile which contains all the features located on these two profiles. Figure 3-5 shows a comparison of the two profiles to establish the union profile. The objective is to find a single profile which contains all the features located on back profile and front profile. This is done by extruding both profiles toward each other and finding the 2D cross section wherever these extruded solid bodies intersect. Figure 3-6 signifies the final union profile, created according to the profiles in Figure 3-5.

Finally, the area of this union profile is computed within an API function created in

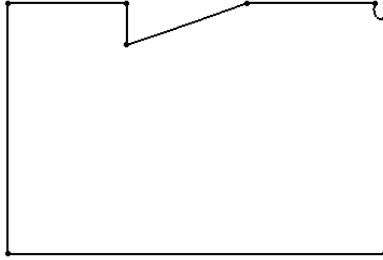


Figure 3-6: Union profile

SolidWorks<sup>®</sup>. Then, the slice volume is calculated by multiplying the union profile area by the slice thickness. At the end, summation of all the slices volumes results in the volume of assembled slices. Volume deviation is found by subtracting the volume of the original model from this volume. All the steps of this process are summarized in Figure 3-7. Here:

$P_i$ : The slice plane;

$V_s$ : The total volume of assembled slices;

$V_a$ : The volume of actual CAD model;

$A_i$ : The area of slice;

$V_i$ : The volume of slice.

This virtual slicing process is conducted in a simulation module which was created in SolidWorks<sup>®</sup>. Also, the simulation module can find the number of slices by counting the number of union profiles created for each thickness vector. The results of the simulation module then are used in the optimization module.

### 3.3 Optimization Methodology

Figure 3-8 (a), is the CAD representation of a hydroforming tool in University of Waterloo. As it is depicted in Figure 3-8 (b), the final laminated tool has less volume deviation with the original CAD model if small slice thicknesses are selected. However, this results higher cutting process costs due to having more 2D profiles to cut. On the other hand, using big slice thicknesses as depicted in Figure 3-8 (c) reduces the cutting process costs, while the volume deviation and consequently the CNC machining cost is increased. Therefore, an optimization is

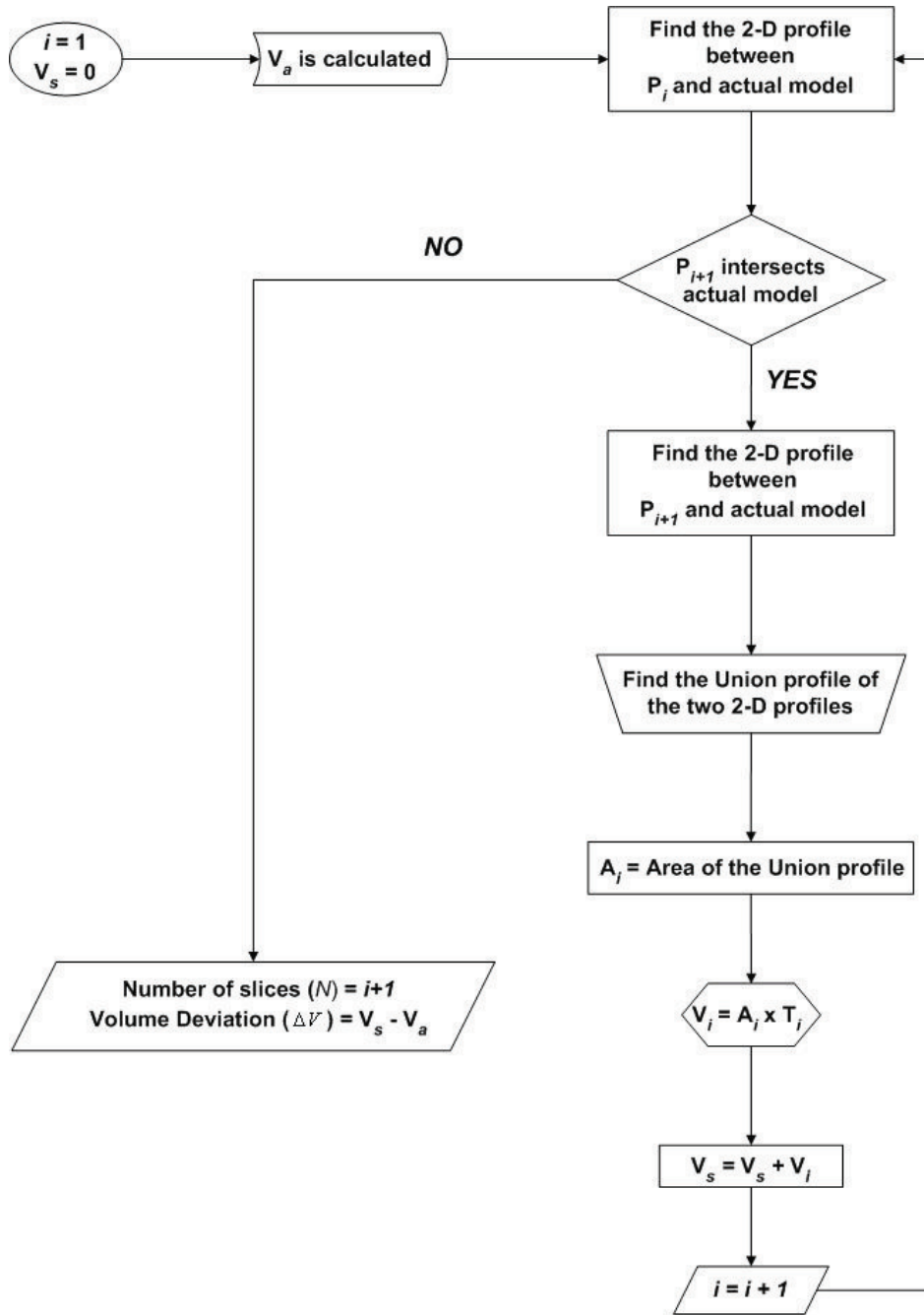


Figure 3-7: Schematic of slicing process in simulation module

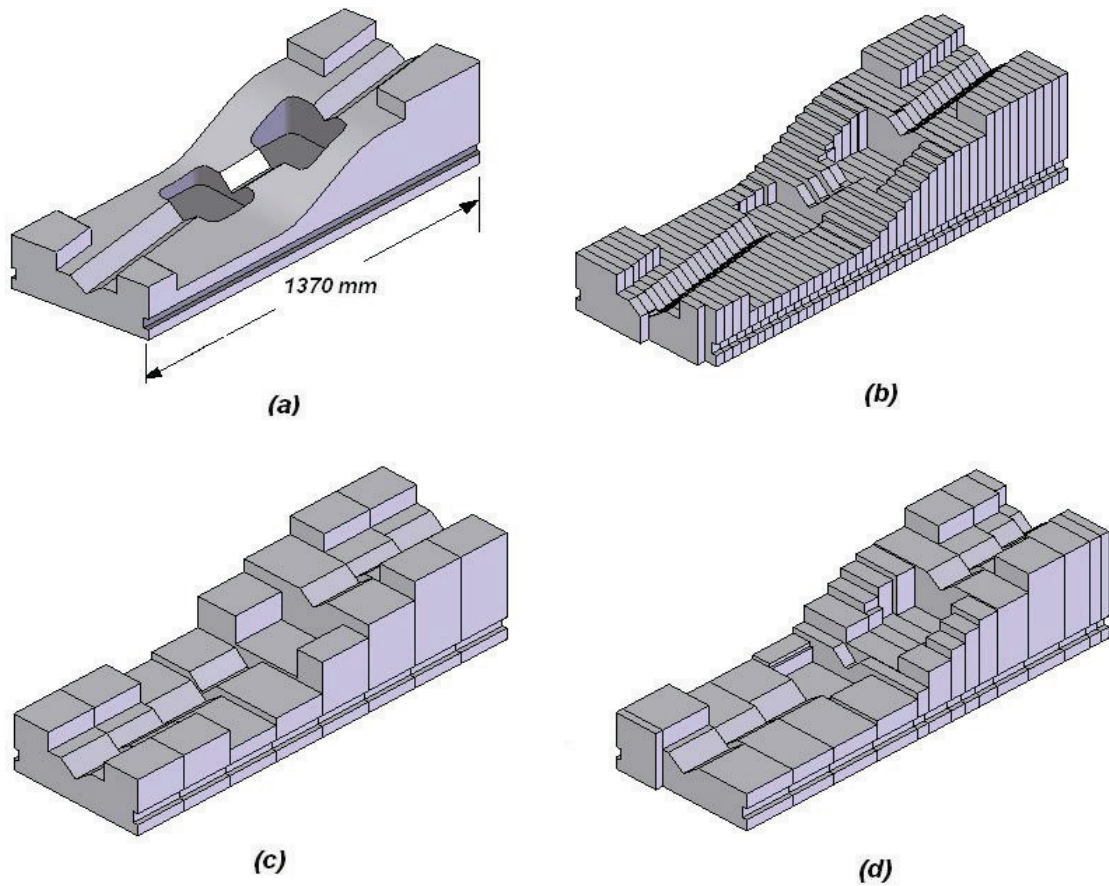


Figure 3-8: (a) A sample model; (b) Uniform slicing with minimum thickness; (c) Uniform slicing with maximum thickness; (d) Adaptive slicing with optimization outcome thicknesses.

needed to suggest variable thicknesses based on CAD model geometry as it is shown in Figure 3-8 (d) to reduce CNC and cutting costs at the same time.

In conclusion, these examples showed that it is needed to find the best configuration of the thicknesses not only to minimize the number of slices covering whole CAD model surface, but also to reduce the volume deviation. So far in industry, the process to determine the layers' thicknesses has been usually performed by well trained technicians. While in this research a novel approach in optimization of laminated tooling process is introduced. The proposed method is a genetic algorithm based optimization which can find the optimum arrangement of the thicknesses based on the CAD model surface geometry.

### 3.3.1 Why Genetic Algorithms?

Figure 3-8(d) shows an arrangement of sheet metals, with variable thicknesses, that create the laminated version of the CAD model presented in 3-8(a). All these thicknesses are selected from a set of commercially available sheet thicknesses such as

$$\{t_i | i \in [1, n]\} \quad (3.1)$$

This is named as the *standard set* and each member of this standard set, such as  $t_i$  is named as a *standard thickness* in this research.  $n$  is the number of the standard thicknesses used in optimization procedure.

Each combination of these thicknesses that can cover the whole CAD model surface is known as a *thickness vector*. Each thickness vector is potentially a solution for the optimization process.

In this particular application, the number of the standard thicknesses is usually up to seven or eight different thicknesses. Also the repetition is absolutely permitted for each standard thickness creating a thickness vector. Therefore, the solution space contains enormous number of thickness vectors.

Consequently, a population based optimization method is needed to consider as many as possible thickness vectors in order to search more areas of the solution space.

Genetic algorithms consist of a class of population based algorithms. They are nature based algorithms that work based on the notion of evolution. As opposed to the traditional optimization methods, GAs work on population of solutions to solve the optimization problem. Therefore, by considering a population of possible solutions, a larger area of solution space can be searched for a global optimum with a lesser chance to trap at a local optima. Moreover, it does not need the derivatives or partial derivatives of objective function. Hence, GAs can be applied to the systems with complicated objective functions.

On the other hand, since each member of the solution space is an arrangement of the thicknesses, it can be simulated by a chromosome. Then, in a real coded GAs, by applying two GAs' operators, crossover and mutation, on the sets of thicknesses, it is possible to change the arrangement of thicknesses in each solution to find the optimum set of thicknesses.

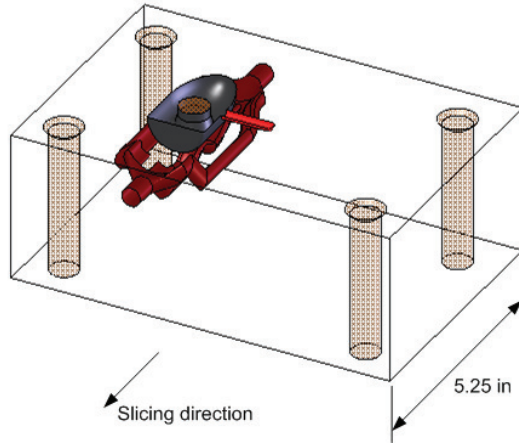


Figure 3-9: A sample CAD model with conformal cooling channels

These benefits make genetic algorithm a good candidate for this optimization problem. It is noted that the GA algorithm is used in this research differs from the classic GAs. The genetic operators used here are slightly different. Also, as it is discussed in Chapter 4, a new crowding method is applied to prevent premature convergence in the population.

In the following sections, the GA algorithm adapted in this research is introduced. Then the simulation results are presented in Chapter 4. More discussion about how genetic algorithm works was also presented in Chapter 2.

### First Generation

Genetic algorithm starts with creating the first generation based on the initial population. Here, the initial population is all combinations of standard thicknesses which are able to cover the CAD model surface. Since there is no limitation to the number of times that an individual size can be used in a thickness vector, the initial population has an enormous number of members. To elaborate, let us consider the model presented in Figure 3-9. Any combination of the standard thicknesses represented by Equation 3.1, such as

$$\{a_j | a_j \in \{t_1, t_2, \dots, t_{n-1}, t_n\}\} \quad (3.2)$$

is a member of the initial population. Each member of the initial population must be able to cover the entire CAD model. This means the selection from the standard set Equation 3.1 to create each thickness vector is continued until

$$\sum_{j=1}^m a_j \geq L \quad (3.3)$$

where  $L$  is the CAD model length and  $m$  is the number of thicknesses need for covering the entire CAD model..

The first generation contains a number of these thickness vectors randomly selected from all the initial solution space, this is called as the *population number*. The population number is defined by the user at the beginning of the G.A. process.

It should be mentioned that the standard set of thicknesses, such as the one presented by Equation 3.1, is selected from a bigger set which is all commercially available sheet thicknesses for that specific material. The thicknesses in the standard set are selected by the user, based on the parameters such as available power of laser cut and also the features on CAD model surface.

### **Objective Function Evaluation**

Figure 3-10 shows the schematic of the standard G.A. process. As depicted in this figure, after the first generation population is created, the objective function is evaluated. Objective function contains all the important variables in the optimization process. Therefore, the value of the objective function can be used as a criterion for finding the optimization solution.

### **Termination Criterion**

Following the Schematic presented by Figure 3-10, the next step after finding the objective function values, or as it is sometimes called, the fitness values for the entire population is to check if the termination criterion is satisfied.

Different termination criteria are suggested in the literature. Some of them, such as fitness convergence, population convergence and gene convergence, continue genetic algorithm procedure until a predefined population convergence occurs in a generation.

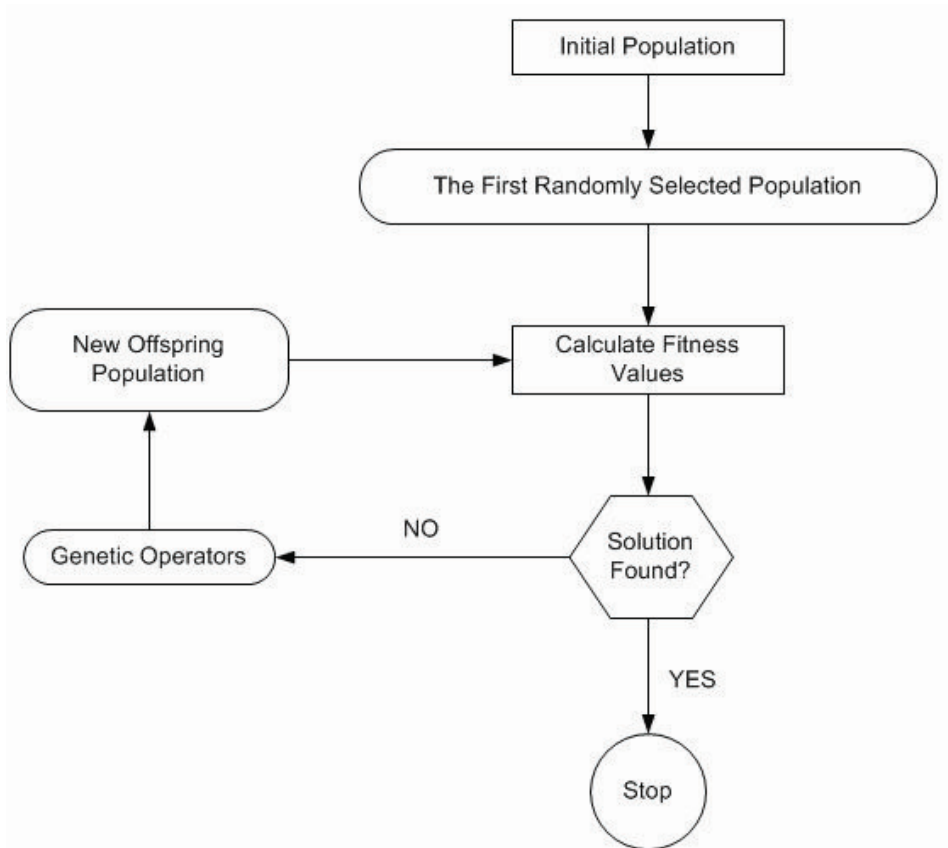


Figure 3-10: Schematic of how genetic algorithm works



The other criterion is *generation number*, which stops the optimization process after a specific number of iterations. Also the *evolution time* criterion stops after a specific calculation time. These criteria are usually used in cases where the objective function calculation needs too much time; therefore, it takes a long time to have a convergence through generations in the optimization process.

For this research, terminating the optimization process can be accomplished by any of these termination criteria. However, since the simulation module needs almost 35 seconds to calculate the volume deviation and the number of slices for each thickness vector, for the first sets of case studies, the number of iterations is chosen as the termination criterion. The results show that the system converges to a steady state solution after a small number of generations.

If the termination criterion is not satisfied yet, the procedure continues to make the next generation.

### **Selection Operator**

Among different selection operators which are introduced through literature, the tournament selection is used for the aim of this research. The tournament selection operator takes some members of the population, randomly. Then the one with the highest fitness value is selected for the next generation. The process continues until the initial next generation's population, named as mating pool is created. The mating pool has the same size as the population size.

### **Crossover Operator**

Crossover is one of the genetic algorithm operators which let the system search more areas of the solution space. It randomly selects two chromosomes from the current population. These are called parental chromosomes. By switching the genes between these parental chromosomes, two new chromosomes, which are considered their "children", are created.

The crossover operator which is used in this research works based on some specific critical sections of the CAD model surface. A critical section, as depicted in Figure 3-11, is a section on the CAD model where the shape of surface is changed drastically. The slice plane locations around these sections have a considerable impact on the volume deviation value. Consequently, it is important to know the effect of changing the slice plane locations on the value of the

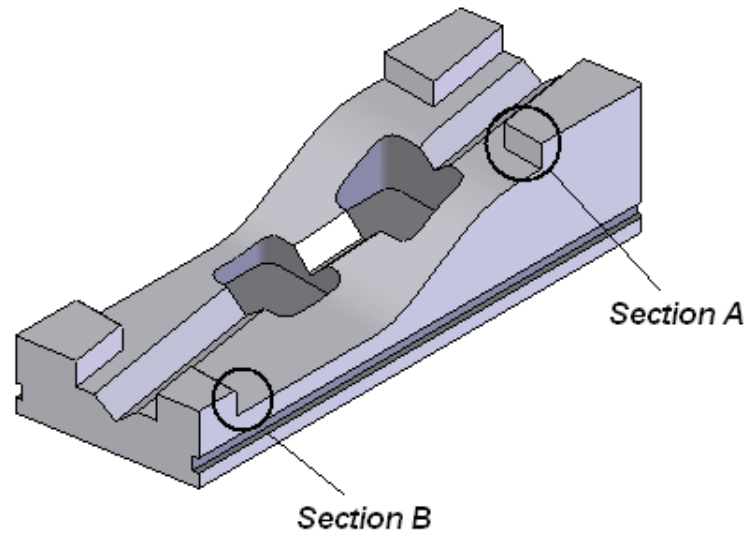


Figure 3-11: A sample CAD model with two critical sections

objective function.

Figure 3-12 shows how the intended crossover operator works. As it can be seen in this figure, sometimes the slice planes do not lie exactly on a critical section. To deal with this situation, the closest slice planes to these specific locations are usually chosen for the crossover operation.

Also, it should be mentioned that changing the thickness arrangements during the crossover operation may result in the entire CAD model length not being covered by some thickness vectors. To deal with this problem, due to the location of the critical section and the location of the two slice planes on either side of this point, different slice planes are selected to switch between the two sets. Table 3.1 presents the different cases that are considered in the crossover process. As it is explained in Table 3.1, in each case the slice planes get involved in the crossover switching process such that the children thickness vectors are still able to cover the entire CAD model.

### **Mutation Operator**

Mutation is a genetic operator that helps the optimization algorithm dodge from a local optimum in order to find a global or at least a better local optimum. It usually changes the value

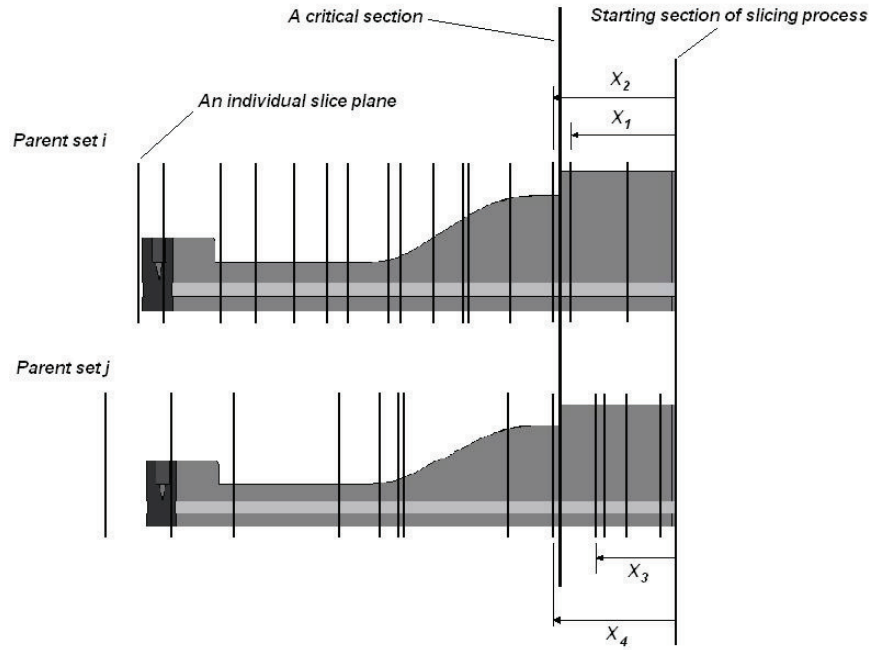


Figure 3-12: Location of the slice planes in either side of critical section

Table 3.1: Different cases in crossover operation

<p><u>Case 1</u></p> <p><math>X_3 &gt; X_1 \ \&amp; \ X_4 &gt; X_2</math></p> <p>All thicknesses after <math>X_3</math> in parent <math>j</math> with the thicknesses after <math>X_1</math> in parent <math>i</math> and all thicknesses after <math>X_2</math> in parent <math>i</math> with the thicknesses after <math>X_3</math> in parent <math>j</math></p>
<p><u>Case 2</u></p> <p><math>X_3 &lt; X_1 \ \&amp; \ X_4 &lt; X_2</math></p> <p>All thicknesses after <math>X_4</math> in parent <math>j</math> with the thicknesses after <math>X_1</math> in parent <math>i</math> and all thicknesses after <math>X_1</math> in parent <math>i</math> with the thicknesses after <math>X_3</math> in parent <math>j</math>.</p>
<p><u>Case 3</u></p> <p><math>X_3 &lt; X_1 \ \&amp; \ X_4 &gt; X_2</math></p> <p>All thicknesses after <math>X_4</math> in parent <math>j</math> with the thicknesses after <math>X_2</math> in parent <math>i</math> and all thicknesses after <math>X_1</math> in parent <math>i</math> with the thicknesses after <math>X_3</math> in parent <math>j</math></p>
<p><u>Case 4</u></p> <p><math>X_3 &gt; X_1 \ \&amp; \ X_4 &lt; X_2</math></p> <p>All thicknesses after <math>X_3</math> in parent <math>j</math> with the thicknesses after <math>X_1</math> in parent <math>i</math> and all thicknesses after <math>X_2</math> in parent <math>i</math> with the thicknesses after <math>X_4</math> in parent <math>j</math>.</p>

$$\mathbf{T} = \{ \mathbf{t}_1, \mathbf{t}_2, \mathbf{t}_3, \mathbf{t}_4, \mathbf{t}_5, \dots, \mathbf{t}_{12}, \mathbf{t}_{13}, \mathbf{t}_{14} \}$$

(a)

$$\mathbf{T} = \{ \mathbf{t}_1, \mathbf{t}_{13}, \mathbf{t}_3, \mathbf{t}_4, \mathbf{t}_5, \dots, \mathbf{t}_{12}, \mathbf{t}_2, \mathbf{t}_{14} \}$$

(b)

Figure 3-13: The effect of internal mutation on a thickness vector. (a) before mutation; (b) after mutation

of a randomly selected gene. In the binary coded genetic algorithm, this means switching from zero to one, or vice versa. In the application of this research, the value of a gene is replaced by another value from the standard set.

To apply the mutation operator in this particular application, a value of a randomly selected gene from a thickness vector has to be changed with another thickness from the standard set. The problem which arises is that, in some cases, the value of the gene is replaced with a smaller value. In such an instance, the possibility of not covering the entire CAD model surface by the newly created thickness vector, exists .

To address this problem, a new mutation operator is designed for the aim of this research. This mutation idea comes directly from biology, where mutation can happen when two genes in a chromosome are misplaced to each other. This type of mutation is developed for this research, to ensure that all the new thickness vectors can cover the entire CAD model surface. In this kind of mutation, which is called internal mutation, two genes are switched together in a thickness vector. The thickness vector, as well as the gene locations are randomly selected. Figure 3-13 illustrates this type of mutation.

After applying the genetic operators, the new offspring is created. As depicted in Figure 3-10, the algorithm now starts to do the same steps for this new generation. The process will continue until the termination criterion is satisfied.

### 3.4 Optimization and Simulation Modules

The optimization module consist of all the genetic algorithm process steps explained so far. Since the objective of this study is to reduce volume deviation and the number of slices at the same time, the objective function has been considered as the following:

$$\Phi(\Delta V, N) = \frac{1}{\beta_1 \Delta V + \beta_2 N} \quad (3.4)$$

Here  $\Delta V$  is the volume deviation between assembled slices and the actual CAD model, and  $N$  represents the number of slices. Also  $\beta_1$  and  $\beta_2$  are user-defined weight coefficients which specify the importance of the volume deviation and the number of slices in the optimization process. It should be mentioned that due to different units are used for  $\Delta V$  and  $N$ , they are not at the same order as  $\beta_1$  and  $\beta_2$ . In such a case, to  $\beta_1$  and  $\beta_2$  show the weight properly, normalization is needed.

As it is depicted in Equation 3.4, to evaluate the objective function  $\Phi$ , the volume deviation and the number of slices values must be found. The procedure of finding these two quantities were explained in Section 3.2. This is a process which virtually creates the laminated model based on the thicknesses of each thickness vector, and find the volume deviation and number of slices correspond to each thickness vector. This is performed in a simulation module created in SolidWorks<sup>®</sup>. Figure 3-14 shows the relation between this simulation module and the optimization module.

As it is shown in Figure 3-14, as soon as the optimization parameters,  $\Delta V$  and  $N$  are found, the results come to the optimization module to be used for the objective function, fitness, calculation. The optimization module is written in VisualBasic, since it is very compatible with SolidWorks<sup>®</sup>. All the genetic algorithm steps then followed in the optimization module, until the termination criterion is satisfied.

More information on how the optimization program works, is presented in Chapter 6. Also, the result of applying the proposed optimization technique on an injection mould tool is presented in the next Chapter.

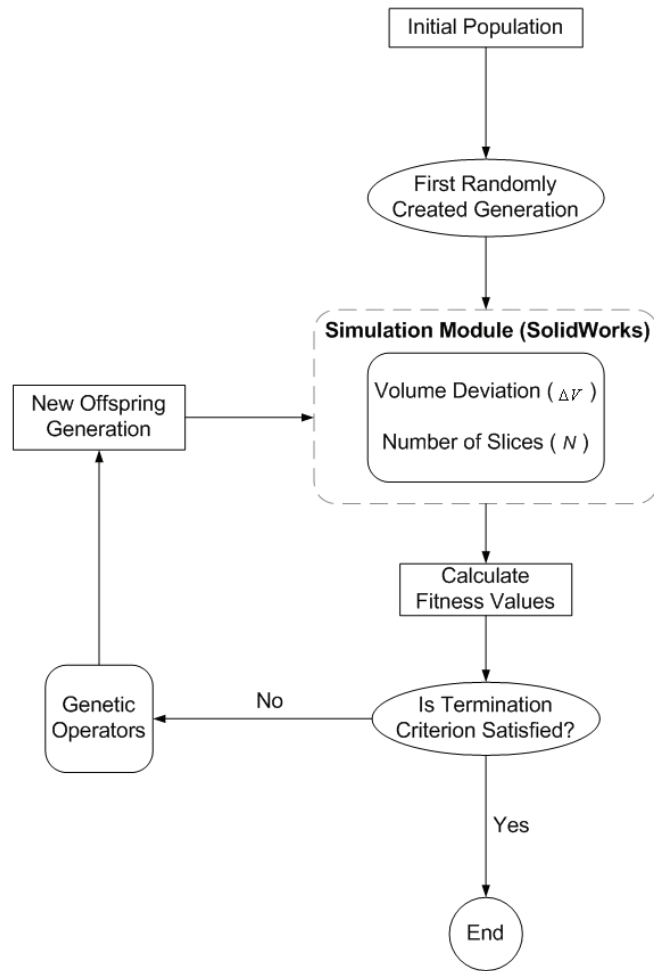


Figure 3-14: Schematic of genetic algorithm procedure in the current research

## Chapter 4

# Optimization Results

### 4.1 Introduction

In this Chapter, the suggested algorithm that was explained in Chapter 3, is applied to some sample CAD models. First a very simple CAD model is selected to test the performance of the proposed method. In the next step, the hydroforming tool in Figure 3-8 undergoes the optimization procedure. Results show how the slice plane locations are improved such that the volume deviation is reduced with the same number of slices. Finally, as an actual experimental test, an injection mold tool is studied based on the proposed on Chapter 3.

### 4.2 Case Studies

#### 4.2.1 Case 1 - A trivial example

The first case is a simple model which is presented in Figure 4-1. This example is employed to show how algorithm works in terms of finding the best locations for slice planes in a very simple case. The first population is created based on a sample standard thicknesses which presented by:

$$\{10, 20, 30, 40\} \quad . \quad (4.1)$$

The population size is 100 which means the program starts with 100 random sets of thick-

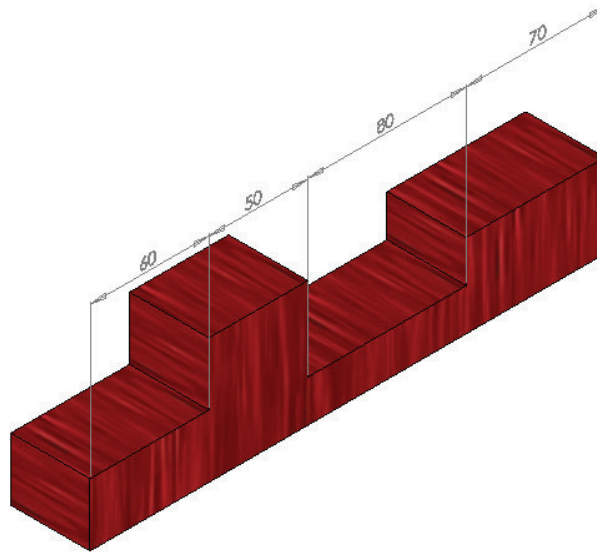


Figure 4-1: First case, a simple model

nesses that covers all the length of the CAD model. By following the same procedure and by crossover and mutation rates equal to 0.6 and 0.04, respectively, Figure 4-2 indicates that all the fitness values at the beginning of the optimization process and after 11 iterations. Note that at the end of process all population members except four of them converge to a unique set; these four sets have been created by mutation and have less fitness value in comparison with other members. This means mutation has a negative effect at this point as the global maximum has already found.

As Figure 4-3 shows, the best relative fitness values after seventh iteration remain almost the same and despite the previous example it is not going to increase again. As Figure 4-4 shows, this happens because the system has already reached its global optimum. It can be seen from Figure 4-4 that final result is the best arrangement of slice planes for this model based on available thicknesses.

In this example, the algorithm was successfully tested for a simple CAD model. In the case of a more complicated CAD model with larger standard thicknesses, the algorithm may need more iterations and bigger population size to converge.



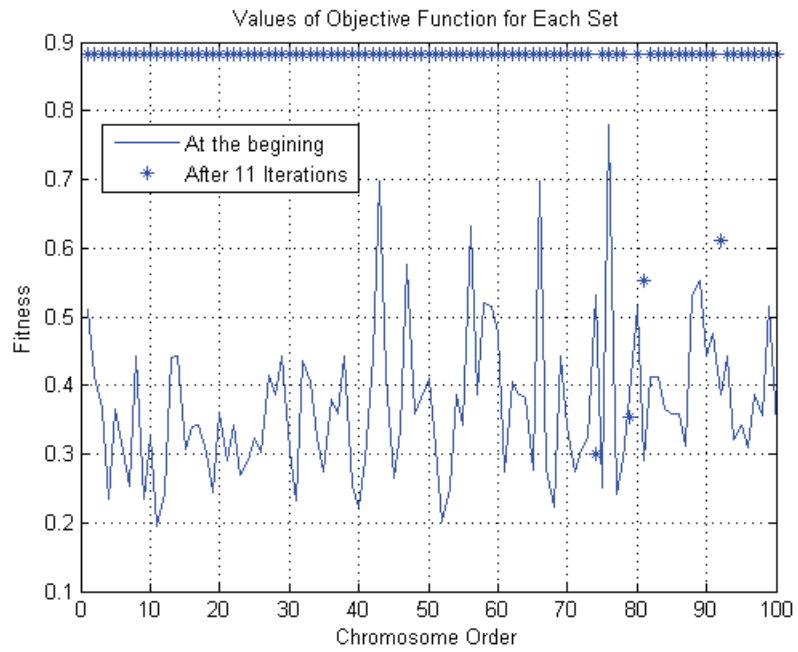


Figure 4-2: Fitness values at the beginning of the optimization process and after 11 iterations.

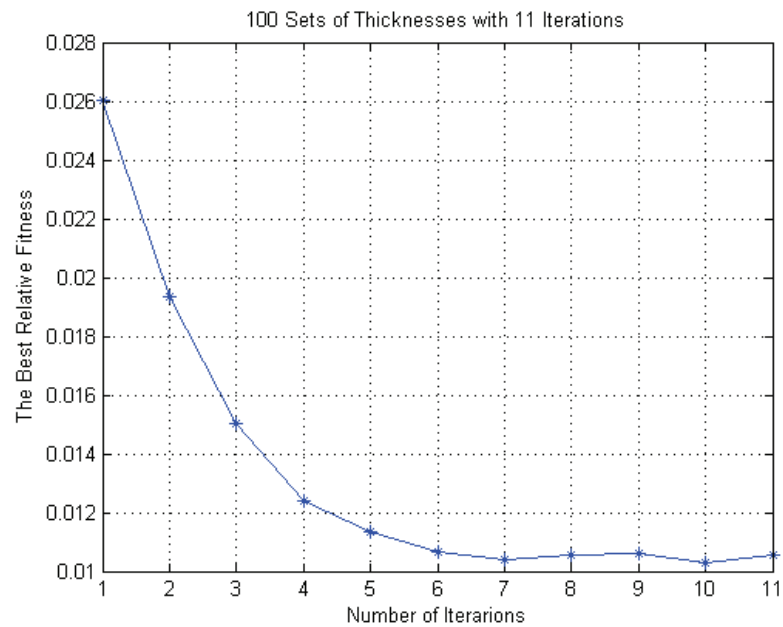


Figure 4-3: The best relative fitness for each iteration.

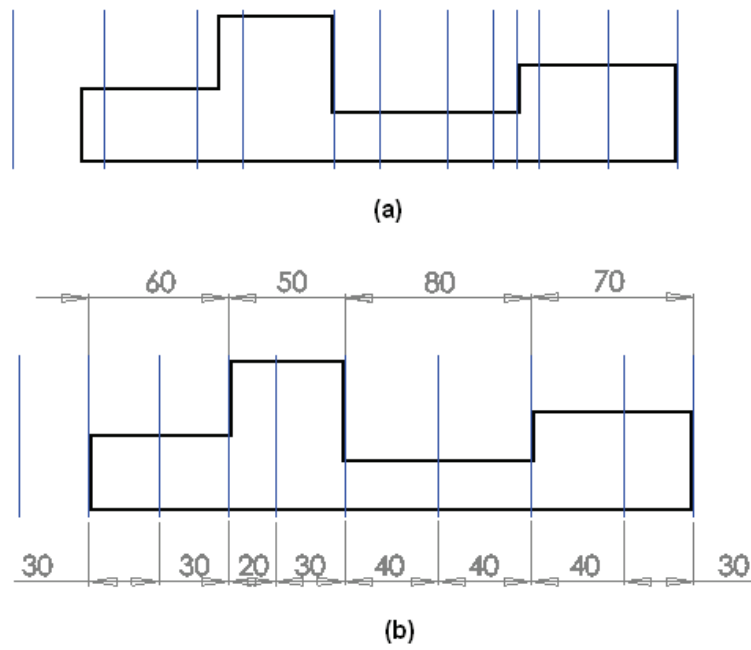


Figure 4-4: Slice planes arrangement; (a) the best set at the first randomly selected population, (b) final result

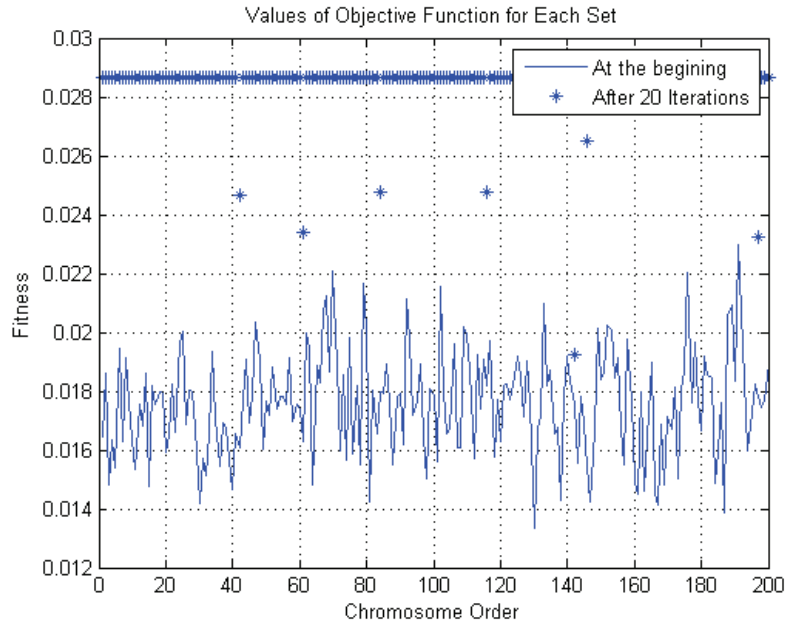


Figure 4-5: Fitness values at the beginning of optimization process and after 20 iterations

#### 4.2.2 Case 2 - Hydroforming tool

The hydroforming tool already presented by Figure 3-8 is presented again as the second case study. The optimization process is started with 200 randomly selected sets. In this example the optimization process is stopped after 20 iterations; the crossover rate is 0.60 and mutation rate is chosen as 0.04. Like the other examples,  $\beta_1 = 3$  and  $\beta_2 = 1$ .

As it is shown in Figure 4-5, after 20 iterations most of the sets have higher fitness values than the first randomly selected sets. Figure 4-6 indicates that the maximum relative fitness is converging to a steady value. To compare the optimization results, the location of plates has been presented in Figure 4-7 in different iterations. In this figure, the results after 5,7,10 and 20 iterations can be compared with each other and the best set in the first generation;

As Figure 4-7 (d) represents, after five iteration, in the area between C and D where the CAD model surface has a significant slope, program uses smaller slice thicknesses compared to Figure 4-7 (c). On the other hand in the area between D and E where the CAD model surface is almost flat, bigger slice thicknesses are used. In order to minimize volume deviation in this area, as Figures 4-7 (c) and (d) indicate, last slice plane is moving towards the step located

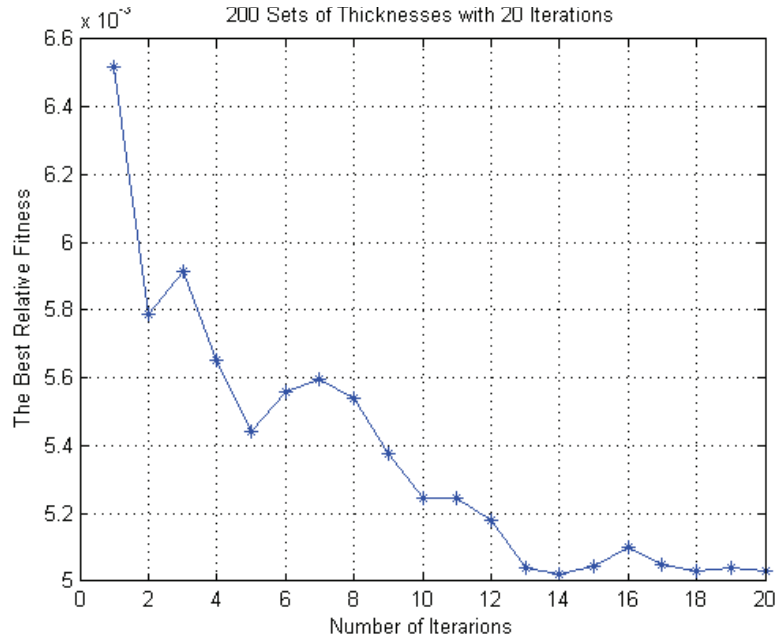


Figure 4-6: The best relative fitness for each iteration.

close to section E. Moreover, from Figure 4-7 (d) to Figure 4-7 (e) only after 2 more iterations program is still trying to find better locations for slice planes in the area between C and D. Therefore after seventh iteration smaller thicknesses are chosen for this area, and also bigger slice thicknesses are used to cover the area between sections D and E from iteration five to seven.

Also from Figure 4-7 (e) to Figure 4-7 (f) the arrangement of slice planes does not have a significant change. It is interesting that the program now is trying to reduce the number of slices from the seventh iteration where it has sixteen slices. After 3 more iterations the program reduces the number of slices by around 10% without increasing  $\Delta V$ . It might not seem a significant effect in this particular example but in reality when there are hundreds of slice planes then ten or even five percent less slices has a significant effect on laser cutting costs.

Finally by continuing the optimization procedure for ten more iterations as it is presented in Figure 4-7 (g), the optimization is focusing on the slices locations in the area between sections A and B. Figure 4-7 (b) indicates the top view of the CAD model, showing a slope between A and B. In this section, less slice thicknesses can cause less volume deviation. This is what

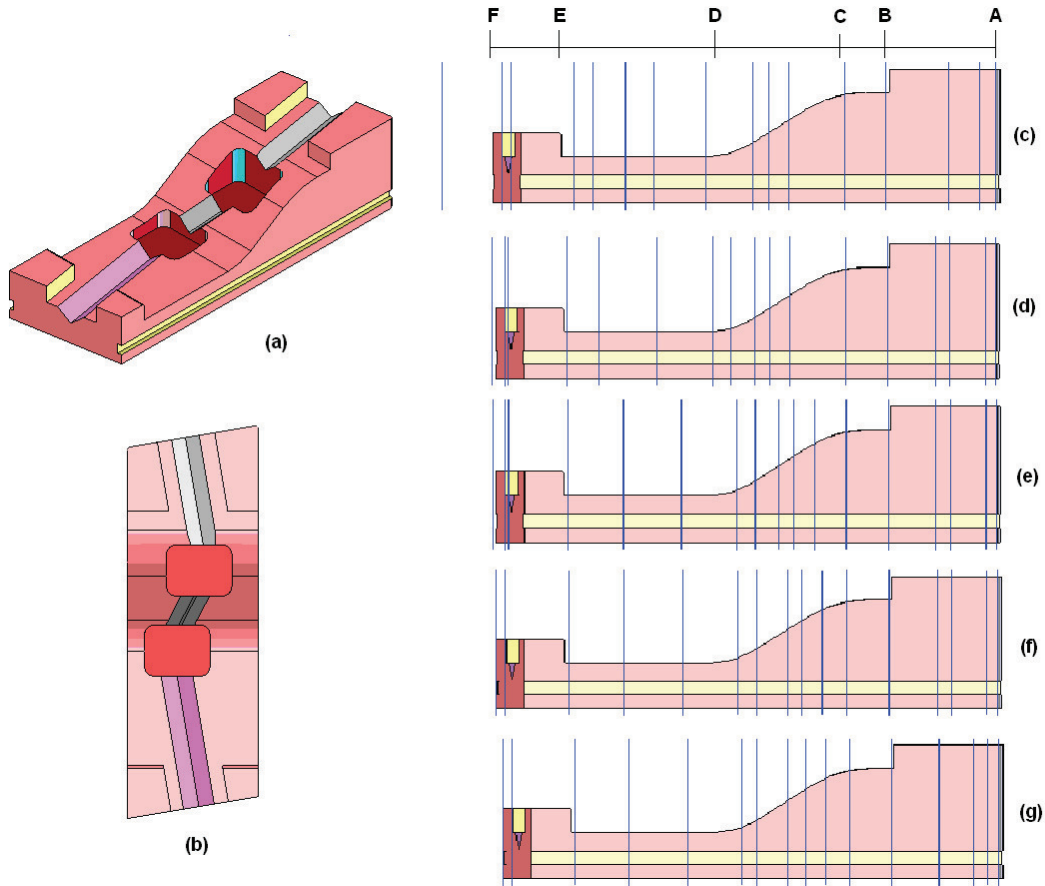


Figure 4-7: Optimization results for 200 population size; (a) Isometric preview of original CAD model, (b) Top view of original CAD model; and The best slice planes locations: (c) For the first randomly selected generation, (d) After 5 iterations, (e) After 7 iterations, (f) After 10 iterations, and (g) After 20 iterations

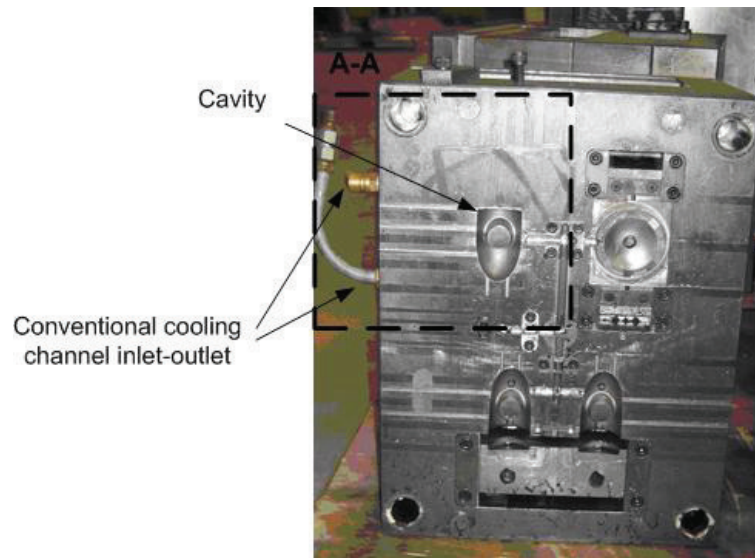


Figure 4-8: The original injection mould tool and the section selected for the case study

the program does from the iteration ten to twenty. As it can be compared from Figure 4-7 (f) and Figure 4-7 (g) while the number of slices in the area between A and B are the same, the program has found a better combination to reduce the volume difference.

### 4.3 Actual Experimental Test

After having these basic case studies, it is now the time to start the actual experimental tests to produce an injection mould tool based on the proposed optimization method. The original injection mould tool is an integrated tool with conventional cooling channels which is used in Webplas injection moulding company in Kitchener, Ontario. As depicted in Figure 4-8, A portion of the tool is selected for the purpose of this research and a CAD model with newly designed conformal cooling channels was created based on this portion. This CAD model was represented by Figure 3-9. The portion of this model which contains the cavity and the cooling channels is considered for the optimization purpose. This portion of the tool is shown in Figure 4-9. Two cases are considered. In each case, all the optimization parameters are the same except in the second case the population size is twice larger than what is selected for the first case.

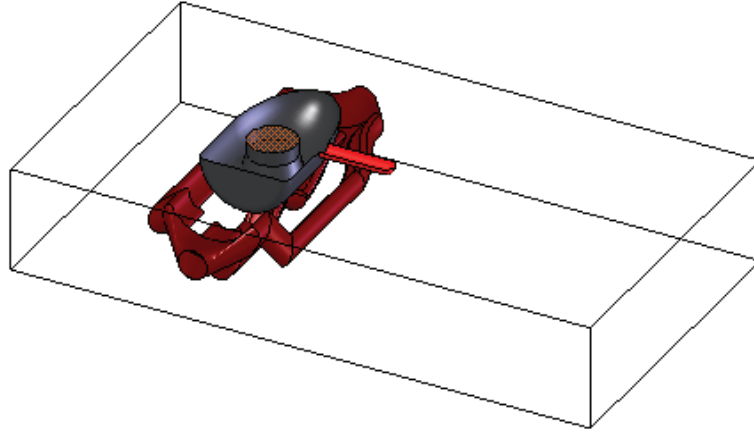


Figure 4-9: The portion of CAD model used in the optimization process

Figure 4-10 presents a better view of the newly designed conformal cooling channels for the tool.

Although the results show improvement in the location of the slice planes, the premature convergence that happens in the population, causes stopping in a local optimum while a better solution is expected. To prevent this premature convergence and also to cut the calculation time, a new crowding method is presented in this chapter. The results based on applying the proposed crowding method show more improvement in the optimization results in comparison with the first set of case studies, while using less calculation time.

In the first case, a population of 50 thickness vectors is created. Then, in the second case, the optimization process is repeated with a population of 100. As the results show, the quality of the solution is improved by having a larger population size. This is due to the postponement of the convergence in population members by a larger population size.

### 4.3.1 Case 1

In this example, the mating pool contains 50 thickness vectors. The termination criterion is the number of generations which stops the optimization process after 20 iterations. The crossover and mutation rates are 0.75 and 0.04, respectively. This value of crossover is a bit higher than what is suggested in literature (0.4 to 0.6). This provide more diversity in the population through generations. Also  $\beta_1 = 3$ , and  $\beta_2 = 1$ , which means having a minimum volume

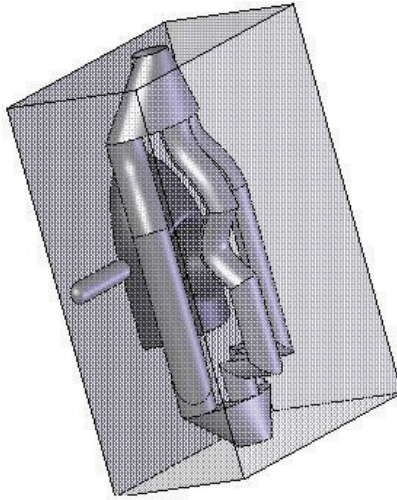


Figure 4-10: A conformal cooling system can follow the cavity shape

deviation is more important than having a minimum number of slices in this optimization process.

As depicted in Figure 4-11, the maximum relative fitness, converges to a steady value after the 8th iteration. Also Figure 4-12 shows that after 8th iteration, system cannot find a better solution. This is a touchstone for the system convergence. This means with a population size of 50, the convergence occurs after 8th iterations and the system is trapped in a local optimum. This confines the system to use only those thicknesses that are in the best set in the 8th iteration. Therefore, due to not having enough resources, the system cannot find a better solution during the next iterations. This is called premature convergence.

Premature convergence prevents the system from searching more areas of the solution space. When this happens, all population members converge to a unique member, a thickness vector here, and the system loses the chance of creating new offspring by applying the genetic operators. If the premature convergence is postponed, the system still has the resources to create new thickness vectors. This leads us to the idea of having a larger population size in order to give the system the chance of searching more areas of the solution space. In this case, the system has more thicknesses available and, consequently, more diversity in the population.

In the next case, the same model is considered with exactly the same optimization parame-



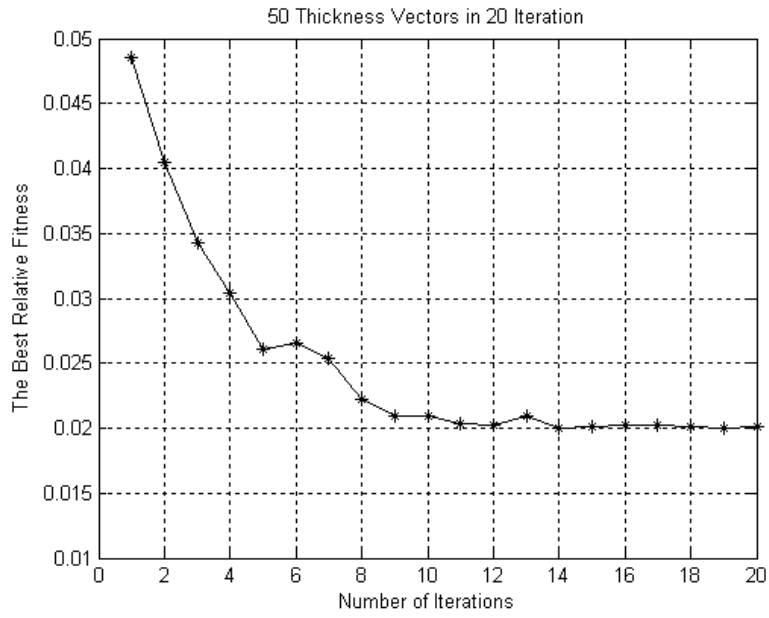


Figure 4-11: The best relative fitness trough iterations for a population size of 50

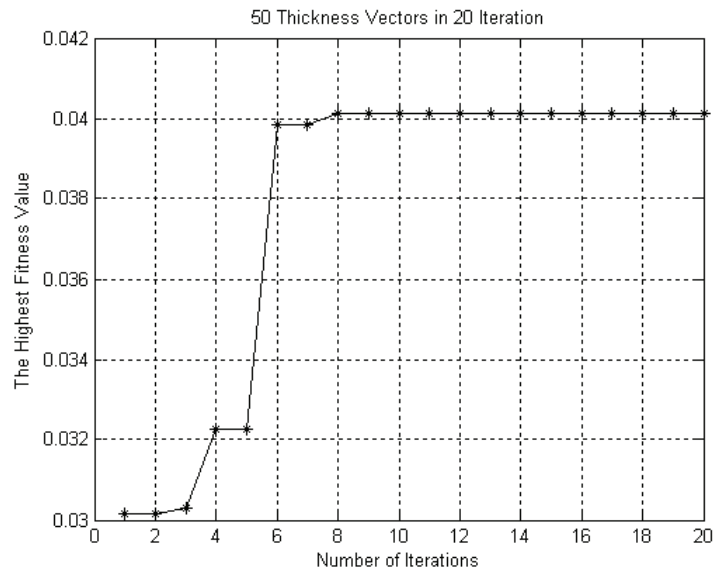


Figure 4-12: The fitness values of the best thickness vectors in each iteration

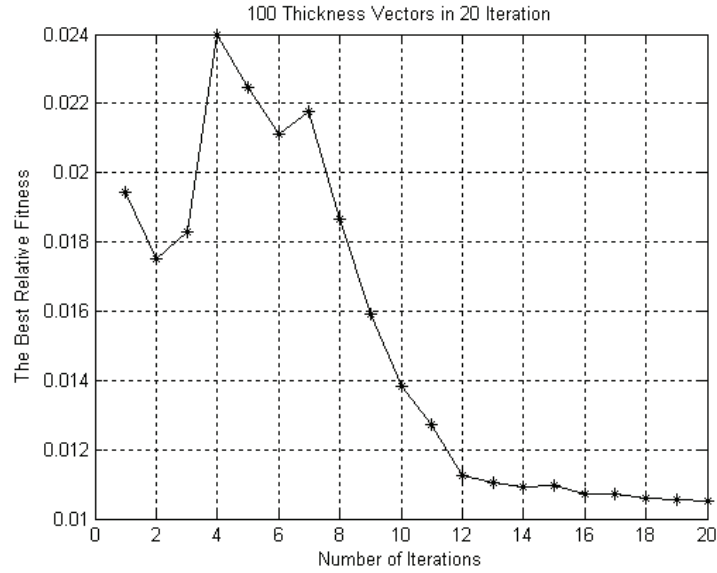


Figure 4-13: The best relative fitness trough iterations

ters, the only difference being the population size. This time, the population size is twice as large as in the first case.

### 4.3.2 Case 2

As depicted in Figure 4-13, the same as the first case, the maximum relative fitness converges to a steady value. The difference in this time is that the convergence happens almost after the 15th iteration. Figure 4-14 shows that the final maximum fitness value in the second case is almost 20 percent higher than the first case. This is due to more opportunity the system has in the second case, to look for a better solution, before being trapped in a local optimum.

Figure 4-15 shows at the end of the optimization process in the second case study, most of the final population members, have higher fitness than the first randomly selected population. This clearly shows how the algorithm can converge to a more reliable solution during optimization process.

Moreover, since as it was mentioned in Section 4.2.1, by choosing  $\beta_1 > \beta_2$  this optimization process focuses more in the volume deviation reduction, Figure 4-16 represents the results in this matter. It shows that at the end, the optimization program can cut the value of the

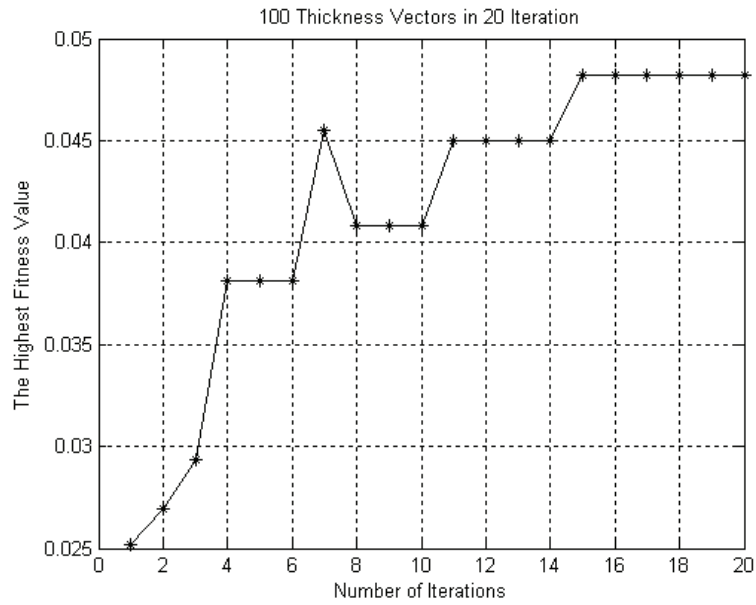


Figure 4-14: The fitness values of the best thickness vectors in each iteration

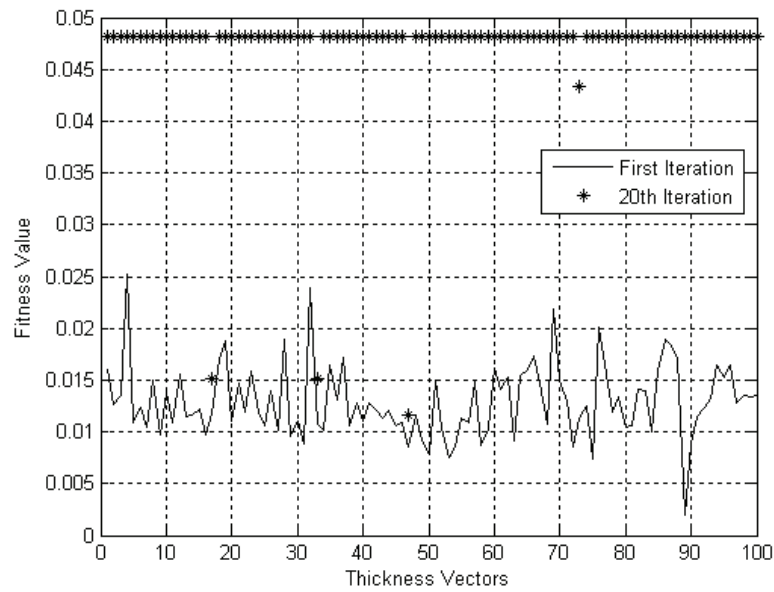


Figure 4-15: Fitness values of all thickness vectors at the first and last iterations

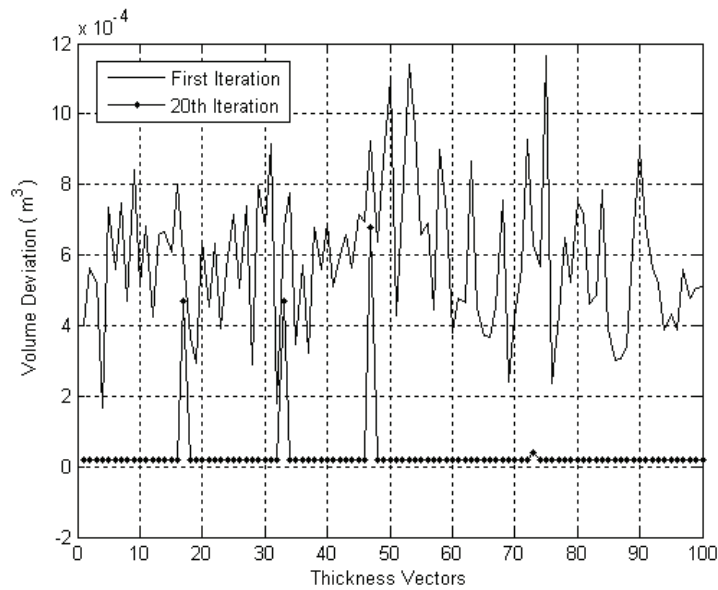


Figure 4-16: Volume deviations of all thickness vectors at the first and last iterations

best volume deviation in the population, to almost 50 percent. This reduction is due to the improvement on slice plane locations during the optimization procedure.

Figure 4-17 provides a better visualization of how the optimization program works. In this figure, the optimization results are presented for the first and last iterations. As depicted here, in some sections such as section-A, where the CAD model and cooling channels surfaces have steep angles with the slicing direction, program uses the sheets with less thicknesses. Moreover, at the end of the optimization process, program uses four slices less than what used at the beginning. This means more than 15 percent reduction in the number of slices. This is another reason for having higher fitness values for the final population members. Therefore, program not only could cut the volume deviation by 50 percent, it also uses less slices to cover the entire CAD model surface.

The results in both cases showed that after a certain number of iterations, the slice plane locations are improved and produced lesser amount of volume deviation. However, as showed in two previous case studies, by choosing a larger population results are more reliable. Since the fitness calculation time is considerably high, almost 35 seconds for each thickness vector, developing a new method to add diversity to the population while having the minimum (or no)

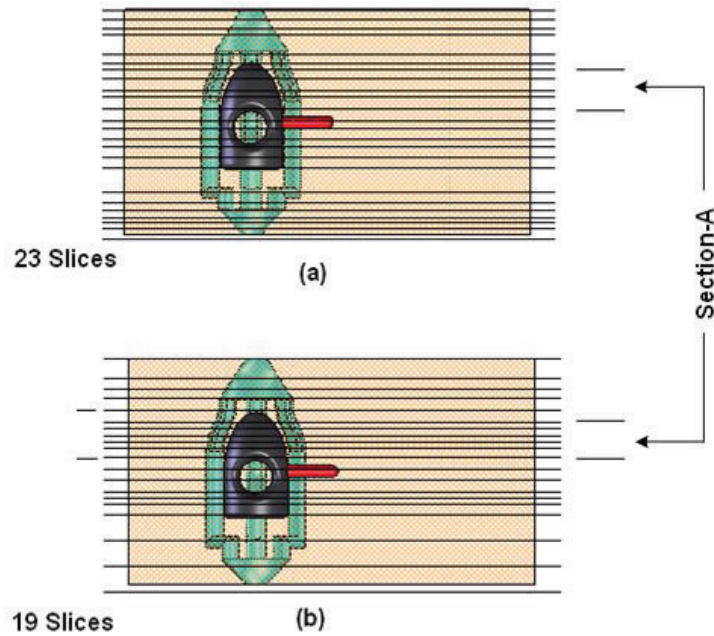


Figure 4-17: The top view of the slice planes arrangement for the second case study, a) The best set in the first generation b) The optimization result

increase in calculation time was considered as the next step in this research.

#### 4.4 Improving the Search Technique

The results in Section 4.2 showed an improvement in the slice planes locations at the end of the optimization process. However, premature convergence in the population is still an issue that causes the algorithm to trap in a local optimum during.

In the following sections, an explanation of premature convergence and a review of methods currently used to prevent this problem, are presented. Then, a new method to improve the search algorithm is introduced. This method prevents premature convergence in the population and allows the algorithm to continue searching for a more reliable solution. Next, three different case studies are presented and their optimization results are discussed.

## 4.5 Premature convergence and its treatment

In the current optimization problem, there are two independent parameters which need to be minimized at the same time, volume deviation and the number of slices. This is what called multi-objective function optimization. Premature convergence is an issue in the optimization of multi-objective functions. It happens when the optimization process gives a local optimum as the solution instead of a global optimum. Genetic algorithms is one of the solution to prevent premature convergence. The mutation operator in genetic algorithm was designed to help the system to escape from a local optimum. Even so, in some cases, the mutation operator effect is not sufficient.

As it is illustrated in Figure 4-15, at the beginning of the optimization process, there are too many thickness vectors that their objective function values are close. Therefore, such a system has too many local optima. During the optimization process, there is always a possibility that the system converges to one of these local solutions. In genetic algorithm, mutation operator was designed to prevent trapping in a local optimum by performing a drastic change in some randomly selected members of the population. In this specific application, mutation operator changes the value of one thickness amongst all thicknesses in a thickness vector. As the it was shown in the examples provided in Section 4.2, this is not enough to prevent premature convergence. As suggested in Section 4.2, increasing the population size helps the system to search a larger area of the solution space. Consequently, the quality of the optimization results is improved by this modification. However, since the slicing process is lengthy, a method is required to not only prevent premature convergence, but also let the genetic algorithms search the solution space more efficiently. Some methods that have been suggested in the literature are presented below.

### 4.5.1 Parallel genetic algorithm and niching methods

Parallel genetic algorithms typically divide the solution space into subpopulations. This helps the system to consider different areas of the solution space. Consequently, the searching performance is increased with this modification. Moreover, the calculation process for each subpopulation can be done on different processors. If the system has the chance of looking for an

optimum in different portions of the solution space, then there is a greater possibility of finding more reliable results.

Although parallel genetic algorithms improve searching performance, having several powerful processors available at the same time is not always possible. This is the disadvantage of the parallel method, which makes it unsuitable for the aim of the current research.

To maintain diversity in the population, there are other methods which are mostly categorized as niching methods. These are biological based methods. In biology, each niche has finite physical resources which have to be shared among the population of that niche. Niching methods divide all members of the population into groups based on their fitness values. Each group, which is named as a niche, represents a group of individuals with almost the same characteristics.

As mentioned in [34], niching methods represent the natural emergence of species in the environment (solution space). Different niching methods are presented in [34] and [35]. Fitness sharing as one of the most important niching methods is described in the following section.

### **Fitness sharing**

Fitness sharing was originally introduced by Holland [35] and then improved by other researchers such as Goldberg and Richardson [36]. Fitness sharing is a nature-based method. In biology, animals use different methods to survive. Some survive by hunting, others by grazing and so on. As mentioned in Beasley et al.[34], each group of animals that uses the same survival technique is referred to as an ecological niche. Since each niche population suffers from a shortage of physical resources, these resources must be shared among all members of the niche population. This pushes all species in an ecological population to create subpopulations in different niches. The size of each niche is directly related to the availability of physical resources for that specific niche. Each maxima means physical resourcefulness; in other words, a niche can exist around it. Consequently, the shared fitness for each individual in a subpopulation is proportionally related to the value of the maxima as well as the number of members in that niche. This model can be used in function optimization.

The question is how the locations of niches can be estimated. This means a criterion is needed to determine whether or not two individuals can be grouped into the same niche.

As Goldberg and Richardson [36] mentioned, two individuals can be in the same niche if the difference between their fitness is smaller than a value called the niche radius. The method to find the niche radius is presented in [37].

Despite its benefits, the niching method has some disadvantages. As pointed out by Smith et al. [9], for niche radius calculation, the differences between the fitness of all individuals in the population should be found. Therefore, the time for niche radius calculation in each generation is added to the time for the standard genetic algorithm. As noted in [9], this time is proportionally related to the second order of the population size. Consequently, by increasing the population size, the time which is needed to complete the calculation for each generation is rapidly increased. This could be a problem, especially when a large population exists, or in the cases where the fitness calculation is lengthy.

All other niching methods, such as *sequential niching method*, *restricted tournament selection*, *standard crowding* and *deterministic crowding*, suffer from the timing problem since they are based on the fitness function calculation for not only the main population, but also other elements such as offspring or members of a subpopulation. Thus, for the application of this research, a new method is needed to maintain population diversity without necessitating extra fitness calculations.

## 4.6 Weak elimination crowding method

Premature convergence, in this specific application, occurs when the system does not have sufficient resources to create new thickness vectors. In other words, the premature convergence is realized when all thickness vectors merge to a unique thickness vector which is a local optimum solution. In this case, the standard thicknesses which can be used by the system are limited to the thicknesses in this locally optimum set. Therefore, a method is needed to provide more resources for creating offsprings during iterations.

The *weak elimination crowding* is the new crowding method which has been designed for the purposes of this research. It gives the system more options for creating new thickness vectors by injecting standard thicknesses into each generation of the population.

In this crowding method, fitness values are calculated for all members of the current pop-



ulation as in regular genetic algorithms. Then all members are ranked based on their fitness values. The  $N$  weakest members of the population are then replaced by  $N$  new randomly created members.  $N$  is calculated by

$$N = C_f M \quad (4.2)$$

where  $C_f$  is the user-defined crowding factor value. This value represents the magnitude of the diversity in the population of  $M$  thickness vectors.

Figure 4-18 shows where the weak elimination crowding method enacts in the optimization process. As depicted in Figure 4-18, after weak elimination crowding method injects new members into the population, the old and new members of the population will undergo crossover and mutation operators to create the next generation.

It should be mentioned that, since the weak elimination crowding method adds diversity to the population, it may take longer time for the system to converge to an optimum. Even with a high value for the crowding factor, convergence is not guaranteed. Therefore, a new termination criterion is developed to match this modified version of genetic algorithm.

#### 4.6.1 Termination criterion

The number of iterations was used as the termination criterion in Section 4.2. Due to the value of the crowding factor, it is possible that the convergence will not take place in the population within a specific calculation time / Number of iterations. Therefore, the termination criterion needs to be modified to stop the process as soon as a solution with a predefined accuracy is found.

The objective function is presented by Equation 3.4. In the newly suggested termination criterion, prior to starting the G.A. process, the ideal result is found based on the most important parameter in the objective function. For example in the case that having the minimum volume deviation is more important than having the minimum number of slices, the best solution with maximum fitness value is generated by the thickness vector which contains only the minimum available thickness. On the other hand, it is possible to check the number of thickness vectors that have a close fitness value to the fitness value created by this uniform slicing with minimum available thickness.

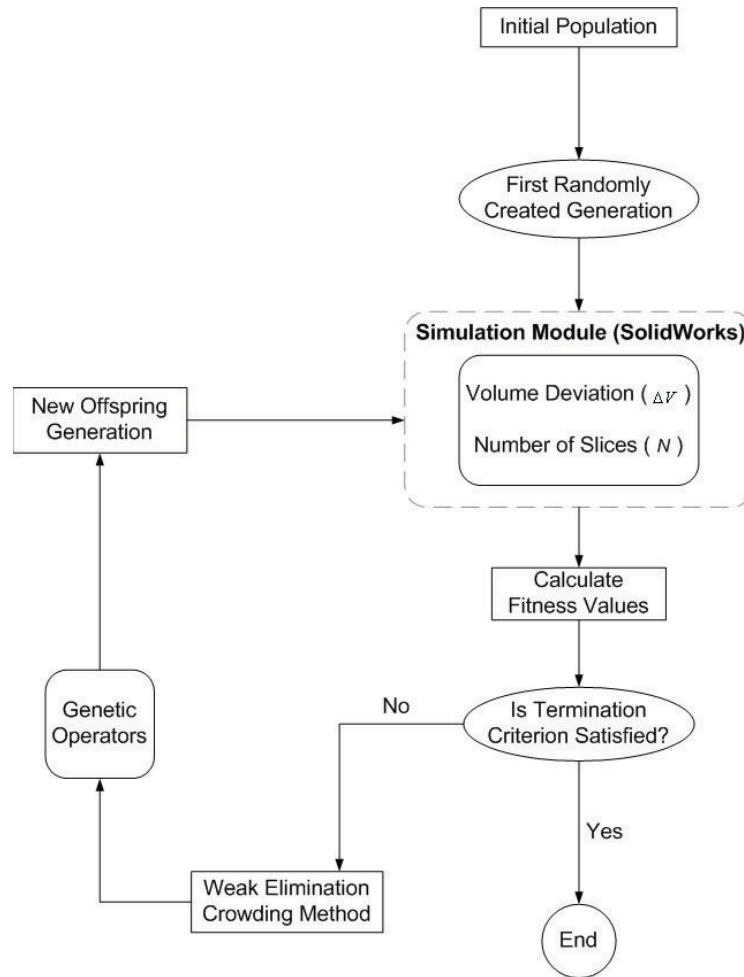


Figure 4-18: Schematic of the modified genetic algorithm procedure in the current research

Also, the value of the volume deviation can be checked for these "strength" chromosomes. The process will stop when a specific user-defined number of chromosomes can generate a low volume deviation. This means the population can now be investigated for the convergence. Moreover, the user can choose the accuracy of the final result by specifying the difference between the best volume deviation in the population and the minimum volume deviation generated by the uniform slicing.

It should be mentioned that the number of generations can still act as a termination criterion, since the program should stop in a situation where there is no convergence to a good local optimum after a specific number of iterations.

In conclusion, the new termination criterion is actually a set of criteria that can be summarized as follow:

- 1) The desirable volume deviation overshoot is selected. This means, as soon as the algorithm finds a thickness set that creates a volume deviation less than a user defined value, it checks the second criterion.

- 2) The second criterion measures the convergence in the population. This can be checked by comparing the value of the maximum fitness in the population and the average fitness value. These values converge when the number of chromosomes with the same fitness value is increased in the population. This is a user-defined difference, which means the optimization process stops as soon as the difference between the maximum fitness and the average fitness in the population is less than or equal to a user-defined value.

- 3) Despite these criteria, as mentioned earlier, a generation criterion is still needed. This criterion stops the program after a specific number of generations when the convergence to the expected solution does not occur. Such a case happens specially when the crowding factor has a high value and switches a high portion, of the population with new members.

## 4.7 Results

The same tool represented by Figure 4-9 is considered for this case study. The standard set for the optimization process is presented by

$$\{1/2'', 7/16'', 3/8'', 5/16'', 1/4'', 3/16'', 5/32''\} \quad (4.3)$$

Before starting the actual optimization process, a pre-run is needed to determine the minimum volume deviation. The result, derived from uniform slicing with a  $5/32''$  thickness value is  $\Delta V = 4.79 \times 10^{-6} m^3$ . This only represents the ideal volume deviation. Although making this tool with the laminas with uniform thickness of  $5/32''$  minimizes the volume deviation, it is more costly due to the increase in laser cutting cost.

Table 4.1 summarizes the results of the optimization program. Three different cases are considered to show the effect of adding the proposed crowding method to the optimization procedure. As shown in this table, the value of  $\beta_1$  is ten times larger than  $\beta_2$  for all three runs, which means the same objective function is used for all runs. Also, the values of two genetic operators are the same for all three runs. However, to show how the population size affects the quality of the solution, the third run has a larger population size than the first and second runs. Furthermore, as depicted in Table 4.1, the crowding factor for the first run is zero. This means the first run uses the standard genetic algorithm as discussed in Chapter 3. The weak elimination crowding method is employed in the second run to prevent premature convergence in the same system. As Table 4.1 shows, the system can reduce the volume deviation value by almost eleven percent simply by using the proposed crowding method. More importantly, it converges to this higher value of fitness, faster than the first run. As explained in Section 4.3.1, a new termination criterion is needed to stop the optimization process as soon as the system can find a reliable solution. This new termination criterion, as a combination of three different criteria, has the following characteristics:

1) The desirable volume deviation overshoot is 30%. This means as soon as the algorithm finds a thickness set that creates a volume deviation less than  $1.3 \times (\text{Min. volume deviation})$  it checks the second criterion.

2) The fitness convergence rate is considered 15%. This means as soon as the difference between the maximum fitness and the average fitness in the population is less than or equal to  $0.15 \times (\text{Max. fitness in population})$ , the optimization process is stopped.

3) As explained in Section 4.5.1, there is still a need for another stop criterion to terminate the algorithm when an appropriate convergence does not occur in the population after a specific

Table 4.1: Different case studies in optimization of injection mould laminated manufacturing

Parameters	Run1	Run2	Run3
$\beta_1$	10	10	10
$\beta_2$	1	1	1
Crossover Rate (%)	50	50	50
Mutation Rate (%)	10	10	10
Population Size	20	20	50
Crowding Factor (%)	0.0	10	10
Number of Iterations	20	13	24
Minimum Volume Deviation after Termination	$7.85 \times 10^{-6}(\text{m}^3)$	$7.08 \times 10^{-6}(\text{m}^3)$	$6.92 \times 10^{-6}(\text{m}^3)$
Number of Slices	14	16	14
Highest Fitness Value after Termination	0.01081	0.011509	0.01202
Calculation Time	233 <i>min.</i>	151 <i>min.</i>	700 <i>min.</i>

amount of time. Therefore the number of iterations can still be used as the final termination criterion. This final criterion which is the number of iterations, is set to 30.

In the final case, to show how an increased population size can affect the optimization results, a population of fifty thickness vectors is considered. However, the other run characteristics are exactly the same as the second run.

Figure 4-19 shows the value of volume deviations for all thickness vectors in the first generation (at the left) and the last generation (at the right), in all three cases. As depicted in Figure 4-19 (a), in the first run, the optimization process can create thickness vectors that reduce the amount of volume deviation. This figure also shows that, at the time of termination (the 20th iteration), almost all thickness vectors produce the same volume deviation. In fact, due to convergence in the population, all thickness vectors are the same.

In the next run, the weak elimination crowding method is employed to improve the search technique. As depicted in Table 4.1, a 10% crowding factor is applied to the same system as in the first run. This means, for a population of twenty thickness vectors, the two weakest chromosomes in each generation are replaced by two newly created thickness vectors. Figure 4-19 (b) shows diversity in the population in the last generation. Therefore, the system can find a set that creates less volume deviation in the second run. The amount of  $\Delta V$  for the second run is  $\Delta V = 7.08 \times 10^{-6} \text{m}^3$ , while the volume deviation that the best set in the first run could create was  $\Delta V = 7.85 \times 10^{-6} \text{m}^3$ . Finally, the program can find a better solution in the second run faster than the first run, as it takes seven iterations, or more than 80 minutes, less to reach

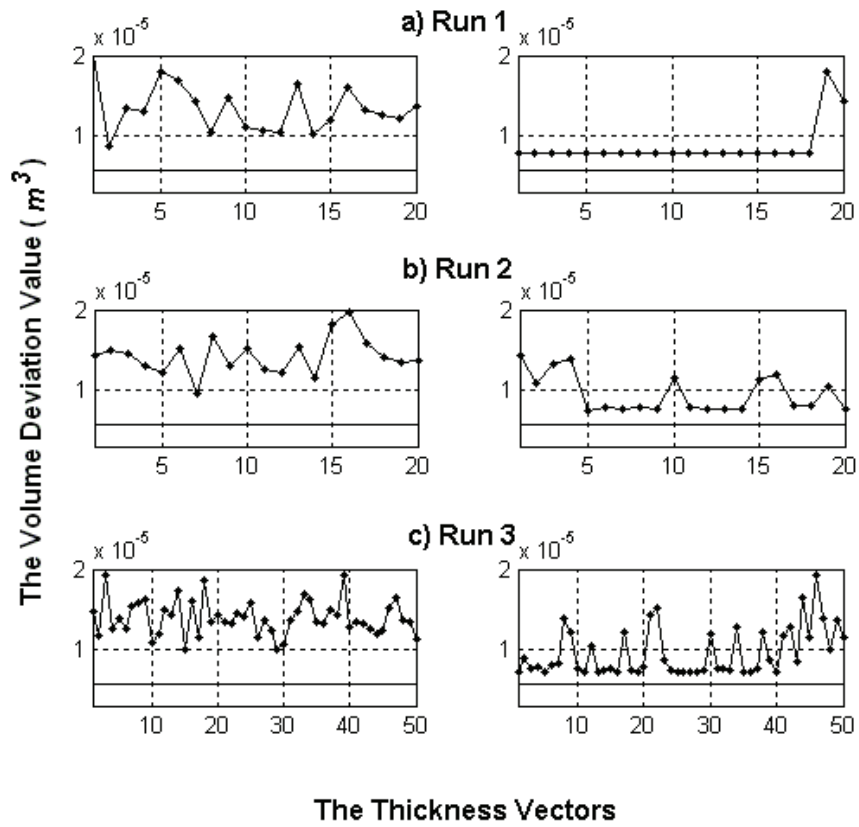


Figure 4-19: Comparison of volume deviations with the ideal value for the first generation in the left and the last generation in the right (— ideal volume deviation, —●— calculated volume deviation)

the solution that satisfies the convergence-based termination criteria.

To show the effect of increasing the population size on the optimization results, in the last case, the test was conducted on a population of fifty thickness vectors, while the other characteristics are the same as in the second run. In this case, the best set creates a lower amount of  $\Delta V = 6.92 \times 10^{-6} m^3$  compared with the first and second runs. Although due to a larger population size, the calculation time needed for this case is higher.

Figure 4-19 shows that, during the different generations of the three runs, the minimum value of volume deviation is getting closer to the ideal value which is  $\Delta V = 4.79 \times 10^{-6} m^3$ . Furthermore, the number of thickness vectors which produce the volume deviations that are close to the one produced by the ideal set, is increased during generations for each run.

Figure 4-20 presents the fitness values of all population members in the first and the last generations in comparison with the average fitness value, for all runs. As shown in this figure, in the first run, due to the premature convergence, almost all members of the last generation produce the same fitness values. This means, the choices for the system to search for an optimum is reduced from one generation to the other. As the results show, the average fitness value at the end of the process in the first run is the lowest one among the three runs.

Consequently, Figure 4-20 displays the effect of the weak elimination crowding method on preventing premature convergence and improving the fitness values. The second run has a 10% crowding factor, while the other run characteristics are exactly the same as the first run. As Figure 4-20 (b) and Table 4.1 show, in the second run, the system can reach a better fitness value with the same population size as the first run. It also can be checked by comparing the values of the average fitness in the first and the second run as well. These results show that with the same conditions, the weak elimination crowding method can improve the quality of the solution for this system. To investigate the effect of the population size on the quality of the solution, another run of the program is considered.

Furthermore, as shown in Figure 4-20 (c) and Table 4.1, in the third run, where the population size is larger than the second run but all other conditions are the same, the value of fitness is improved. However, with an increased population size, it takes longer for both termination criteria to be satisfied. This can be seen in Table 4.1.

As depicted in Figure 4-21, the highest fitness values are improved through the generations,

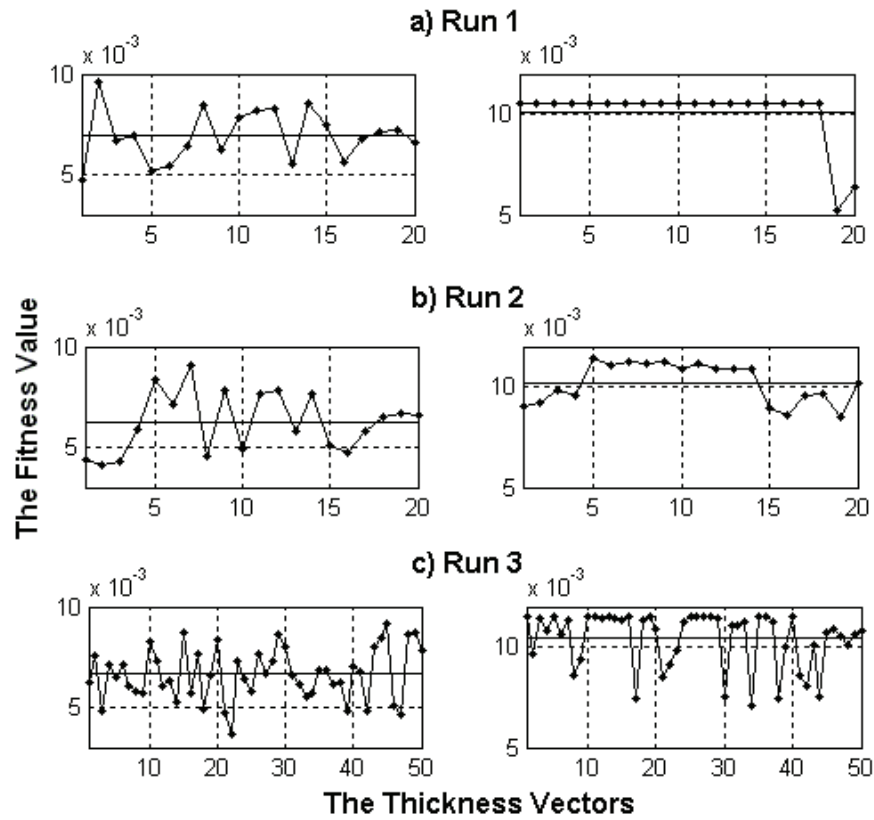


Figure 4-20: Comparison of fitness values with the average value at the first generation in the left and the last generation in the right(— average fitness value, —●— calculated fitness value)



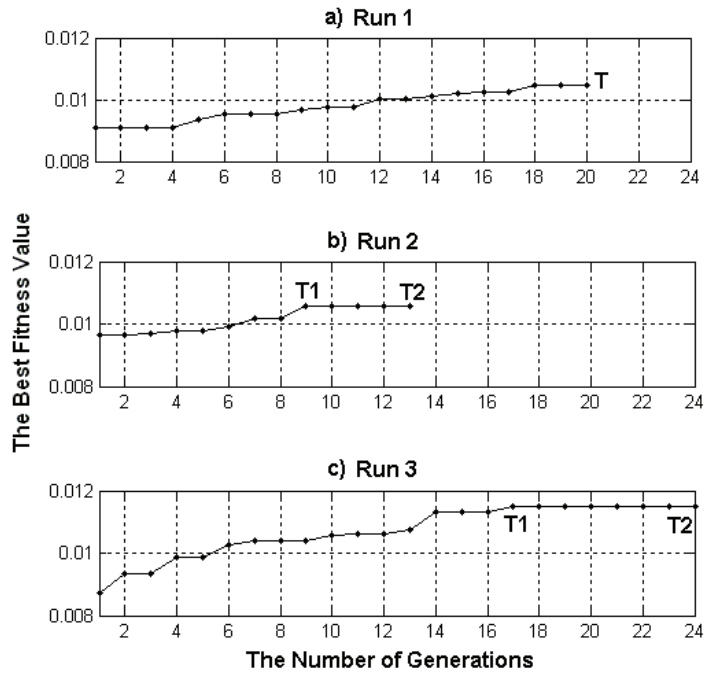


Figure 4-21: The best fitness value in each generation. T: the unique termination criterion is satisfied; T1: the first termination criterion is satisfied; T2: the second termination criterion is satisfied.

in each run. It should be mentioned that, as this figure shows, the best fitness value remains the same in the last few generations for all runs. This is due to the convergence that occurs in the population in the final generations.

In the first run, the system found an optimum in the eighteenth iteration. However, in the last two generations (see Figures 4-19 (a), and 4-20 (a)), the system has no longer a good chance to improve the fitness, since all thickness vectors are now the same.

In the second run, as depicted in Figure 4-21 (b), system can satisfy the first termination criterion in the ninth iteration. However, it still needs more iterations to fulfill the second termination criterion. This is due to the crowding method that injects new members into the population at every generation.

Finally, as Figure 4-21 (c) shows, since a larger population is used for the third run, it takes more generations for the system to satisfy the convergence criterion, in comparison with the second run. However, the maximum fitness value is improved in the third run.

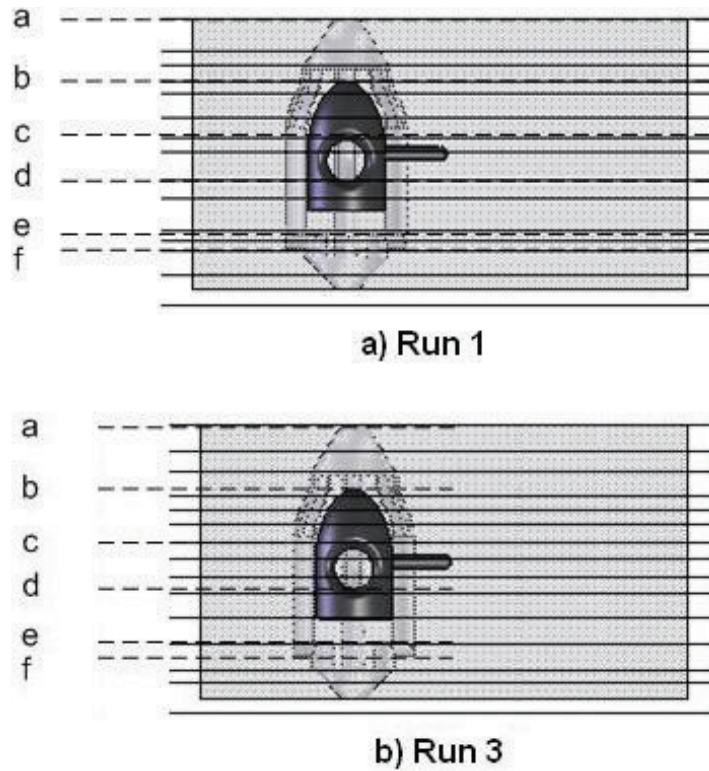


Figure 4-22: The top views of the results for the first and last runs

Figure 4-22 illustrates a comparison between the first and third run results. The figure shows how the weak elimination crowding method helps the optimization process reach better results. The top views of the slice planes arrangement on the CAD model for these two runs are provided here. For ease of discussion, the CAD model surface is divided to some sub-areas.

Although in the area between sections a and b, the slice planes arrangement in the two runs are similar, the difference in the section between b and c is well distinguished. As depicted in Figure 4-22 and Figure 4-23, the cavity and the cooling channels have curved surfaces in this area. Therefore, thinner slices are needed to reduce uncertainty between the CAD model surface and assembled slices. As depicted in Figure 4-22, the program is able to use more slice planes with thinner thicknesses in the third run for this area to cover the curvature in both the cavity and the cooling channels surfaces. Also, in the area between c and d, it can be seen that the slice plane locations in the third run create less material removal for the slices. Moreover, there is another section which shows a significant difference between these two runs results. In

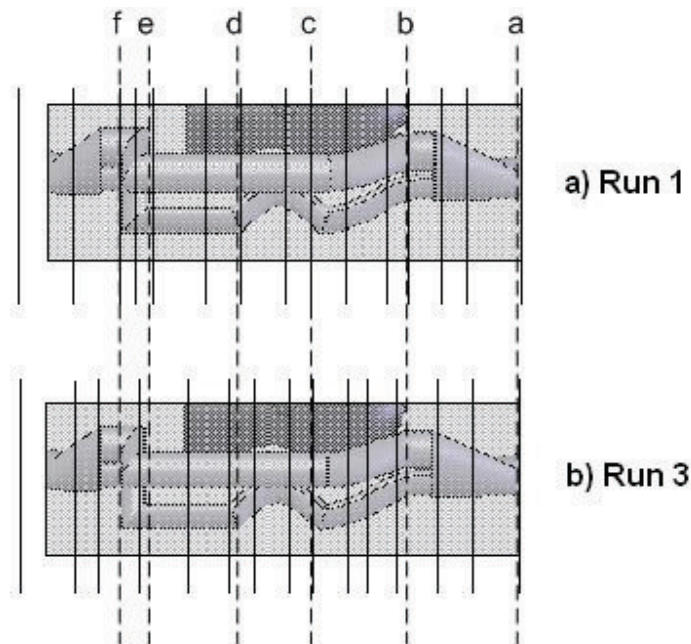


Figure 4-23: Side views of results for the first and last runs

the area between d and e, where the cavity ends, there is a considerable change in the CAD model surface shape. Therefore, having a slice plane close to this point can significantly reduce the amount of material removal in the final product. As seen in Figure 4-22, this is exactly what the program has done at this area in the third run.

Also, in the first run, the program uses two thin slices in the area between e and f, while in the third run the program puts more slice planes behind section f. This is a better arrangement that creates less material removal in the portion of the CAD model which is behind section e.

Furthermore, the number of slices in both runs is the same. This means the third run can reduce the amount of volume deviation in comparison with the first run, without raising the number of slices.

Finally, it should be mentioned that testing larger population sizes to find a more reliable solution is not necessary at this time, as the main aim of this paper is to show how the suggested method can improve the quality of the solution.

## 4.8 Conclusion

In this chapter, an injection mould tool with conformal cooling channel was designed based on a conventional tool which was working in Webplas injection mould company. A modified genetic algorithm was used to find the best locations of slice planes in laminated tooling process. The genetic algorithm explained in Chapter 3 applied to the first two case studies to show how it may be trapped in a local optimum after a few iterations. As it was shown in these case studies, premature convergence can not be detected even by choosing a larger population size.

A weak elimination crowding method was introduced and implemented for the application of this research to prevent premature convergence. This technique significantly reduces the processing time for finding the optimum thickness vector. In the second set of case studies, the new crowding method was applied to the CAD model, and the results showed a significant improvement in fitness values. At the same time, the effect of the population size was also studied.

Although the slicing direction in the current research is constant, slicing in different directions may result in more improvement in the fitness value. Therefore, the slicing direction can be treated as an optimization parameter in further studies. In the next Chapter, the methods to find the best slicing direction based on the CAD model surface geometry is introduced.

## Chapter 5

# Slicing Direction Optimization in Laminated Dies

### 5.1 Introduction

So far in this research, the combination of sheet metal thicknesses was considered as the only effective parameter on volume deviation reduction in laminated tooling. In the current chapter, slicing direction as another important parameter in laminated tooling optimization is considered.

Slicing direction in laminated tooling is usually selected manually. In this chapter, a new method to find the best slicing direction for the entire tool is introduced. This helps to find the best slicing direction faster and more accurate. The suggested method is based on surface analysis of the CAD model which is conducted by using the stereolithographical (STL) representation. The STL representation was briefly discussed in Section 3.1.1.

The effect of CAD model surface topology on producing volume deviation is first discussed. Then the procedure to find candidate slicing directions is explained, and the relation between surface normal vectors and the candidate directions is studied. Also some examples are presented to show the performance of the suggested method. Finally a method for global search for the best slicing direction(s) is introduced.

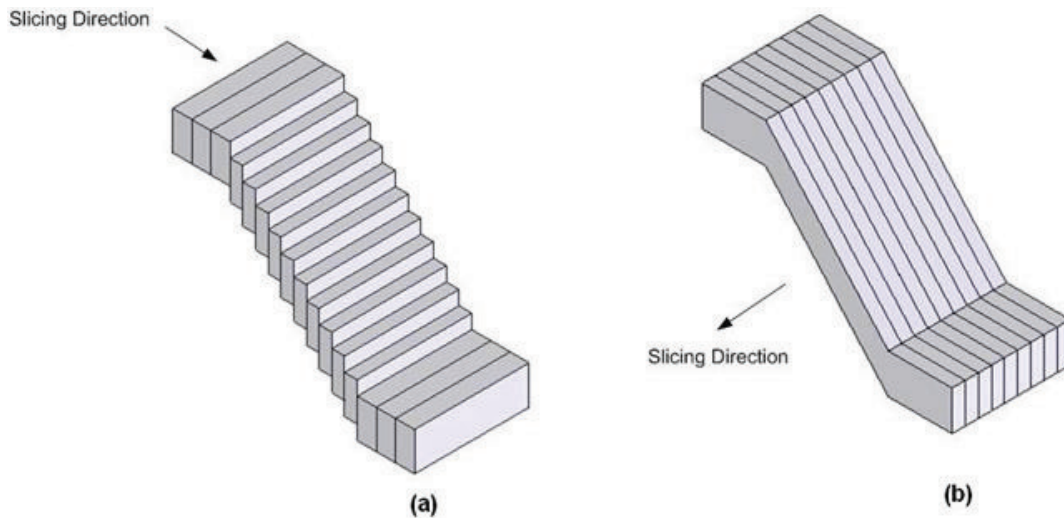


Figure 5-1: A change in slice direction from (a) to (b) eliminates the volume deviation value

## 5.2 The Effect of Surface Topology on Slicing Direction

In addition to slice thicknesses, direction of slicing is another parameter that can be considered for surface quality improvement in laminated tooling. Figures 5-1 and 5-2 visualize the effect of different slicing directions on volume deviation reduction. As depicted, the direction taken in Figure 5-1 (b) produces zero volume deviation, whereas by adding two new features to the model, as depicted in Figure 5-2 (a), the situation is completely changed. Figure 5-2 (b) shows that there is still a possibility of having no volume deviation if the slicing is done in two different directions which are selected based on the CAD model geometry.

In volume deviation calculation for a CAD model in a specific direction, its entire surface is considered as a combination of tiles. Each tile is a sub-surface of the CAD model that can be considered as a planar surface. In some cases such as what presented by Figure 5-3 (a), the entire CAD model surface is a combination of planar sub-surfaces, tiles. However in the case of having non-planar surfaces, the STL representation of that specific non-planar surface is considered. Such a case is studied in Section 5.3

Figure 5-3 shows how different values of extra volume are produced based on the choice of slicing direction. As shown in this figure, there is no extra volume in the case presented by Figure 5-3 (d), whereas in Figures 5-3 (b) and 5-3 (c), different values of extra volume are

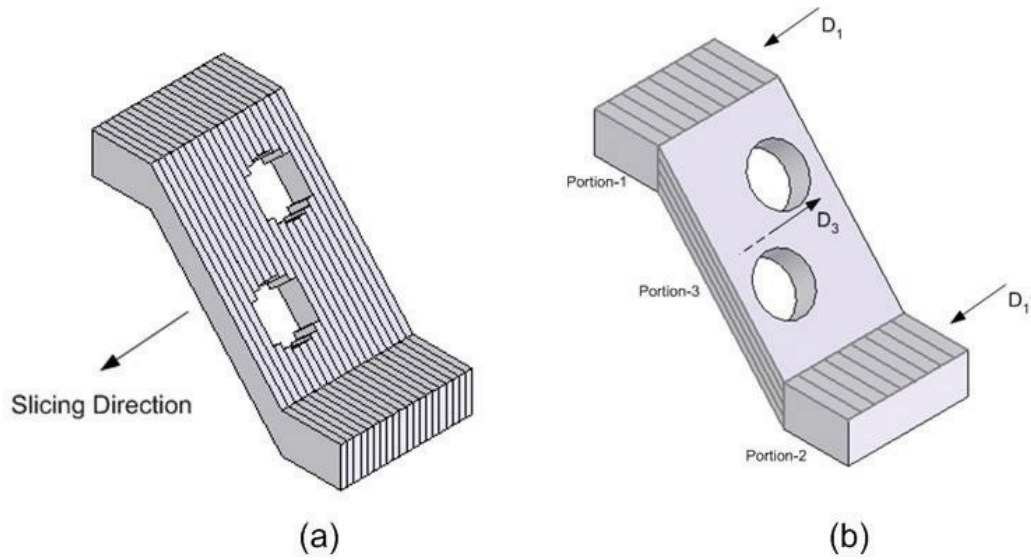


Figure 5-2: The effect of different slice directions on the slicing process performance

produced on tile 6 due to the different angles between slicing directions and the normal of this tile. These examples show that a criterion is needed to determine whether or not a tile produces extra volume. The error triangle, which is introduced in the following, is defined as a quantity for the extra volume estimation of a tile.

### 5.2.1 Error Triangle

As depicted in Figure 5-4, an error triangle is the triangle created between each slice and actual CAD model surface. In this figure,  $t$  is the slice thickness along the slicing direction and  $l$  represents the length of the first approximation of the CAD model surface between the two consecutive slices. Also,  $c$  is the cusp height and  $\alpha$  is the angle between  $d$  (slicing direction) and a surface normal  $\vec{N}$ . Finally,  $l'$  is the misplacement length between two consecutive slices.

The error triangle area which is called cusp area, could be used as a representation of the value of extra volume in a tile. This area can be found by either of the two following formulas:

$$A = \frac{1}{2}lt \cos \alpha \quad (5.1)$$

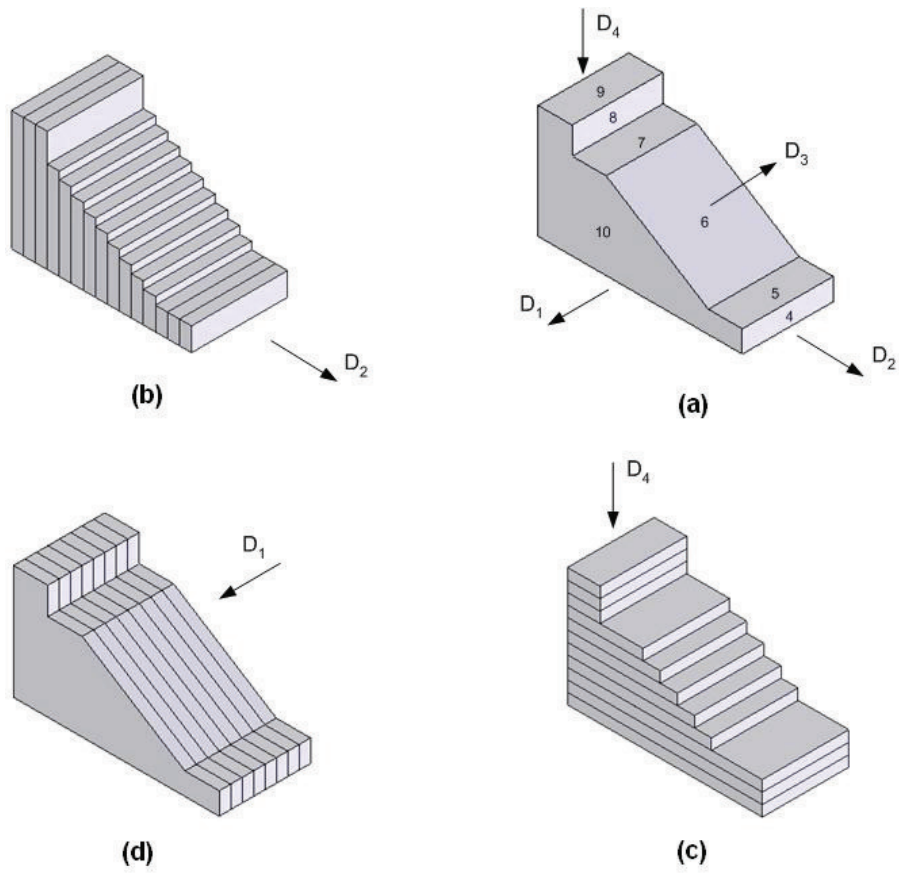


Figure 5-3: CAD model tile behavior in different slice directions

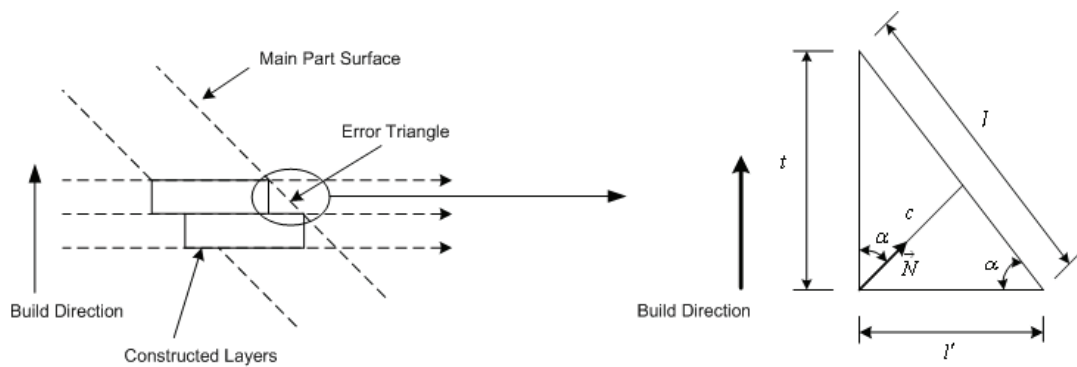


Figure 5-4: Error triangle



$$A = \frac{1}{2}ll' \sin \alpha \quad (5.2)$$

From Equations (5.1) and (5.2), it is understood that when the slicing direction is either perpendicular or parallel to the surface normal vector, the cusp area and consequently the volume deviation is zero.

This can be considered as the basic rule in the best direction investigations. Among all the tiles creating the entire CAD model surface, the volume deviation on a tile in a specific slicing direction is zero, when the area of its error triangle is zero, or in other words: its normal vector is perpendicular or parallel to the slicing direction. Such a tile which creates negligible volume deviation is defined as a *well-located tile* and its normal vector is referred to as a *co-operator normal vector* for that specific direction.

### 5.3 Surface Analysis Method

As mentioned in Section 5.2, tiles that are parallel or perpendicular to the slicing direction result in a zero error triangle area and do not produce any extra volume in the slicing process.

The proposed method to find the best slicing direction, considers all the normal vectors as the potential solutions. Therefore, the best way to evaluate the slicing efficiency of each normal vector is to investigate its situation against all tiles on the CAD model surface.

Figure 5-5 represents the model shown in Figure 5-3 (a), with the normal vector corresponding to each tile. It is important to note that the three tiles and their normal vectors cannot be visualized in this figure. As can be seen, three different directions:  $D_1, D_2$  and  $D_4$  are investigated. Among these three directions, only  $D_1(\vec{N}_{10})$  is parallel or perpendicular to all normal vectors, as both other directions,  $D_2$  and  $D_4$ , are non-parallel and/or non-perpendicular to  $\vec{N}_6$ . Therefore, as depicted in Figures 5-3 (b), 5-3 (c) and 5-3 (d), during the slicing process these directions create extra volume on the tile that  $\vec{N}_6$  belongs to.

It is anticipated that larger tiles produce higher extra volume than smaller tiles. Therefore, in the proposed searching process, besides the number of normal vectors that are parallel or perpendicular to a specific direction, the magnitude of the area of the tile that belongs to each normal vector has a sizable impact on the results.

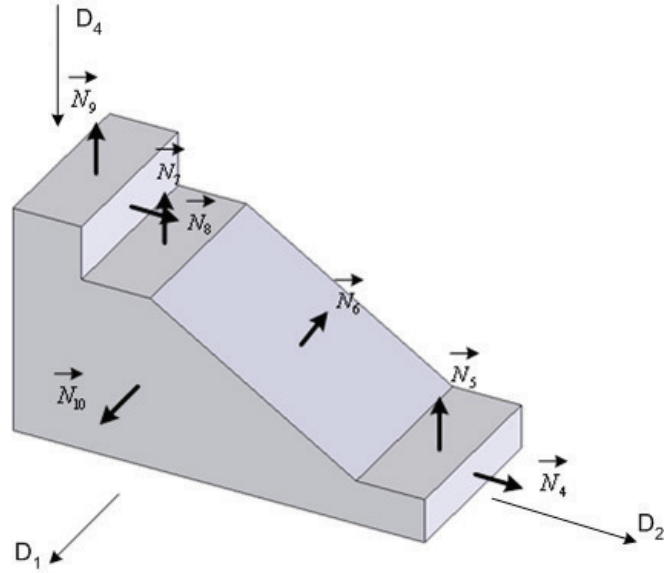


Figure 5-5: Tiles and normal vectors on a sample model

Figure 5-6 represents the proposed direction finding algorithm. Here  $\vec{N}_i$  is the normal vector of tile  $i$ , and  $\vec{A}_i$  represents the area of that tile.

Explaining Figure 5-6, each normal vector  $\vec{N}_i$  is compared to other normal vectors to find the normal vectors parallel or perpendicular to that. This is done by performing Dot and Cross products between  $\vec{N}_i$  and all other normal vectors. The summation of the areas of the tiles whose normal vectors are parallel or perpendicular to  $\vec{N}_i$  is found in next step. The normal  $\vec{N}_m$  which produces the highest value between these summations represents the slicing direction which produces the minimal amount of extra volume in assembled slices.

As explained earlier in this section, a normal vector is defined as the unit vector perpendicular to a planar surface. Therefore, in a non-planar tile, finding this quantity as well as the tile area requires further calculation.

A non-planar tile, such as that presented in Figure 5-7, can be approximated by a number of planar triangles, as shown in Figure 5-8. This is a Stereolithographical (STL) representation of the tile. Tata et al. [31] defines STL as: “a tessellated representation where the solid model is represented by a number of three-sided planar facets (triangles).” The idea of STL files is employed from rapid prototyping for investigation of non-planar tiles in the current work.

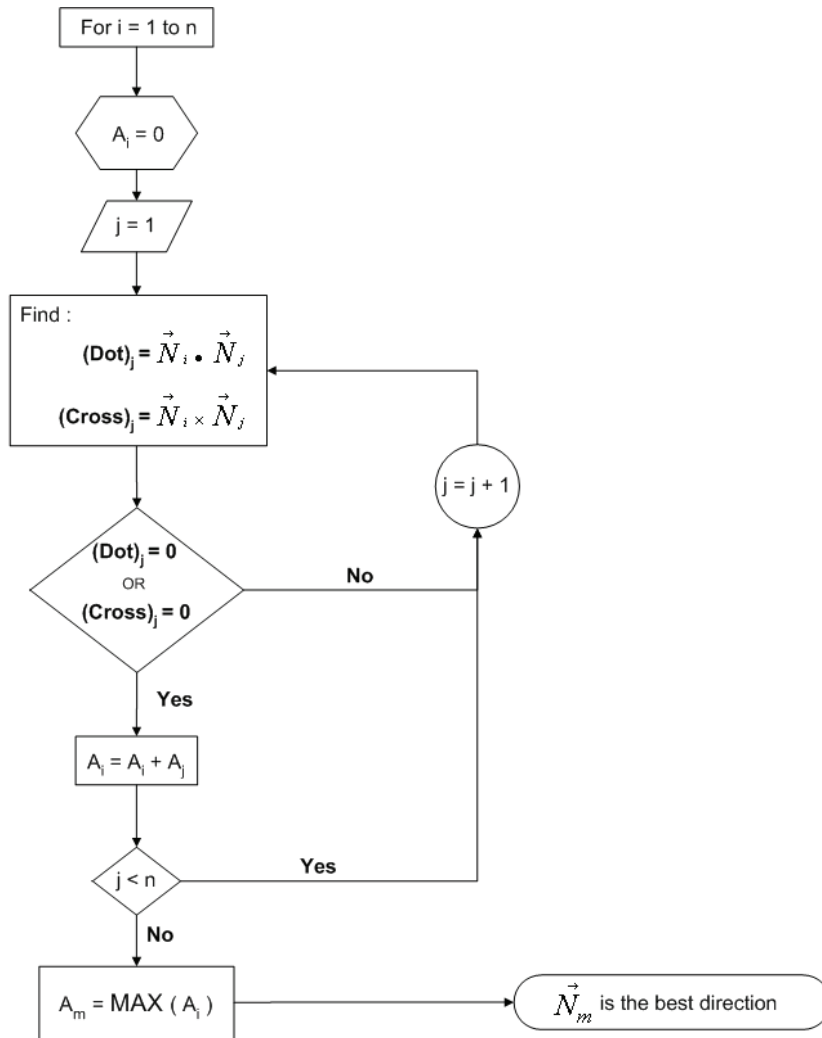


Figure 5-6: Suggested algorithm for optimal direction finding

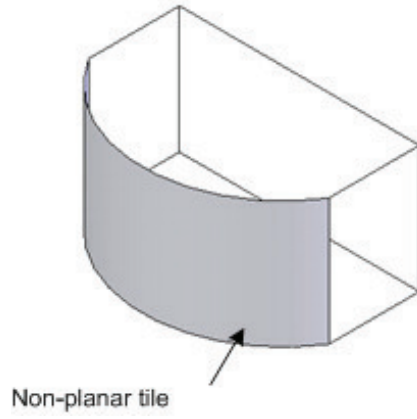


Figure 5-7: A non-planar tile in a CAD model

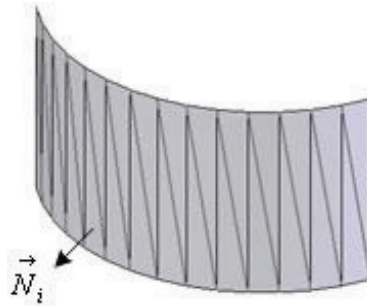


Figure 5-8: Planar representation of a non-planar tile

Table 5.1: Co-operator normal vectors and the areas of well-located tiles for model in Figure 5.9

Candidate Directions	The Co-operator Normal Vectors	Summation of Well-Located Tile Areas on Whole Part ( $mm^2$ )
$D_1$	$\vec{N}_1, \vec{N}_2, \vec{N}_3, \vec{N}_4, \vec{N}_5,$ $\vec{N}_6, \vec{N}_7, \vec{N}_8, \vec{N}_9, \vec{N}_{10}$	8800
$D_2$	$\vec{N}_1, \vec{N}_2, \vec{N}_3, \vec{N}_4, \vec{N}_5,$ $\vec{N}_7, \vec{N}_8, \vec{N}_9, \vec{N}_{10}$	7300
$D_3$	$\vec{N}_2, \vec{N}_6, \vec{N}_{10}$	4300
$D_4$	$\vec{N}_1, \vec{N}_2, \vec{N}_3, \vec{N}_4, \vec{N}_5,$ $\vec{N}_7, \vec{N}_8, \vec{N}_9, \vec{N}_{10}$	7300

## 5.4 Direction Analysis Results

### 5.4.1 Single direction

The goal of the first example is to find a single direction as the best direction for the entire CAD model surface. The investigated model, as well as all potential solutions, i.e., all normal vectors, are shown in Figure 5-9. As depicted in this figure, all normal vectors can be classified into four different directions. The co-operator normal vectors and the summations of the areas of the well-located tiles for each direction  $D_i$  are presented in Table 5.1.

Based on the explanation provided in Section 5.3, the best slicing direction for the CAD model in Figure 5-9 is  $D_1$ , as it has the highest value of well-located tile areas. Figure 5-3 (d) shows that the extra volume on assembled slices in direction  $D_1$  is zero.

### 5.4.2 Multiple Directions

#### Case 1

The proposed algorithm can also suggest dissimilar slicing directions for different portions of a CAD model. Figure 5-2 (b) illustrates an application where variable slicing directions provide

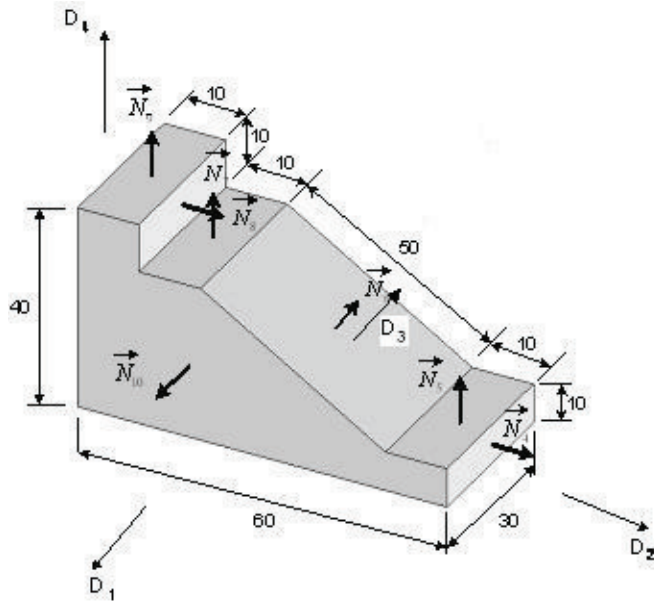


Figure 5-9: A sample model without non-planar tiles (Dimensions are in millimeter)

greater reduction in the extra volume of the final product.

As explained in Section 5.2.1, the area of well-located tiles is the criterion to finding the best slicing direction. Referring once again to Table 1, when the values of well-located areas for two different directions, such as  $D_1$  and  $D_2$  or  $D_1$  and  $D_4$ , are close, either  $D_2$  or  $D_4$  may provide a performance that is just as good or even better than  $D_1$  in some portions of the CAD model. In such a case, there is always an inclination for having more than one slicing direction. The candidates, such as  $D_1$ ,  $D_2$  and  $D_4$  that may get involved in the multiple direction slicing process, are defined as the *favorite directions*. Favorite directions are the directions that have higher well-located tile areas than others. Indeed, in each portion of CAD model, the value of well-located areas for each favorite direction can be used as the criterion to choose the best candidate direction for that specific portion.

To elucidate this, consider the model presented in Figure 5-10. It should be noted that here,  $A'_1$ ,  $A'_2$ ,  $A'_3$ ,  $A'_4$ , and  $A'_5$  are the tiles in the locations behind the seen. Figure 5-11 shows the STL representation of non-planar features  $A_6$  and  $A_7$ .

Again, all normal vectors can be categorized into four different directions. Table 5.2 sum-

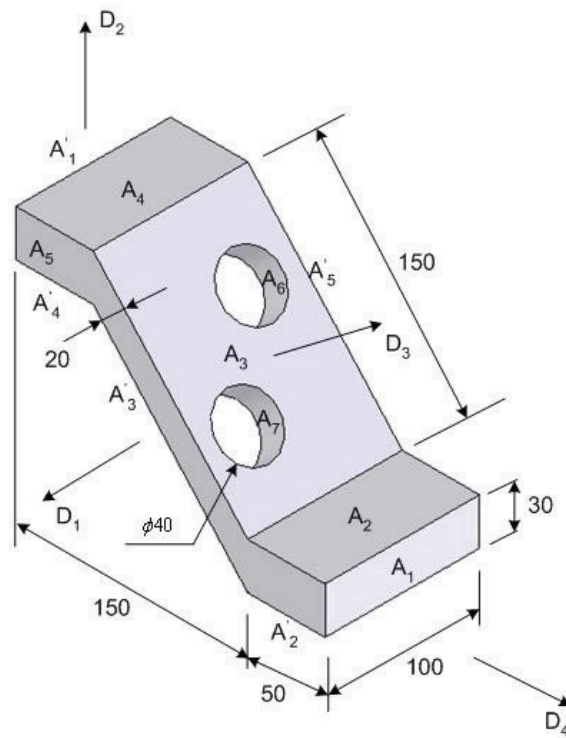


Figure 5-10: A sample model with non-planar tiles (Dimensions are in millimeters)

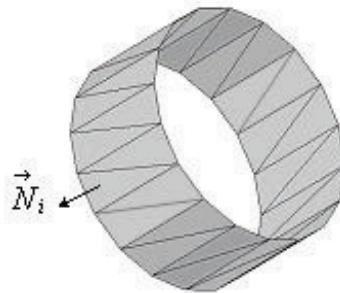


Figure 5-11: STL representation of tile  $A_6$  or  $A_7$

Table 5.2: Co-operator normal vectors and the areas of Well-located tiles for model in Figure 5.10

<b>Candidate Directions</b>	<b>The Co-operator Normal Vectors</b>	<b>Summation of All Well-Located Tile Areas (<math>mm^2</math>)</b>
$D_1$	$\vec{N}_1, \vec{N}'_1, \vec{N}_2, \vec{N}'_2,$ $\vec{N}_4, \vec{N}'_4, \vec{N}_5, \vec{N}'_5$	38000
$D_2$	$\vec{N}_1, \vec{N}'_1, \vec{N}_2, \vec{N}'_2,$ $\vec{N}_3, \vec{N}'_3, \vec{N}_4, \vec{N}'_4,$ $\vec{N}_5, \vec{N}'_5$	62976
$D_3$	$\vec{N}_1, \vec{N}'_1, \vec{N}_2, \vec{N}'_2,$ $\vec{N}_4, \vec{N}'_4, \vec{N}_5, \vec{N}'_5$	38000
$D_4$	$\vec{N}_3, \vec{N}'_3, \vec{N}_5, \vec{N}'_5,$ $\vec{N}_6, \vec{N}_7$	42000

marizes the values of well-located areas for each candidate direction. It is understood from this table that the best slicing direction for the entire model is  $D_2$ . Nonetheless, the user may want to check the performance of all or some of the directions in different portions of CAD model.

Theoretically, the slicing direction can be changed as many times as the user wishes. However, due to the challenges in the joining process, it is preferable to limit the slicing directions to two or three. Referring to Table 2,  $D_4$  has the closest value of well-located area to what belongs to  $D_2$ , therefore,  $D_2$  and  $D_4$  are considered as the favorite directions in this example.

As depicted in Figure 5-12, to start multiple direction analysis, the sample model in Figure 5-10 is divided into three different portions, P1, P2, and P3.

Table 5.3 displays the surface analysis for the two favorite directions  $D_2$  and  $D_4$  in each portion. As Table 3 shows,  $D_2$  provides a better performance in the first and last portions; while in the middle portion it is better to change the slicing direction from  $D_2$  to  $D_4$ . This is due to the higher value of the well-located areas that  $D_4$  generates in P2.

Figure 5-13 visualizes the effectiveness of each favorite direction on the entire CAD model



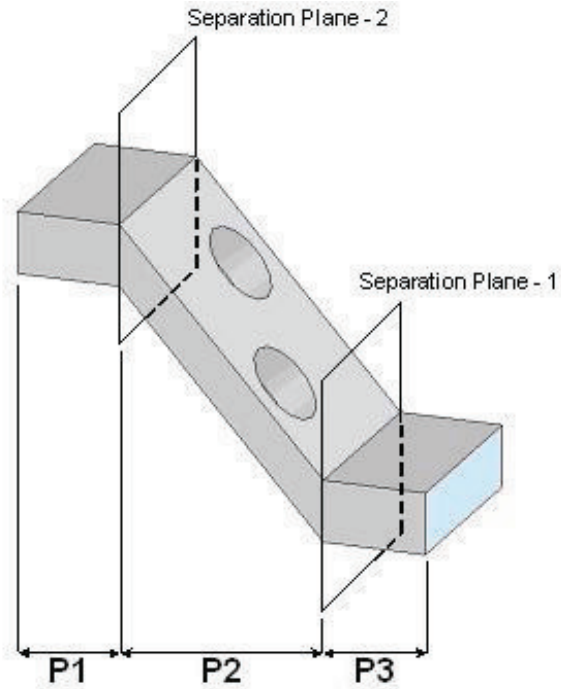


Figure 5-12: Model is divided into different portions to investigate different slicing directions

Table 5.3: Areas of well-located tiles in different portions for the model in Figures 5.10 and 5.12

<b>Favorite Directions</b>	<b>Summation of Well-Located Tile Areas (<math>mm^2</math>) (P1)</b>	<b>Summation of Well-Located Tile Areas (<math>mm^2</math>) (P2)</b>	<b>Summation of Well-Located Tile Areas (<math>mm^2</math>) (P3)</b>
$D_2$	16000	<b>30976</b>	16000
$D_4$	3000	<b>33000</b>	3000

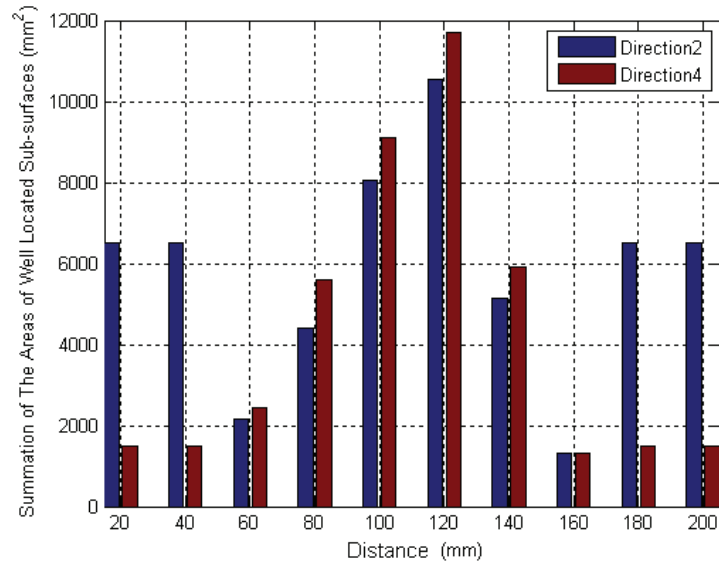


Figure 5-13: Performance of each favorite direction on CAD model

surface. As depicted in this figure, the first favorite direction,  $D_2$ , has a better performance than  $D_4$  starting from the left. However, after 50 mm, it is the second favorite direction,  $D_4$ , which takes over  $D_2$ . This is portion P2 in Figure 5-12. Finally, in portion P3, direction  $D_2$  again provides a better surface quality than  $D_4$ .

## Case 2

Here, the tool in Figure 5-14 is considered for multiple-slicing-direction analysis. This is a hydroforming die which is used at the University of Waterloo.

Figure 5-15 indicates three favorite directions for this tool. The CAD model is then divided into three consequent portions, as depicted in Figure 5-16. Figure 5-17 visualizes the performance of these three favorite directions on the entire CAD model surface. The best slicing direction(s) for this tool can be selected based on the results provided in Figure 5-17. For example, in the middle portion of the tool, P2, Direction 2, which is the second favorite direction shows a better performance than the others, while at the beginning, P1, Direction 1 is the better choice.

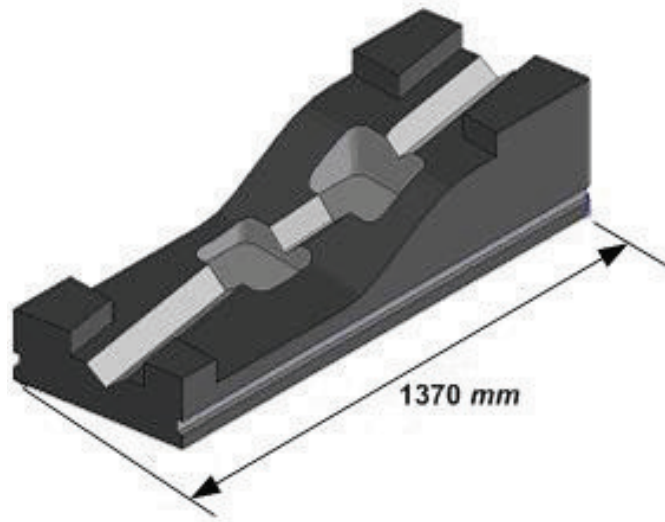


Figure 5-14: The hydroforming tool

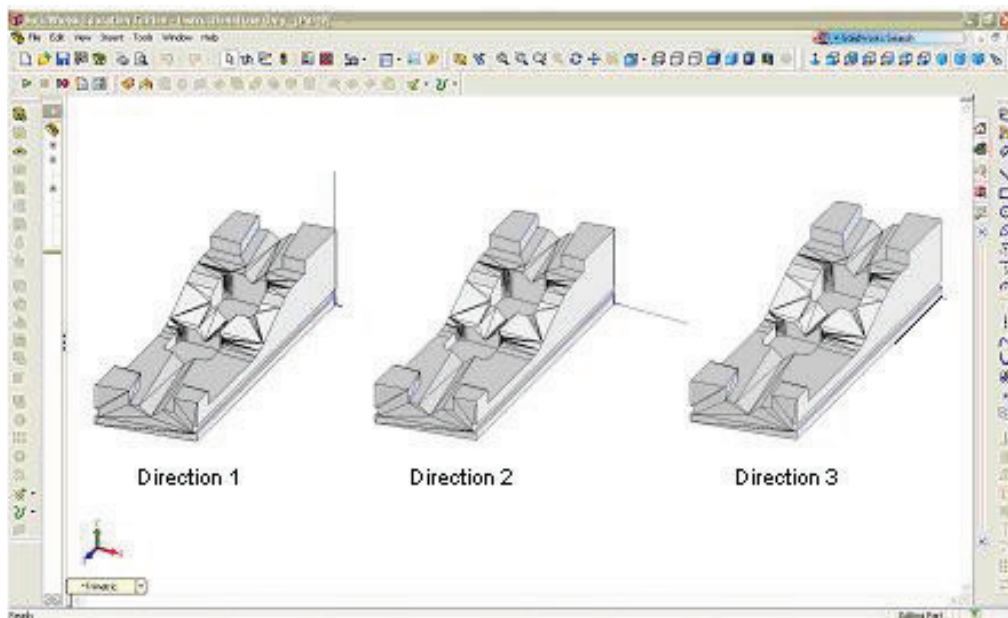


Figure 5-15: The suggested slicing directions from program output

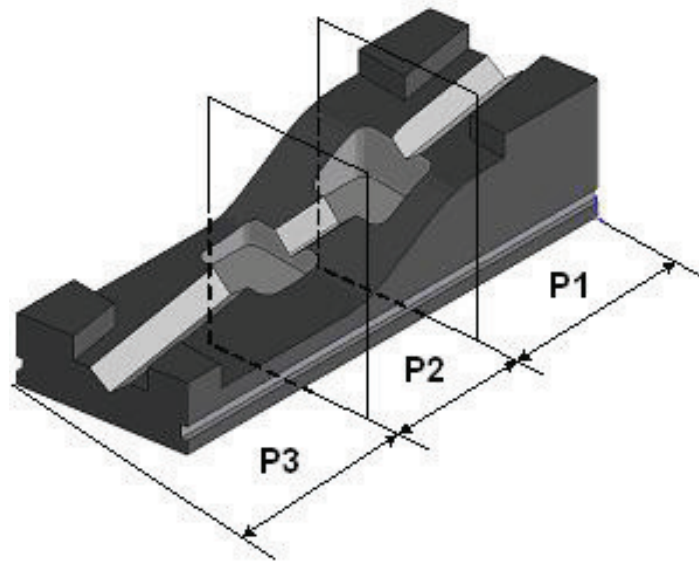


Figure 5-16: Model is divided to different territories to investigate different slicing directions

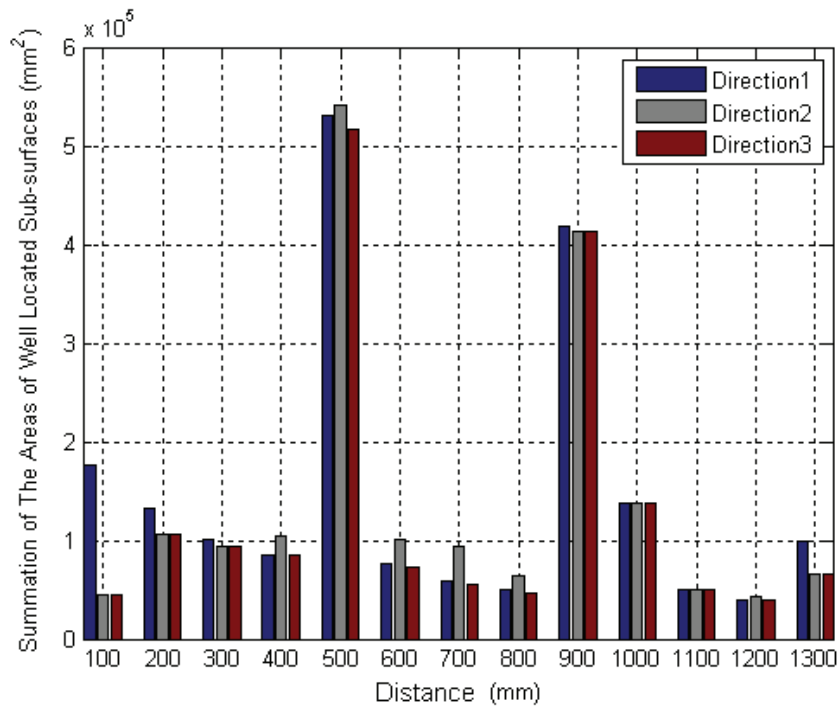


Figure 5-17: Performance of each favorite direction based on CAD model length

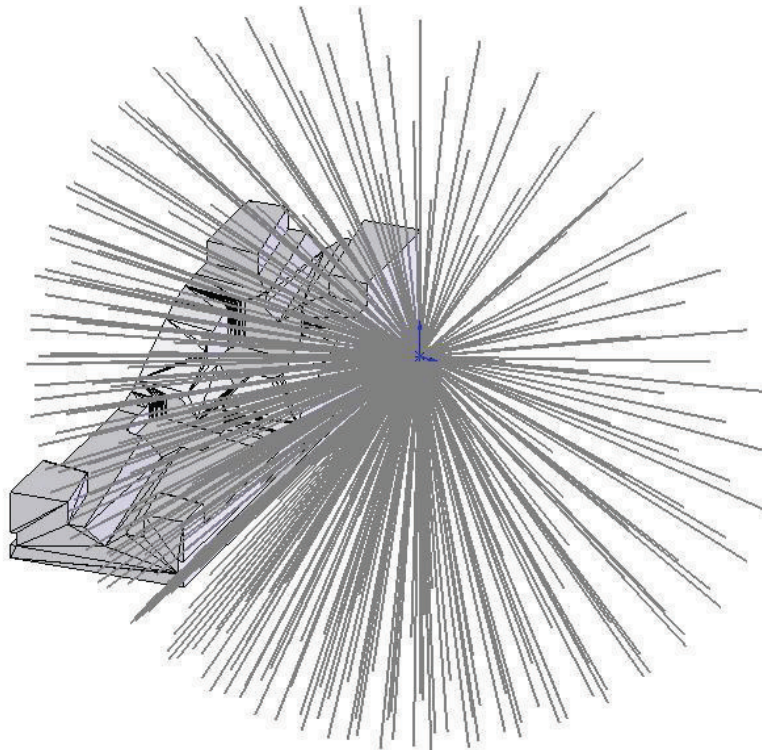


Figure 5-18: All potential slicing directions in the space

## 5.5 Global Search for The Best Direction

The method proposed in the previous sections is based on tile normals. Here, instead of considering only the tile normals, the search is conducted to find the best slicing direction among all possible directions in space. This will neglect the chance of missing an optimum slicing direction by considering only the normal vectors. However, the outcomes show that for the same model, the result of the search is exactly the same in both methods.

To construct the slicing directions such that the entire space get covered, in a cylindrical coordinate system the angles  $\phi$  and  $\theta$  are changed from  $-90^\circ$  to  $180^\circ$   $-90^\circ$  to  $90^\circ$ , respectively, with the increment of  $10^\circ$ , as shown in Figure 5-18. This makes a set of  $28 \times 19 = 532$  possible directions. It should be noted that, by reducing the increment, more potential directions are created and tested. However, in this case, the calculation time is an issue.

The algorithm in Figure 5-6 is re-considered in Figure 5-19. As indicated in this figure, in

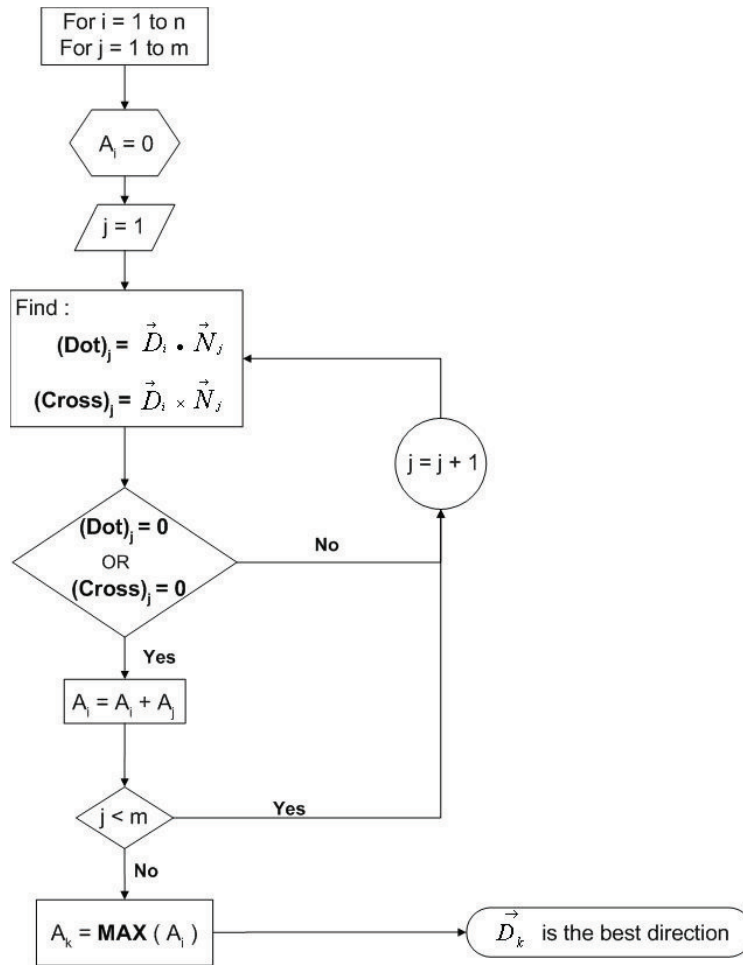


Figure 5-19: Suggested algorithm for globally optimal direction search

the global search instead of comparing each tile normal with others, each of the directions  $\vec{D}_i$  presented in Figure 5-18 undergoes a dot and product operation with all normal vectors. The steps in Figure 5-19 are almost the same as those presented in Figure 5-6, except that here,  $n$  is the number of potential slicing directions. As depicted in Figure 5-19, based on the magnitude of the well-located tile areas produced by each potential direction, the best candidate slicing direction(s) is selected.

Figure 5-20 shows the results of the global best direction(s) search. This shows the amount of well-located tile areas for all potential directions. As depicted in this figure, the directions which produce a considerable amount of well-located tile areas can be classified as six directions.

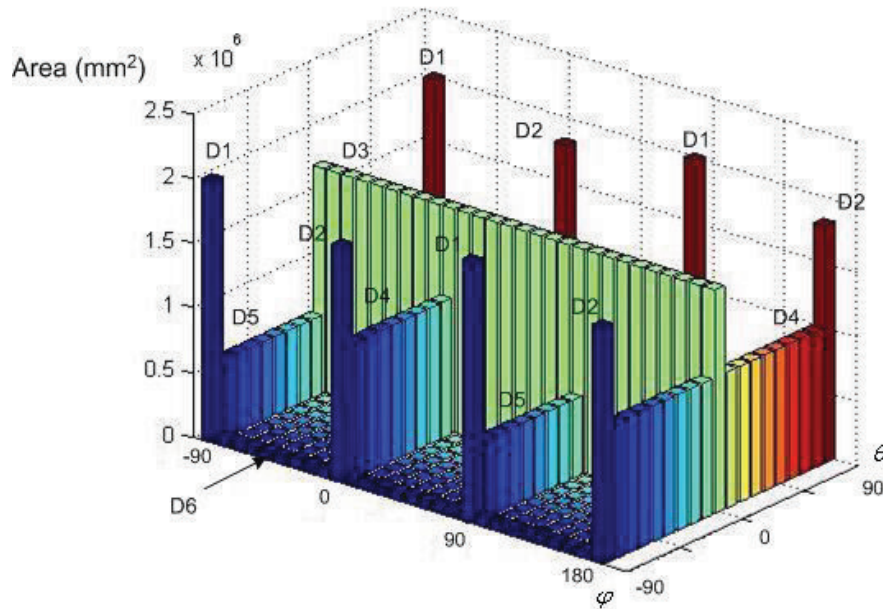


Figure 5-20: Histogram of well-located tile areas produced by favorite directions,  $D_1$  to  $D_6$

Figure 5-21 compares these favorite directions based on the well-located tile areas. From the results in Figures 5-20 and 5-21, the first three candidate directions are presented in Figure 5-22.

## 5.6 Conclusion

The slicing direction as one of the most important parameters affecting surface jaggedness in laminated tooling process was investigated in this chapter. An analytical method based on the situation between normal vectors was proposed to determine the best slicing direction based on the geometry of CAD model surface.

In some cases, based on the close performances of the output directions of the single direction study, user may decide to conduct a multiple directional study as well. In such a case there is a possibility that having different slicing directions generates less surface jaggedness. Therefore, a method to investigate different slicing directions was also proposed in this chapter. The

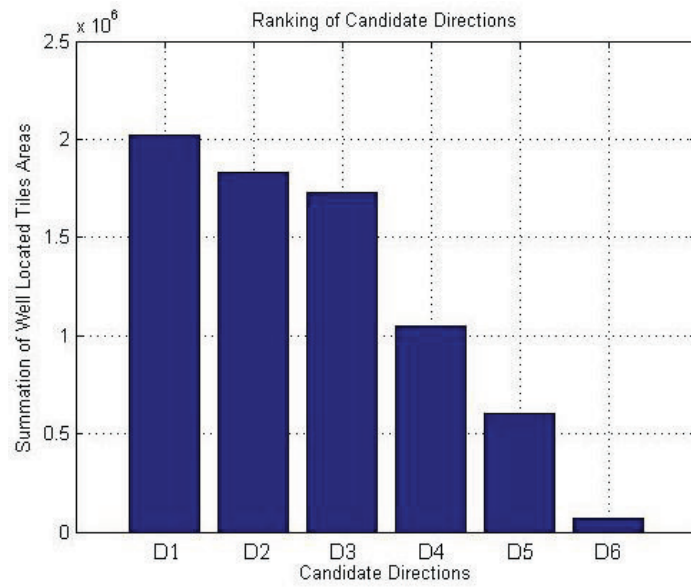


Figure 5-21: Rank of favorite slicing directions

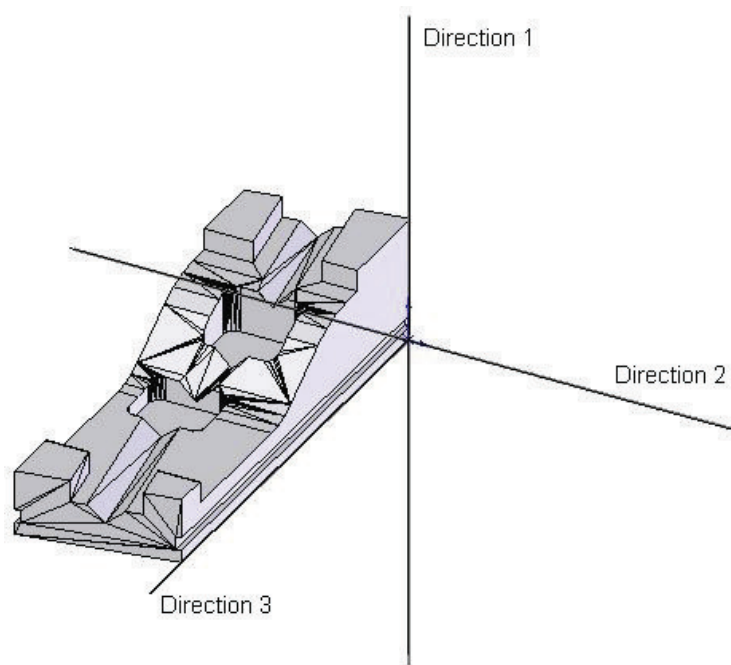


Figure 5-22: The outcomes of the global best direction investigation



suggested algorithm is able to find the best slicing direction for different portions of the entire CAD model surface.

Moreover, in the proposed method there was still a poor possibility that a good direction, which is not among the normal vectors, is omitted. To solve this problem, a set of all potential directions was created, and then the suggested method was conducted on whole population of these directions. Although the results in both cases are the same, the second approach is always suggested for a more reliable solution. However, the first approach is faster.

## Chapter 6

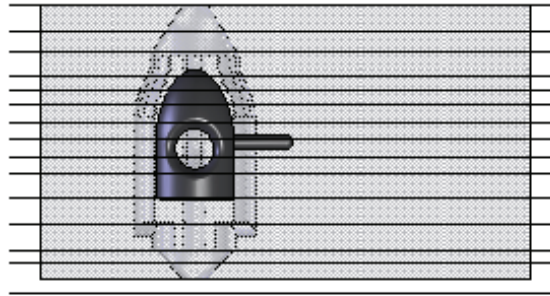
# Experimental Analysis

### 6.1 Introduction

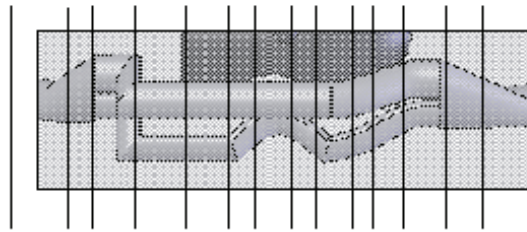
In the current chapter, the experimental results are presented. The laminated tool with conformal cooling system, which was already presented in Figure 4-9 is taken from the design to production and the process steps are followed from the beginning to the end. The same tool with conventional cooling channels is also tested to compare its performance with the laminated tool. The laminated tool was designed and built by the author. Other research group members were also involved in the other parts of this experimental analysis. M. K. Ghovanlou was the researcher who studied the joining process and applied her research outcome to the fabrication process. Also, J. Seo investigated the optimum sensor locations for cooling channels performance measurements. Also J. Benninger was the CNC technician who performed the CNC machining in the final assembly.

The slice thicknesses used in fabrication process are the outcome of the program in the third run in Section 4.6. The final tool is tested to show its improvement in production time and the cooling system performance.

The optimization program, is discussed in the Appendix A. Here, as mentioned earlier, the proposed method is applied to an injection mould for fabricating a new laminated die with conformal cooling channels. The results both for conventional and laminated moulds are presented at the end.



**a) Front view**



**b) Side view**

Figure 6-1: Slice planes location at the end of optimization procedure

## 6.2 Experimental Results

Figure 6-1 shows the optimum thickness vector for the part shown in Figure 4-9. This is the output of the third run in Section 4.6, which is used as the final result of the optimization in the fabrication process .

For the example considered in this work, the fabrication of the laminated tool began with laser cutting the lamina according to the best thickness vector. Figure 6-2 depicts an individual slice after laser cutting process. As it can be seen in this figure, besides cavity and cooling channel profiles, each slice has three guide holes which assist in the assembling process to prevent sliding slices on each other.

After cutting, the sheets are bonded together using brazing. Figure 6-3 shows the laminated tool after the brazing process. The portions of the rods outside of the assembled slices will be removed during CNC machining.

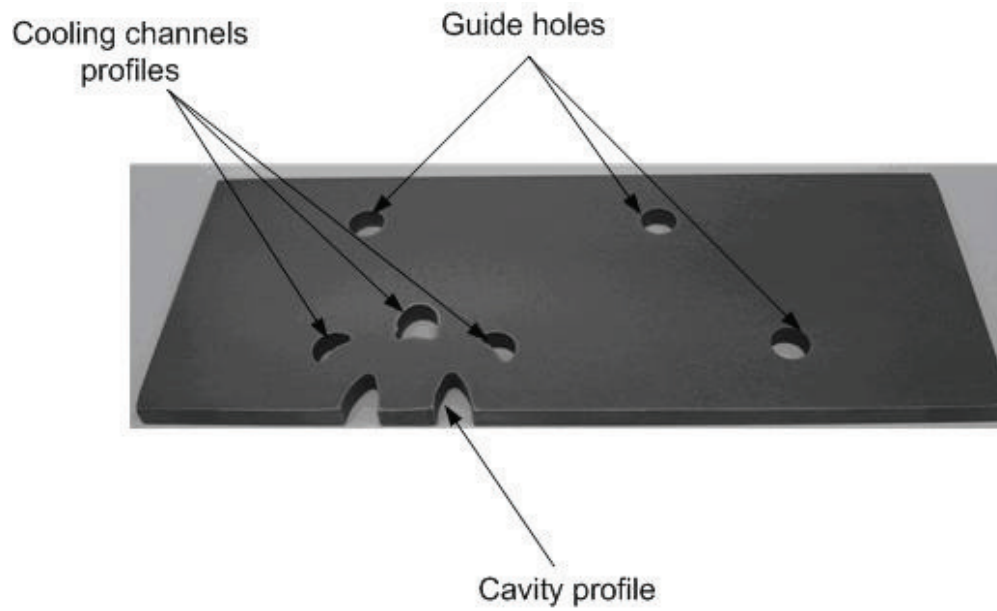


Figure 6-2: One sample after laser cutting process

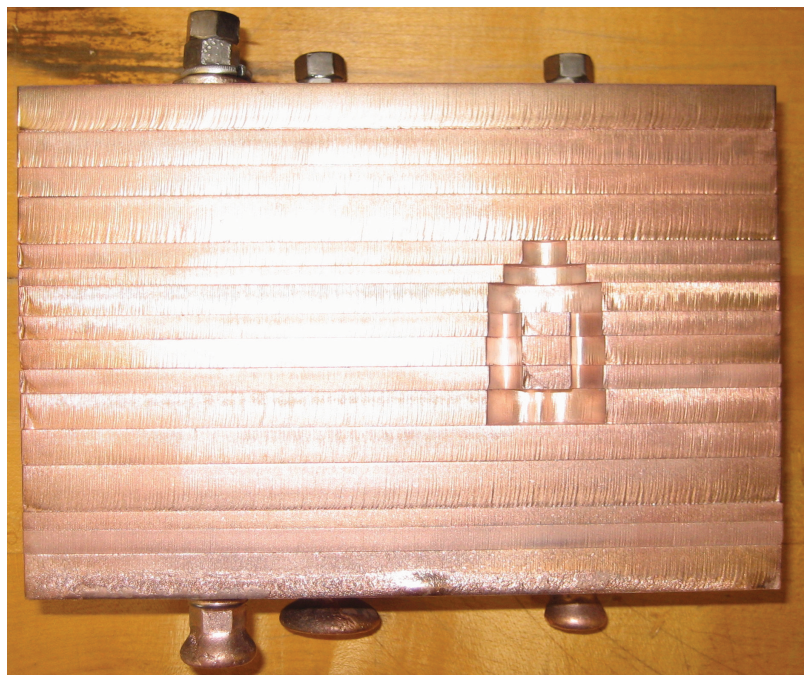


Figure 6-3: The laminated tool after brazing process

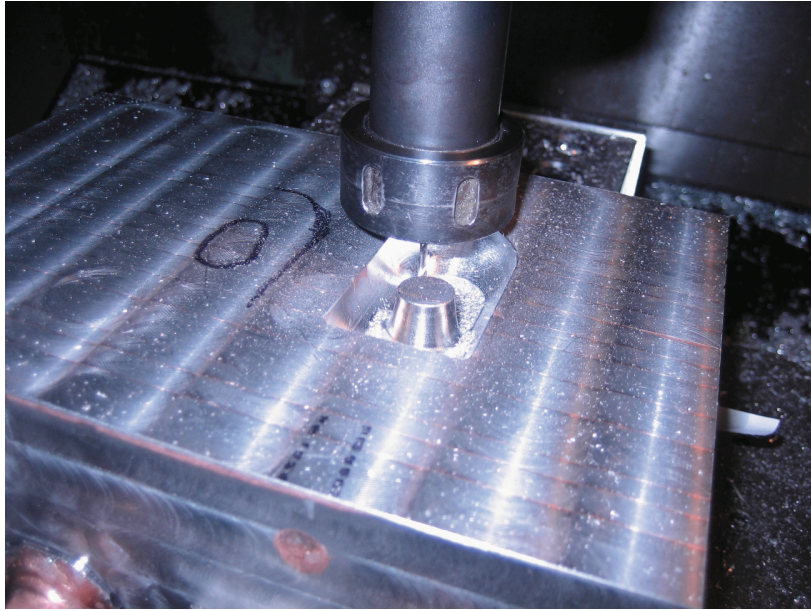


Figure 6-4: The CNC machining process

The final step in laminated tooling process is CNC machining. The machining step will remove stair case effects on the tool surface and bring it to near net shape. Here, as shown in Figure 6-4, the brazed assembly is machined based on the data from the CAD model presented in Figure A-3. The CNC machining process was done on an OKK 3-axis CNC machine.

The machining time to finish the sides of the laminated tool is almost equal to the time required for a traditional tool which is made from a block of material. However, as it can be seen in Figures 6-3 and 6-4, in the inside of the cavity, only the stair step effects needs to be removed, and this results in a reduction in the machining time.

For this test piece, the time spent for finishing the cavity in the laminated tool was almost 15 minutes while the estimated time to make the same cavity from a block of material in traditional process is almost 15% higher. It should be added that more machining time reduction is expected while creating a larger tool.

On the other hand, one of the crucial issues in laminated tools manufacturing is to provide a reasonable surface quality of the cavity. This is more important especially in injection mould or hydroforming tools where a high surface quality for the part produced by the tool is needed.



Figure 6-5: Inside of the cavity and joined layers

As Figure 6-5 shows, CNC machining can provide an acceptable surface quality for the cavity in this test tool.

To investigate the performance of the laminated mould with conformal cooling channels, and also to make sure there is no leakage through the cooling system or the cavity, the tool went through the production tests.

Figure 6-6 shows the laminated injection mould tool during the production tests. The tests were conducted on an 83 ton Battenfeld 750, toggle machine. It has a 9oz. or 257 gram shot capacity and the screw diameter is 40mm.

Firstly, no leakage was reported during the tests either from inside the cavity or along the cooling channels. As depicted in Figure 6-6, the cavity is properly filled during the injection process. Figure 6-7 shows the final product of injection moulding which is a plastic part used in the furniture industry. As depicted in this figure, the final part has an excellent surface quality, which means not only the surface of the cavity has been finished properly during CNC post processing, but also there is no leakage inside the cavity. This implies that in this laminated tool, the brazing process can provide enough strength to hold the sheets.

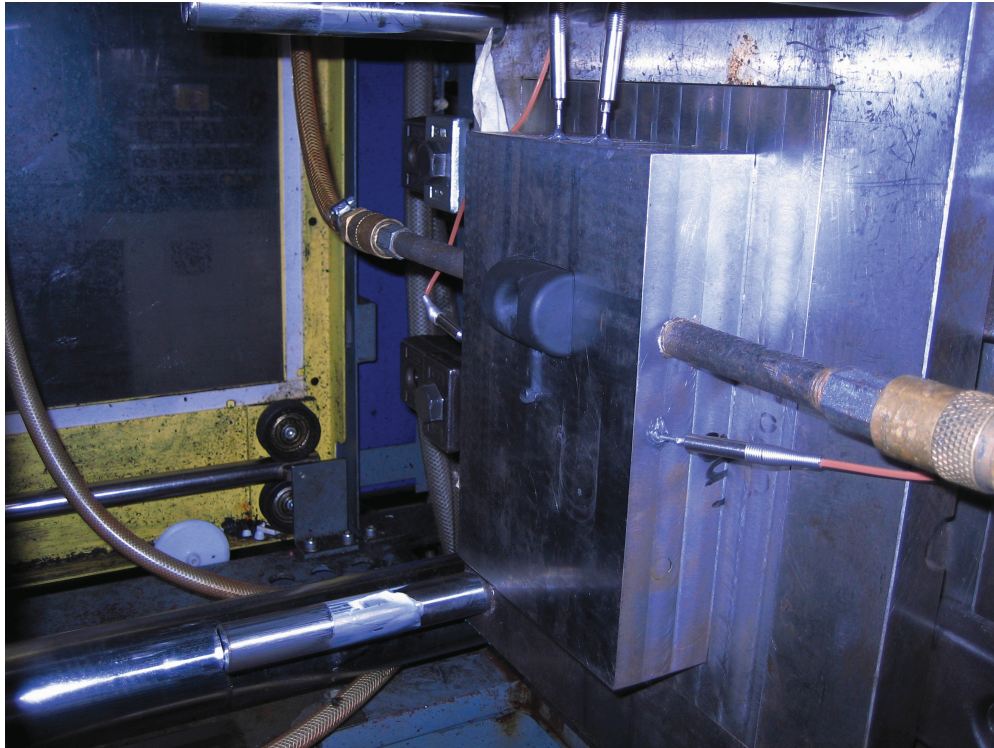


Figure 6-6: The laminated injection mould tool during the operation, with the sensors installed to investigate the cooling channels performance



Figure 6-7: The final product



Table 6.1: Operation results for conventional and conformal cooling channels for the sample injection mould tool

<b>Process</b>	<b>Time required (Sec.) (Conventional cooling system)</b>	<b>Time required (Sec.) (Conformal cooling system)</b>
Boost	2	2
Hold	16	16
<b>Cool</b>	<b>50</b>	<b>25</b>
Ejection	22	22
<b>Total</b>	<b>90</b>	<b>65</b>

Table 6.1 compares the performance of the proposed conformal cooling channel with the conventional one. An injection moulding process consists of boosting, holding, cooling, and ejection. As depicted in Table 6.1, with the conventional cooling channels, the time for cooling the injected mould is 50 seconds. This time then reduced to 25 seconds in the tool with conformal cooling system. This means almost a 50% reduction in the cooling time, without any negative effect on the quality of the product. This reduction is due to the ability of conformal cooling channels to follow the cavity. Moreover, considering the whole injection moulding process, the 50% reduction in cooling time means a 25% reduction in overall cycle time.

### 6.3 Conclusion

In this chapter, a mould already in production line with conventional cooling channels, was reproduced by the laminated tooling technique with conformal cooling channels based on the proposed optimization method, in Chapter 4.

Results clearly indicated that using the optimized set of available sheets can reduce the post-processing (CNC) cost by almost fifteen percent in comparison with the traditional method of creating this cavity.. It should be mentioned that considering the size of the tool in this experimental study, more reduction in machining time is expected for larger tools.

On the other hand, conformal cooling channels created for the tool by the proposed optimization method could provide better cooling performance than conventional cooling channels.

Results of the experimental tests showed a fifty percent reduction in the cooling time for this tool. Since the highest amount of the time for the whole injection moulding process belongs to the cooling process, a fifty percent reduction in the cooling time causes almost thirty five percent reduction for the whole process time. This is just for the using of conformal cooling system for this tool.

## Chapter 7

# Concluding Remarks and Future Works

### 7.1 Thesis Contributions

In this thesis, the laminated tooling as one of the most effective methods to create injection mould tools with complex cavity shapes was investigated. The problem of having the optimum sort of commercially available thicknesses such that the post processing and cutting costs are minimized, was studied. The main output of this research is a genetic algorithm based optimization procedure which starts with the CAD model of the tool and then based on the standard set of thicknesses provide the best slice locations. Whereas, the process of finding the best slice locations in laminated tooling has been conducted manually so far in the tool making industry.

As the next step, slicing direction as an important parameter in volume deviation reduction in laminated tools fabrication was investigated. A method to find the best slicing direction based on CAD model surface geometry was proposed. The suggested method can provide not only the best slicing direction for the entire model, but also different slicing direction for individual portions of the model, as well.

Finally the experimental analysis based on the suggested method was conducted. A tool which has been already used in an injection mould company, in Waterloo Ontario was selected. This original tool had conventional cooling system. A new laminated tool, based on this con-

ventional tool, was designed with conformal cooling channels. Testes could prove that not only the conformal cooling channel results a significant improvement in cooling time, but also the suggested optimization method can provide an acceptable arrangement of standard thicknesses for laminated tools fabrication.

The contributions of this research are classified as:

### **7.1.1 Volume deviation and number of slices were minimized at the same time**

The objective function in this optimization process considers volume deviation and number of slices minimization, at the same time. As it was presented in Chapters 3 and 4, the outcome of the optimization process is a set of available thicknesses which produces the minimum amount of volume deviation while using the minimum number of sheets.

### **7.1.2 Considering a set of available sheets in the optimization process**

The proposed optimization method presented in Chapter 3 considers a set of sheets as standard set. The standard set is a set of commercially available thicknesses. In the most optimization methods in the literature, the optimization process output was a set of thicknesses for the entire CAD model, no matter if these thicknesses were available or not. Therefore, having a set of thicknesses as the optimization constraint is one of the contributions of this research.

### **7.1.3 A customized version of genetic algorithm was proposed for this specific application**

The nature of this optimization problem forced researchers to customize the standard real coded genetic algorithm for this specific application. First, as it is discussed in Chapter 3, new crossover and mutation operators were developed. Then in Chapter 4, a new crowding method was designed to prevent the premature convergence.

### **7.1.4 Geometry of CAD model was considered for slice thickness calculations**

Considering the geometry of CAD model in slice thickness calculations resulted adaptive slice thicknesses.

### **7.1.5 Slicing direction as an important parameter in laminated tools optimization was studied. An analytical method to find the best slice direction was developed**

Before this research was presented, the direction of slicing in laminated tooling was selected manually. Whereas, here an analytical method was developed to find the best slicing direction based on the geometry of CAD model surface. Also, variable slicing direction to have lesser amount of volume deviation was investigated and the method developed in Chapter 5, expanded to be able to suggest different slice directions based on the geometry of different portions of CAD model.

### **7.1.6 A user friendly software for laminated dies manufacturing**

In the proposed method, the entire optimization and slicing processes were conducted automatically with minimum interface with the user. SolidWorks<sup>®</sup> was used for the slicing procedure simulation and the genetic algorithm based optimization was conducted in VisualBasic. The outcome of thesis is presented as a user friendly software which can find the best thickness vector considering volume deviation and number of slices minimization.

### **7.1.7 Experimental analysis to show the performance of the suggested method was performed**

The proposed optimization method was applied on an injection mould tool. The selected tool had a conventional cooling channel. Author designed a new tool with conformal cooling channels and then applied the proposed method on that to find the best set of thicknesses for making its laminated model. The tool was created and tested and as the results in Chapter 6 shows, conformal cooling channels can reduce the cooling time by almost 50%.

## **7.2 Future Work**

In the following, some of the topics which can be considered as the extension to this research are listed:

- In the current research, crowding factor is a user defined constant, while as a further investigation, it can be defined as a parameter dependent on the rate of the convergence in the population.
- The direction study presented in this research can be applied to an actual model in order to produce a laminated tool with optimized multiple slicing directions. This will show the performance of the proposed method in order to minimize the volume deviation.
- Experimental test on a larger tool with focus on using lamination process on the injection mould inlet can show how the effect of injected material on the final product can be reduced.
- The proposed directional study is based on volume deviation minimization. The number of slices can be also considered as another parameter in searching for the best direction.
- Two approaches were introduced for directional study, in this research. As one of the future steps, some guide lines can be introduced to help the user to pick one of these approaches for the directional study.

## Appendix A

# Optimization Program

The methodology of the optimization was already explained in Chapter 3. Here a brief explanation of how the optimization program works, is presented. Also, at the end, a copy of the optimization code is attached.

As depicted in Figure A-1, after running the program, it asks about the number of slicing direction(s). Either in a single direction or a multiple directions slicing process, the slicing direction(s) can be selected either by the user or by the program. In the case of the direction(s) found by the program, a direction module based on the method explained in Chapter 5, finds the optimum slicing direction(s). Here as shown in Figure A-1 a user defined single slicing direction is considered.

In the case of user defined multiple slicing direction, program asks the user to input the locations of changing the slicing direction as well as the slicing angles along Z axis, as represented in Figure A-2.

If user prefers the program finds the slicing directions, then as shown by Figure A-3, the CAD model length and the gain value are the only parameters that program needs to start the direction analysis as discussed in Chapter 5. Referring to Figure 5-17, the gain value is the length of equal intervals on CAD model. The amount of well located tile areas are calculated on each of these intervals, then the best direction is found in each interval based on its well located tile area.

The last step before running the program is to input the genetic algorithm related information. As Figure A-4 shows, there are default values for most of the variables, however, user still

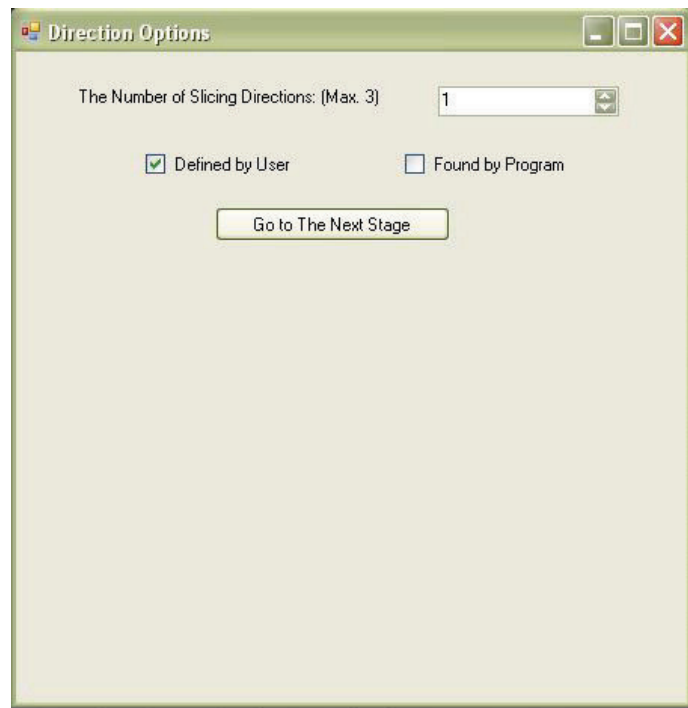


Figure A-1: The first dialog box in the program



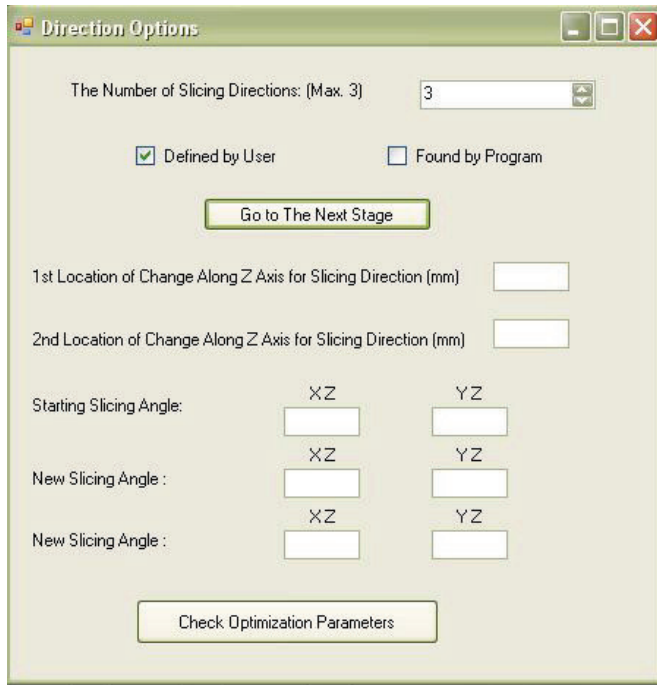


Figure A-2: Dialog box to input the multiple direction slicing information

is able to change each of them.

After all inputs are provided for the program, it starts performing the optimization procedure. Figures A-5 and A-6 are two snap shots of running the simulation module. Figure A-5 represents the slice plane selection to find its intersection with the CAD model and Figure A-6 shows the final shape of an individual slice.

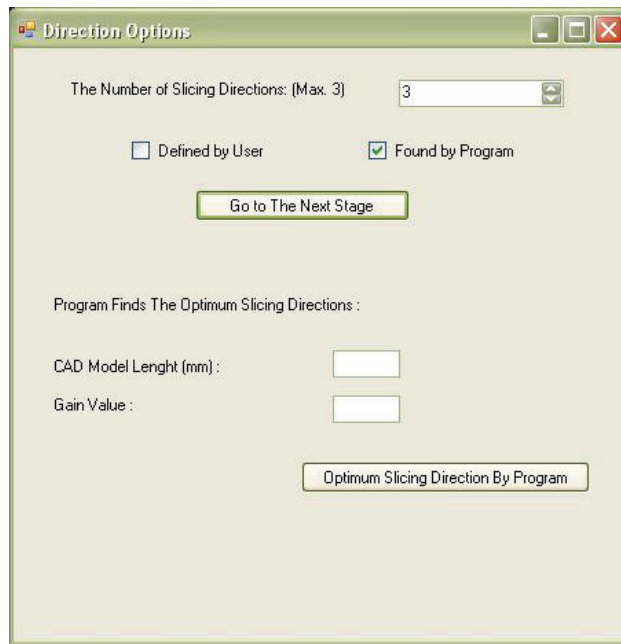


Figure A-3: CAD model length and gain value are needed if the slicing direction(s) is found by the program

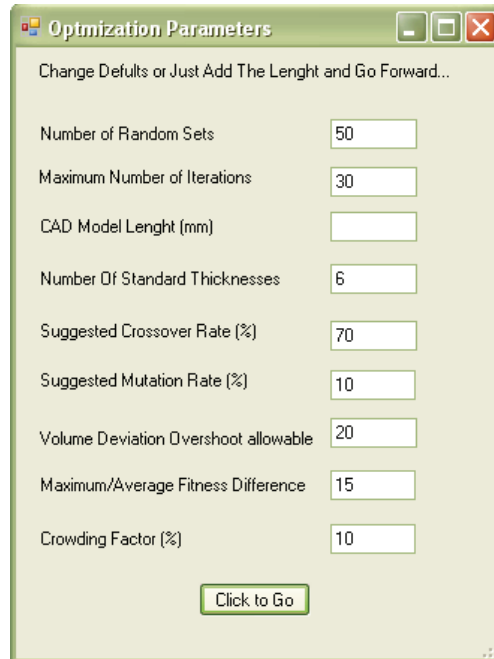


Figure A-4: Optimization parameters input dialog box

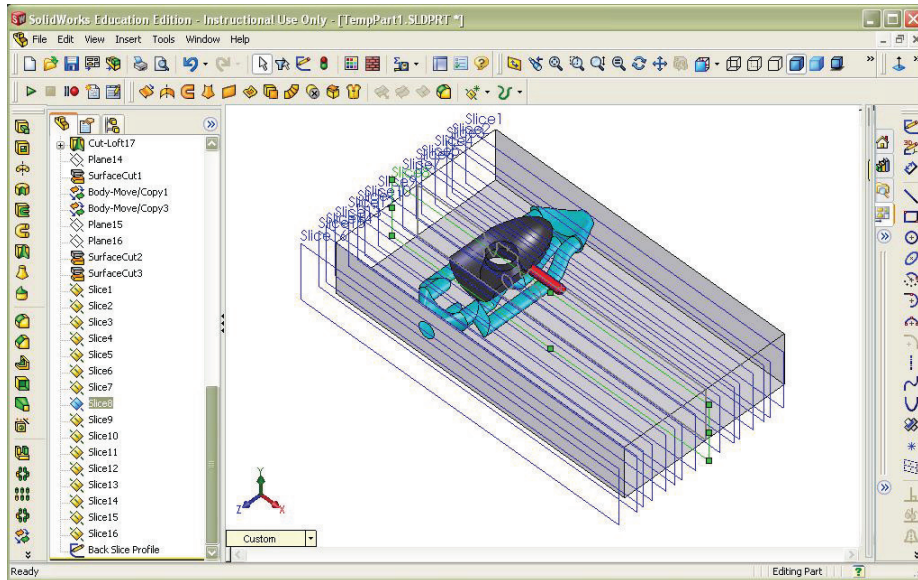


Figure A-5: The intersection of a slice plane with the actual model

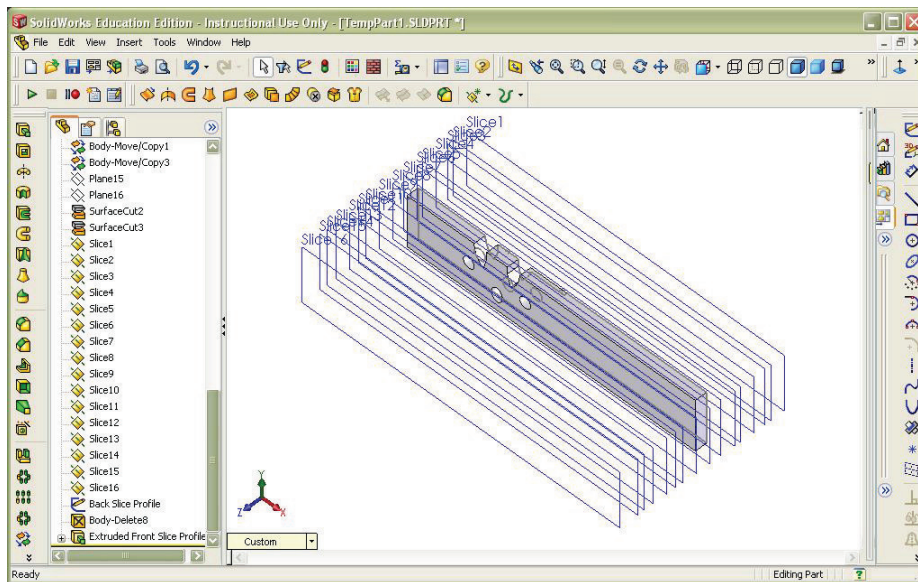


Figure A-6: An individual slice built by the program

# Bibliography

- [1] Yoo S.; Walczyk D.F., “An advanced cutting trajectory algorithm for laminated tooling,” *Rapid Prototyping Journal*, vol. 11, no. 4, pp. 199–213, 2005.
- [2] Brink J.; Lee A.; Anderson D.; Ramani K., “Cad model decomposition for wirepath,” *Rapid Prototyping Journal*, vol. 10, no. 5, pp. 288–296, 2004.
- [3] Nakagawa T.; Kunieda M.; Liu S.D., “Laser cut sheet laminated forming dies by diffusion bonding,” *Proceedings of the 25th International Machine Tool Design and Research Conference*, pp. 505–10, 1985.
- [4] Himmer T.; Nakagawa T.; Anzai M., “Lamination of metal sheets,” *Computers In Industry*, vol. 39, pp. 27–33, 1999.
- [5] Dickens P.M., “Principles of design for laminated tooling,” *International Journal of Production Research*, vol. 35, no. 5, pp. 1349–1357, 1997.
- [6] Kulkarni P.; Dutta D., “An accurate slicing procedure for layered manufacturing,” *Computer Aided Design*, vol. 28, no. 9, pp. 683–697, 1996.
- [7] Dolenc A.; Makela I., “Slicing procedures for layered manufacturing techniques,” *Computer-Aided Design*, vol. 26, no. 2, pp. 119–126, February 1994.
- [8] Hope R.L.; Roth R.N.; Jacobs P.A., “Adaptive slicing with sloping layer surfaces,” *Rapid Prototyping Journal*, vol. 3, no. 3, pp. 89–98, 1997.
- [9] Smith R.F; Forrest S.; Perelson A.S., “Searching for diverse, cooperative population with genetic algorithms,” *TCGA Report No. 92002, University of Alabama*, 1992.

- [10] Smith T.S.; Farouki R.T.; Al-Kandari M., “Optimal slicing of free-form surfaces,” *Computer Aided Geometric Design*, vol. 19, pp. 43–64, 2002.
- [11] Lee K.H.; Choi K., “Generating optimal slice data for layered manufacturing,” *International Journal of Advanced Manufacturing Technology*, vol. 16, pp. 277–284, 2000.
- [12] Majhi J.; Janardan R.; Smid M.; Gupta P., “On some geometric optimization problems in layered manufacturing,” *Computational Geometry, Theory and Applications*, vol. 12, pp. 219–239, 1999.
- [13] Cormier D.; Unnanon K.; Sanni E., “Specifying non-uniform cusp height as a potential aid for adaptive slicing,” *Rapid Prototyping Journal*, vol. 6, no. 3, pp. 204–211, 2000.
- [14] Haipeng P.; Tianrui Z., “Generation and optimization of slice profile data in rapid prototyping and manufacturing,” *Journal of Materials Processing Technology*, vol. 187–188, pp. 623–626, 2007.
- [15] Dai J.; Luo W.; Jin M.; Zeng W.; He Y., “Geometric accuracy analysis for discrete surface approximation,” *Computer Aided Geometric Design*, vol. 24, pp. 323–338, 2007.
- [16] Renner G.; Ekart A., “Genetic algorithms in computer aided design,” *Computer Aided Design*, vol. 35, pp. 709–726, 2003.
- [17] Chandan K.; Choudhury A.R., “Volume deviation in direct slicing,” *Rapid Prototyping Journal*, vol. 11, no. 3, pp. 174–184, 2005.
- [18] Zhao Z.; Laperriere L., “Adaptive direct slicing of solid model for rapid prototyping,” *International Journal of Production Research*, vol. 38, no. 1, pp. 69–83, 2000.
- [19] Himmer T.; Techel A.; Nowotny S.; Beyer E., “Recent developments in metal laminated tooling by multiple laser processing,” *Rapid Prototyping Journal*, vol. 9, no. 1, pp. 24–29, 2003.
- [20] Gibbons G.J.; Hansell R.G.; Norwood A.J.; Dickens P.M., “Rapid laminated die cast tooling,” *Assembly Automation*, vol. 23, no. 4, pp. 372–381, 2003.

- [21] Hur J.; Lee K., “The development of a cad environment to determine preferred build-up direction for layered manufacturing,” *International Journal of Advanced Manufacturing Technology*, vol. 14, pp. 247–254, 1998.
- [22] Paul B.K.; Voorakarnam V., “Effect of layer thickness and orientation angle on surface roughness in laminated object manufacturing,” *Journal of Manufacturing Processes*, vol. 3, no. 2, pp. 94–101, 2001.
- [23] Massod S.H.; Rattanawong W.; Iovenitti P., “Part build orientations based on volumetric error in fused deposition modelling,” *International Journal of Advanced Manufacturing Technology*, vol. 16, pp. 162–168, 2000.
- [24] Massod S.H.; Rattanawong W.; Iovenitti P., “A generic algorithm for part orientation system for complex parts in rapid prototyping,” *Journal of Materials Processing Technology*, vol. 139, no. 1-3, pp. 110–116, 2003.
- [25] Bryden B.G.; Wimpenny D.I.; Pashby I.R., “Manufacturing production tooling using metal laminations,” *Rapid Prototyping Journal*, vol. 7, no. 1, pp. 52–59, 2001.
- [26] Schwartz M., *Brazing*, ASM International, second edition, 2003.
- [27] Walczyk D.F.; Hardt D.E., “A new rapid tooling methods for sheet metal forming dies,” *Proceedings of the 5th international conference on rapid prototyping*, pp. 275–89, 1994.
- [28] Yoo S.; Walczyk D.F., “An adaptive slicing algorithm for profiled edge laminae tooling,” *International Journal of Precision Engineering and Manufacturing*, vol. 8, no. 3, pp. 64–70, 2007.
- [29] Fakhreddin O.Karray and Clarence De Silva, *Soft Computing And Intelligent Systems Design (Theory, Tools and Applications)*, Pearson Education Limited, first edition, 2004.
- [30] William W.Melek, *ME780: Computational Intelligence, Course Handouts*, Department of Mechanical Engineering, University of Waterloo, Summer 2007.
- [31] Tata K.; Fadel G.; Bagchi A.; Aziz N., “Efficient slicing for layered manufacturing,” *Rapid Prototyping Journal*, vol. 4, no. 4, pp. 151–167, 1998.

- [32] Leong K.F.; Chua C.K.; Ng Y.M., “A study of stereolithography file errors and repair. part 1 generic solution,” *The International Journal of Advanced Manufacturing Technology*, vol. 12, pp. 407–414, 1996.
- [33] Tai I. Y.; Walczyk D.F., “Development of a computer aided manufacturing system for profile edge lamination tooling,” *Journal of Manufacturing Science and Engineering*, vol. 124, pp. 754–761, August 2002.
- [34] Beasley D.; Bull D.R.; Martin R.R., “A sequential niche technique for multimodal function optimization,” *Evolutionary Computation*, vol. 1, pp. 101–125, 1993.
- [35] Holland J.H., *Adaptation in Natural and Artificial Systems*, University of Michigan Press, 1975.
- [36] Goldberg D.E.; Richardson J., “Genetic algorithm with sharing for multimodal function optimization,” *Proceeding of The Second International Conference on Genetic Algorithms, Pittsburgh*, 1987.
- [37] Deb K.; Goldberg D.E.; Richardson J., “An investigation of niche and species formation in genetic function optimization,” *Proceeding of The Third International Conference on Genetic Algorithms, San Mateo, CA*, 1989.